Study on isoprene emission from leaves of bamboo species

Tingwei Chang

2021

Contents

Figure Index

Table Index

Chapter 1

Introduction

1.1. Impact of Isoprene on Atmospheric Chemistry

Isoprene (2-methyl-1,3-butadiene) is one of the major biogenic volatile organic compounds (BVOCs) in the atmosphere, with an estimated annual carbon emission of approximately 400–700 Tg, accounting for approximately 50–70 % of the total terrestrial BVOC emissions (Guenther et al., 2006, 2012; Sindelarova et al., 2014). This amount is almost equivalent to global methane emission recorded between 2008 and 2017 (410–660 Tg of carbon per year) (Saunois et al., 2020) and can be 4–7 times of the total global anthropogenic emissions for non-methane volatile organic compounds (Kansal, 2009; Middleton, 1995). Several global estimation studies have revealed large-scale emissions of plant-based isoprene.

These emissions can impact atmospheric chemistry and negatively affect air quality. Isoprene and its oxidation products (methyl vinyl ketone and methacrolein) react with nitrogen oxides (NO_x) to form ozone (O_3) in the troposphere (Kamens et al., 1982; Paulson et al., 1992; Paulson and Seinfeld, 1992; Teng et al., 2017), thus, worsening the air quality. This effect has been recorded in urban green environments where both isoprene and NO_x are highly abundant (Biesenthal et al., 1997; Dreyfus et al., 2002; Duane et al., 2002; Pang et al., 2009; Geng et al., 2011; Fierravanti et al., 2017). Additionally, BVOCs are estimated to be the largest source of secondary organic aerosol (SOA) mass globally, releasing 12–70 Tg of SOA per year (Kanakidou et al., 2005). As the most abundant BVOC, isoprene is a major precursor for the formation of SOAs either through photo-oxidation under low atmospheric NO_x or through acid-catalyzed oxidation with hydrogen peroxide (Claeys et al., 2004a, b). A chamber study on the photo-oxidation of isoprene demonstrated that 1–6 % mass of isoprene formed SOA depends on isoprene and NO_x concentration (Kroll et al., 2005, 2006).

As a highly reactive chemical, isoprene competes for radicals and potentially alters the lifespan of methane in the atmosphere; however, this depends on the isoprene to NO_x ratio (Poisson et al., 2000; Spivakovsky et al., 2000; Collins et al., 2002; Pike and Young 2009; Archibald et al., 2011). BVOC emissions could be an overlooked carbon emission pathway, thus, considering BVOC fluxes, including isoprene, when quantifying carbon cycling in forest ecosystems become necessary (e.g., Guenther, 2002; Luyssaert et al., 2007; Okumura et al., 2008; Chapin et al., 2009). Generally, the impact of isoprene on the global warming potential can be significant (Fehsenfeld et al., 1992; Pike and Young 2009).

1.2. An Overview of Plant-Source Isoprene Emission

1.2.1. Biochemical process of isoprene synthesis in plant leaves

Plants produce dimethylallyl pyrophosphate (DMAPP) through 2-C-methyl-D-erythritol 4-phosphate/1-deoxy-D-xylulose 5-phosphate (MEP/DOXP) pathways and convert it to isoprene. This process incorporates pyruvate (pyr) and glyceraldehyde 3-phosphate (g3p) into a 5-carbon skeleton (DOXP) and transform into multiple metabolic intermediates to become DMAPP (Schwender et al., 1997; Rohmer, 1999; Lichtenthaler, 1999). The formation of the intermediates is highly related to photosynthetic chemistry, where the reducing agent (nicotinamide adenine dinucleotide phosphate, NADPH) and energy equivalent (adenosine triphosphate, ATP) are required and limited by the electron transport chain in the light reaction (Brüggemann and Schnitzler, 2002; Rosenstiel et al., 2002; Rasulov et al., 2009; 2018). Apart from the MEP/DOXP pathway, plants can also produce DMAPP through the mevalonate (MVA) pathway. The enzyme isoprene synthase (IspS) is located only in the stromal side of the thylakoid membrane of chloroplasts; therefore, isoprene is produced only in chloroplast-containing organ, such as leaves (Wildermuth and Fall, 1996; 1998; Sasaki et al., 2005). IspS catalyzes the conversion of DMAPP to isoprene and diphosphate (Silver and Fall, 1991; Sasaki et al., 2005; Oku et al., 2014).

1.2.2. Causes of isoprene emission by plants

There are multiple hypotheses for the production of isoprene in plants. Isoprene can stabilize thylakoid membranes, by enhancing the packing of lipid tails, to protect leaves from heat and oxidative damages (Sharkey and Singsaas, 1995; Sharkey, 1996; Loreto and Velikova, 2001; Siwko et al., 2007; Vickers et al., 2009). Isoprene production also helps dissipate the excess energy absorbed by photosynthetic pigments; it dissipates less potential heat energy through non-photochemical quenching that is similar to the function of fluorescence quenching (Way et al., 2011; Pollastri et al., 2014). Isoprene can also quench reactive oxygen species, thereby reducing the oxidative damage to leaves (Loreto et al., 2001). Recently, by studying the RNA interference-mediated suppression of isoprene emission in gray poplar (hybrid of *Populus alba* and *Populus tremula*) and the effects of isoprene fumigation on *Arabidopsis thaliana*, it was established that isoprene concentrations induce changes in the expression of many gene networks that are important for stress responses and plant growth (Behnke et al., 2010; Harvey and Sharkey, 2016). Base on this find, Zuo et al. (2019) further indicated that isoprene affects growth and stress tolerance by directly regulating gene expression, suggesting its role as a signaling molecule in plants.

However, the energy required for isoprene production is quite high. Each isoprene molecule produced via the MEP/DOXP pathway requires 20 ATP and 14 NADPH (Sharkey and Yeh, 2001). Moreover, it causes carbon loss, which is disadvantageous to plant growth (Sharkey and Loreto, 1993). Therefore, isoprene emissions vary among plant species and depending on the environmental conditions (Sharkey and Loreto, 1993; Monson et al., 2013).

1.2.3. History of model development of isoprene emission from plant leaves

Since the first report of isoprene emission from plants (Sanadze, 1957), researchers have been interested in developing a model to explain the variability in isoprene flux among different plant species. To evaluate the impact of plant-emitted isoprene post-haste, the earlier models were developed with limited knowledge of isoprene biosynthesis mechanism in plants. The first systematic model was proposed by Tingey et al. (1979) where the isoprene emission from an oak species (*Quercus virginiana*) was considered. In conjunction with studies indicating that plant isoprene emissions depend on environmental factors such as light and temperature (Sanadze and Kalandadze, 1966; Rasmussen and Jones, 1973), this model featured with a logistic function of either the leaf temperature or the light intensity as driving variables. Although the proposed algorithm does not consider the mechanism of catalytic reaction and carbon loss, most of the coefficients have to be verified empirically to fit the observations.

Another model was proposed by Guenther et al. (1991) basing on observations on *Eucalyptus* sp. with light intensity, leaf temperature, relative humidity, and atmospheric CO_2 concentration as the driving factors. Guenther et al. (1991) also introduced the concept of an emission flux, defined for a standard set of conditions (light intensity at 1000 μmol m^{-2} s^{-1}, leaf temperature at 30 °C, relative humidity at 40%, and atmospheric CO_2 concentration at 330 ppmv), known as the "basal isoprene emission flux." By multiplying this flux with the corresponding coefficients, calculated by measuring the value of each factor, a simulated instantaneous isoprene emission flux could be obtained. This model was modified with only light intensity and leaf temperature as drivers (relative humidity and atmospheric CO_2 concentration were negligible when considered across the range of conditions normally encountered by leaves), and was named the G93 model (Guenther et al., 1993). The current global BVOC estimation method (i.e., Model of Emissions of Gases and Aerosols from Nature, MEGANv3.1) is based on this framework. This model requires only a basal isoprene emission flux and determined environmental condition to estimate the isoprene emission dynamic. The simulated basal isoprene emission flux can also be obtained by reverse calculation of the isoprene emission flux with its corresponding light intensity and leaf temperature. However, the G93 model is still based on empirically conducted value of coefficients without a consideration of underlying biosynthetic stoichiometry. Since basal isoprene emission varies with time, the G93 model may fail to reproduce the values with a basal isoprene emission flux derived a few hours to a few days ago. Another problem is that isoprene emission ability may vary among leaves or individual plants, thus, complicating the determination of a representative basal isoprene emission flux for a plant species.

The newer models were supported by an improved knowledge of the biochemical and physiological mechanisms controlling the isoprene emission flux. For example, Martin et al. (2000) developed a model based on three processes that potentially limit isoprene synthesis, i.e., pyruvate supply to provide the substrate for isoprene carbon, ATP supply for phosphorylation to DMAPP, and the rate of isoprene synthesis from DMAPP. This model uses the same driving factors as those of the empirical model (light intensity, temperature, and CO_2 concentration). The difference is that the functions and coefficients were determined based on theoretical considerations, according to the underlying processes.

Subsequently, Niinemets and Reichstein (2002) developed a model that involves an algorithm based on leaf photosynthetic electron transport to simulate isoprene emission with its energy requirements. They successfully reproduced isoprene emissions from *Liquidambar styraciflua* and *Quercus* spp.; however, fewer empirical coefficients were considered.

Morfopoulos et al. (2014) developed a model based on the hypothesis that isoprene biosynthesis depends on a balance between the supply of photosynthetic reducing agent and the demand for carbon fixation. This model estimates isoprene using intercellular CO_2 concentration and light intensity, by hypothesizing that the NADPH used in isoprene production is dependent on the extent to which the NADPH requirements of the Calvin–Benson and photorespiratory cycles are satisfied.

The greatest limitation in these process-based models is the absence of critical stoichiometric information of isoprene biosynthesis, including the proportion of metabolites and reductive agents channeled from the MEP pathway and photosynthetic pentose phosphate pathway, respectively. Therefore, current isoprene emission estimation is highly dependent on observations, regardless of the usage of an empirical model or process-based model. Plant isoprene emission is more frequently estimated by empirical models (e.g., Guenther et al., 1993; Guenther et al., 2006; Guenther et al., 2012) than the process-based models currently. To use empirical models, a species-specific basal isoprene emission flux is required. Generally, basal isoprene emission fluxes are directly observed under certain light and temperature conditions (usually 1000 μmol m^{-2} s^{-1} and 30 °C, respectively) or simulated by isoprene emission models (e.g., Guenther et al., 1993). However, the basal isoprene emission flux is not always constant and can be altered by long-term weather conditions (e.g., temperature acclimation and drought) (Rasulov et al., 2010; Jiang et al., 2018). Furthermore, the response of simulated isoprene emission flux to instantaneous leaf temperature did not fit the actual reaction for several tropical plant species (Keller and Lerdau, 1999; Oku et al., 2008). These results further revealed evidence and knowledge of isoprene biosynthesis, suggesting a need to revise the empirical models with a process-based approach for better reproducibility.

1.2.4. Database of the isoprene emission capacity of plant species

Different plant species may demonstrate different isoprene emission capabilities. For instance, *Eucalyptus* spp. and *Quercus* spp. have been recognized as significant isoprene emitters (e.g., He et al., 2000; Geron et al., 2001; Okumura et al., 2008), while some species (e.g., *Acer* spp.) had undetectable isoprene emissions (Zimmerman, 1979; Evans et al 1982; Winer et al., 1983). Furthermore, isoprene emission ability could vary among species within a genus (e.g., *Quercus* spp., Tani and Kawawata, 2008). Therefore, it is necessary to record the data from numerous species to accurately estimate the global isoprene emissions from plants. The current global estimation model (MEGANv3.1) requires a basal emission flux and uses the calculated coefficients of light, temperature, leaf age, soil moisture, leaf area index, and CO_2 inhibition, to fit the instantaneous condition of the subject zone. The basal emission flux is usually defined as the emission flux under standard light intensity and leaf temperature (Guenther et al., 1993). Previous studies have shown that the estimation of global isoprene emissions is highly sensitive to basal isoprene emission fluxes.

This section shows the isoprene emission data, measured using the enclosed chamber method, from 41 studies including 244 plant species within 55 families. Note that different studies have used different parts of the plants to apply the enclosure method (e.g., leaf enclosure, branch enclosure, and whole plant enclosure). The emission flux may represent one or both of the two forms (mass-based and area-based). Because most of the studies did not measure the emission flux under standard light or temperature conditions, the data were normalized to simulate a light intensity of 1000 μmol m^{-2} s^{-1} and a leaf temperature of 30 °C by using the following algorithm and its parameter set (Guenther et al., 1993):

$$I_B = I/(L \cdot T) \qquad \text{(Equation 1-1)},$$

where I is the isoprene emission flux at a given light intensity and leaf temperature conditions, I_B is the basal emission flux, and L and T are calculated variables determined by functions of light intensity and leaf temperature, respectively. L is defined as follows:

$$L = \alpha \cdot C_L \cdot \text{PPFD}/\sqrt{1 + \alpha^2 \cdot \text{PPFD}^2} \qquad \text{(Equation 1-2)},$$

where α (0.0027) and C_L (1.066) are empirical coefficients of light response. T is defined as follows:

$$T = \exp\left(C_{T1} \cdot [T_L - T_s]/[R \cdot T_s \cdot T_L]\right)/\left(1 + \exp\left[C_{T2} \cdot \{T_L - T_M\}/\{R \cdot T_s \cdot T_L\}\right]\right) \qquad \text{(Equation 1-3)},$$

where R is the gas constant (8.314 J K^{-1} mol^{-1}), T_s is the leaf temperature under standard conditions (303.15 K); T_L (K) is the leaf temperature at the time of sampling; C_{T1} (95000 J mol^{-1}) and C_{T2} (230000 J mol^{-1}) are the empirical coefficients; and T_M (314 K) is an empirical coefficient of the temperature of maximum isoprene emission (Table 1-1). A constant temperature and light dependence based on Guenther et al. (1993) for every species is assumed for this normalization, since information on the actual quantities are not yet available.

Some species demonstrated considerable basal isoprene emission fluxes (e.g., *Elaeis guineensis*, *Robinia pseudoacacia*, and *Quercus laevis*), while some others demonstrated no emission (e.g., *Pinus canariensis*, *Adenostoma fasciculatum*, and *Citrus limon*), indicating a large inter-species variation (Table 1-1). This suggests that observation is essential for the realistic evaluation of basal isoprene emission flux for each species. Furthermore, large differences in basal isoprene emission flux within a species (e.g., *Liquidambar styraciflua*, *Quercus alba*, and *Quercus rubra*) were observed after repeated examinations. Discrepancies may occur because of different isoprene collection approaches, long-term variations, or heterogeneity in the morphological and physiological states among the measured leaves. This situation complicates the determination of a reliable basal isoprene emission flux for a plant species. Furthermore, some plant species were observed less frequently but exhibited considerable basal isoprene emission fluxes, such as bamboo species.

The increase in the importance of bamboo, due to their increasing numbers in the area, makes it inevitable to evaluate isoprene emissions of the plant. However, only 2 out of 17 species (i.e., *Phyllostachys pubescens* and *Pleioblastus hindsii*; Chang et al., 2012) are assigned emission flux values based on the observations available in "MEGAN2019b vegetation type EF" (https://bai.ess.uci.edu/megan/data-and-code#h.p_UD2ckP0JM58D), the current default database of MEGANv3.1, while the remaining 15 species were assigned assumed values. Other studies on isoprene emission flux from bamboo leaves (i.e., Okumura et al., 2018; Table 1-1) recorded the emission fluxes for a limited number of leaves within a short period that is insufficient to represent the dependence of isoprene emission on light and leaf temperature. These studies also cannot account for the variability and determining factors of basal isoprene emission flux in bamboo leaves. Thus, expanding the isoprene emission database for bamboo species, to evaluate the isoprene emission flux from their leaves, is of utmost importance.

Table 1-1 Basal isoprene emission of 233 plant species within 55 families. The emission flux was represented in two forms of unit (mass-based form, μg g^{-1} h^{-1}; area-based form, nmol m^{-2} s^{-1}); following abbreviations are used: NR = not reported, BDL = below detection limit, and NED = no emissions detected. In *E* (stands for enclosure) column, following abbreviations are used: L = leaf enclosure, B = Branch enclosure, and P = whole plant enclosure. In *N* (stands for normalization) column, following abbreviations are used: S = simulated by Guenther et al. (1993), D = Direct observed under standard light intensity and leaf temperature.

Family	Species	Isoprene emission		*E*	*N*	Reference
		μg g^{-1} h^{-1}	nmol m^{-2} s^{-1}			
Aceraceae	*Acer floridanum*	BDL	NR	B	S	Winer et al. (1983)
	Acer rubrum	NED	NR	B	S	Zimmerman (1979)
	Acer saccharinum	NED	NR	P	D	Evans et al. (1982)
Altingiaceae	*Liquidambar formosana*	92.22	NR	B	S	Chang et al. (2012)
	Liquidambar styraciflua	35.3	NR	P	S	Corchonoy et al. (1992)
	Liquidambar styraciflua	17.8	NR	P	D	Evans et al. (1982)
	Liquidambar styraciflua	68	37	L	D	Geron et al. (2001)
	Liquidambar styraciflua	70	NR	L	S	Guenther et al. (1996b)
	Liquidambar styraciflua	71	NR	L	S	Guenther et al. (1996a)
	Liquidambar styraciflua	3.5	NR	B	S	Zimmerman (1979)
Anacardiaceae	*Astronium graveolens*	NR	26	L	D	Keller and Lerdau (1999)
	Pistacia vera	NED	NR	B	S	Winer et al. (1992)
	Rhus ovata	BDL	NR	B	S	Winer et al. (1983)
	Schinus molle	NED	NR	P	S	Corchonoy et al. (1992)
	Schinus molle	NED	NR	B	S	Winer et al. (1983)
	Schinus terebinthifolius	NED	NR	P	S	Corchonoy et al. (1992)
	Schinus terebinthifolius	BDL	NR	B	S	Winer et al. (1983)
	Spondias mombin	NR	33	L	D	Keller and Lerdau (1999)
Annonaceae	*Annona hayesii*	NR	9	L	D	Keller and Lerdau (1999)
	Xylopia frutescens	NR	15	L	D	Keller and Lerdau (1999)
Apocynaceae	*Carissa macrocarpa*	BDL	NR	B	S	Winer et al. (1983)
	Nerium oleander	BDL	NR	B	S	Winer et al. (1983)
	Nerium oleander	NED	NR	B	S	Zimmerman (1979)
Aquilfoliaceae	*Ilex cassine*	NED	NR	B	S	Zimmerman (1979)
Arecaceae	*Acrocomia vinifera*	NR	20	L	D	Keller and Lerdau (1999)
	Elaeis guineensis	172.9	NR	L	D	Cronn and Nutmagul (1982)
	Phoenix dactylifera	15.8	NR	B	S	Winer et al. (1983)
	Sabel palmetto	4.7	NR	B	S	Zimmerman (1979)
	Serenoa repens	8.9	NR	B	S	Zimmerman (1979)
	Socratea exorrhiza	NR	14.5	L	D	Lerdau and Throop (1999)
	Thrinax morrisii	NR	35	L	D	Lerdau and Keller (1997)

Table 1-1 (Continued)

Family	Species	Isoprene emission		*E*	*N*	Reference
		μg g^{-1} h^{-1}	nmol m^{-2} s^{-1}			
Arecaceae	*Wasingtonia filifera*	9.9	NR	B	S	Winer et al. (1983)
	Xylosma congestum	6.8	NR	B	S	Winer et al. (1983)
Berberidaceae	*Nandina domestica*	25.1	NR	B	S	Winer et al. (1983)
Bignoniaceae	*Jacaranda mimosifolia*	NR	NR	P	S	Corchonoy et al. (1992)
	Jacaranda mimosifolia	NED	NR	B	S	Winer et al. (1983)
	Tecomaria capensis	BDL	NR	B	S	Winer et al. (1983)
	Trichostema lanatum	0	NR	P	S	Winer et al. (1983)
Burseraceae	*Bursera simaruba*	NR	32	L	D	Lerdau and Keller (1997)
	Protium panamense	NR	46.3	L	D	Lerdau and Throop (1999)
	Trattinnickia aspera	NR	55.1	L	D	Lerdau and Throop (1999)
Buxaceae	*Buxus sempervirens*	20	NR	B	S	Owen et al. (1998)
Calophyllaceae	*Calophyllum longifolium*	NR	11.9	L	D	Lerdau and Throop (1999)
	Marila laxiflora	NR	11.2	L	D	Lerdau and Throop (1999)
Capparaceae	*Capparis cyanophollophora*	NR	25	L	D	Lerdau and Keller (1997)
	Capparis indica	NR	23	L	D	Lerdau and Keller (1997)
Caprifoliaceae	*Sambucus simponii*	NED	NR	B	S	Zimmerman (1979)
	Viburnum rufidulum	NED	NR	B	S	Zimmerman (1979)
Clusiaceae	*Symphonia globulifera*	NR	16.8	L	D	Lerdau and Throop (1999)
Compositae	*Artemesia californica*	0	NR	B	S	Arey et al. (1995)
	Artemesia californica	BDL	NR	P	S	Winer et al. (1983)
Convolvulaceae	*Bonamia maripoides*	NR	18	L	D	Keller and Lerdau (1999)
Connaraceae	*Cnestidium rufescens*	NR	26	L	D	Keller and Lerdau (1999)
Cupressaceae	*Cunninghamia lanceolata*	0.11	NR	B	S	Chang et al. (2012)
	Cupressus forbesii	0	NR	B	S	Arey et al. (1995)
	Cupressus sempervirens	0	NR	B	S	Winer et al. (1983)
	Juniperus chinensis	0	NR	B	S	Winer et al. (1983)
	Metasequoia glyptostroboides	0	NR	B	S	Chang et al. (2012)
Dilleniaceae	*Doliocarpus major*	NR	32	L	D	Keller and Lerdau (1999)
Ericaceae	*Arctostaphylos glandulosa*	NED	NR	B	S	Arey et al. (1995)
	Arctostaphylos glauca	BDL	NR	B	S	Winer et al. (1983)
	Erica arborea	6.4	NR	B	S	Hansen et al. (1997)
	Erica arborea	18	NR	B	S	Owen et al. (1997)
	Erica multiyora	2	NR	B	S	Owen et al. (1997)
	Erica multiyora	2	NR	B	S	Owen et al. (1998)

Table 1-1 (Continued)

Family	Species	Isoprene emission		*E*	*N*	Reference
		μg g^{-1} h^{-1}	nmol m^{-2} s^{-1}			
Euphorbiaceae	*Croton discolor*	NR	100	L	D	Lerdau and Keller (1997)
	Hevea brasiliensis	7.5	NR	L	D	Cronn and Nutmagul (1982)
	Macaraunga triloba	45.3	NR	L	D	Cronn and Nutmagul (1982)
	Mallotus paniculatis	NR	NR	L	D	Cronn and Nutmagul (1982)
Fabaceae	*Albizia julibrissin*	70.21	NR	B	S	Chang et al. (2012)
	Cytisus sp.	27	NR	B	S	Owen et al. (1997)
	Dioclea guianensis	NR	43	L	D	Keller and Lerdau (1999)
	Dussia munda	NR	30.7	L	D	Lerdau and Throop (1999)
	Genista scorpius	11	NR	B	S	Owen et al. (1998)
	Lonchocarpus longifolium	NR	53	L	D	Lerdau and Throop (1999)
	Pictetia aculute	NR	50	L	D	Lerdau and Keller (1997)
	Robinia pseudoacacia	151	45	L	D	Geron et al. (2001)
	Robinia pseudoacacia	17.8	NR	B	S	Khedive et al. (2016)
	Spartium junceum	6.4	NR	B	S	Owen et al. (1997)
Fagaceae	*Quercus acuta*	NR	0	L	S	Tani and Kawawata (2008)
	Quercus acutissima	NR	0	L	S	Tani and Kawawata (2008)
	Quercus agrifolia	77	50	L	D	Geron et al. (2001)
	Quercus agrifolia	35.3	NR	B	S	Winer et al. (1983)
	Quercus aliena	NR	18.3	L	S	Tani and Kawawata (2008)
	Quercus alba	NR	48	L	D	Fall and Monson (1992)
	Quercus alba	125	79	L	D	Geron et al. (1997)
	Quercus alba	99	NR	L	S	Harley et al. (1997)
	Quercus alba	7.8	NR	B	S	Lamb et al. (1983)
	Quercus alba	78	28	L	D	Litvak et al. (1996)
	Quercus alba	NR	33	L	S	Sharkey et al. (1991)
	Quercus alba	92	50	L	D	Geron et al. (2001)
	Quercus berberidifolia	73	51	L	D	Geron et al. (2001)
	Quercus borealis	19.7	NR	P	D	Evans et al. (1982)
	Quercus borealis	40.4	NR	B	S	Flyckt (1979)
	Quercus chrysolepis	48	93	L	D	Geron et al. (2001)
	Quercus coccinea	115	NR	L	S	Harley et al. (1997)
	Quercus coccinea	20.1	NR	B	S	Lamb et al. (1983)
	Quercus dentate	NR	30	L	S	Tani and Kawawata (2008)
	Quercus douglasii	71	41	L	D	Geron et al. (2001)
	Quercus dumosa	5.2	NR	B	S	Arey et al. (1995)
	Quercus dumosa	54.4	NR	B	S	Winer et al. (1983)

Table 1-1 (Continued)

Family	Species	Isoprene emission		*E*	*N*	Reference
		μg g^{-1} h^{-1}	nmol m^{-2} s^{-1}			
Fagaceae	*Quercus engelmannii*	39	27	L	D	Geron et al. (2001)
	Quercus falcata	112	57	L	D	Geron et al. (2001)
	Quercus frainetto	133.95	30.72	B	S	Steinbrecher et al. (1997)
	Quercus garryana	59.2	NR	B	S	Lamb et al. (1986)
	Quercus gambelii	121	NR	L	S	Guenther et al. (1996b)
	Quercus gambelii	132	NR	L	D	Harley et al. (1996)
	Quercus glauca	NR	0	L	S	Tani and Kawawata (2008)
	Quercus incana	45.6	NR	B	S	Zimmerman (1979)
	Quercus kelloggii	78	39	L	D	Geron et al. (2001)
	Quercus laevis	151	79	L	D	Geron et al. (2001)
	Quercus laevis	51	NR	L	S	Guenther et al. (1996a)
	Quercus laevis	24.3	NR	B	S	Zimmerman (1979)
	Quercus laurifolia	10.4	NR	B	S	Zimmerman (1979)
	Quercus lobata	86	39	L	D	Geron et al. (2001)
	Quercus lobata	3.4	NR	B	S	Winer et al. (1992)
	Quercus mongolica var. crispula	NR	27.3	L	S	Tani and Kawawata (2008)
	Quercus myrsinaefolia	NR	0	L	S	Tani and Kawawata (2008)
	Quercus myrtifolia	15.2	NR	B	S	Zimmerman (1979)
	Quercus nigra	81	46	L	D	Geron et al. (2001)
	Quercus nigra	24.6	NR	B	S	Zimmerman (1979)
	Quercus phellos	93	48	L	D	Geron et al. (2001)
	Quercus phellos	32.2	NR	B	S	Zimmerman (1979)
	Quercus prinus	44	23	L	D	Geron et al. (2001)
	Quercus prinus	71	NR	L	S	Harley et al. (1997)
	Quercus prinus	6.5	NR	B	S	Lamb et al. (1983)
	Quercus pubescens	78	NR	B	S	Owen et al. (1998)
	Quercus pubescens	90.73	16.68	B	S	Steinbrecher et al. (1997)
	Quercus robur	76.6	NR	B	S	Isidorov et al. (1985)
	Quercus rubra	67	30	L	D	Geron et al. (2001)
	Quercus rubra	112	NR	L	S	Isebrands et al. (1999)
	Quervus rubra	14.8	NR	B	S	Lamb et al. (1983)
	Quercus rubra	NR	38	L	D	Loreto and Sharkey (1990)
	Quercus rubra	77	43	L	D	Sharkey et al. (1996)
	Quercus salicina	NR	0	L	S	Tani and Kawawata (2008)
	Quercus serrata	NR	42.9	L	S	Okumura et al. (2008)
	Quercus serrata	NR	27.8	L	S	Tani and Kawawata (2008)

Table 1-1 (Continued)

Family	Species	Isoprene emission		*E*	*N*	Reference
		μg g^{-1} h^{-1}	nmol m^{-2} s^{-1}			
Fagaceae	*Quercus sessilifolia*	NR	0	L	S	Tani and Kawawata (2008)
	Quercus stellata	73	50	L	D	Geron et al. (2001)
	Quercus stellata	84	NR	L	S	Guenther et al. (1996a)
	Quercus variabilis	NR	0	L	S	Tani and Kawawata (2008)
	Quercus velutina	157	72	L	D	Geron et al. (2001)
	Quercus velutina	97	NR	L	S	Harley et al. (1997)
	Quercus velutina	18.9	NR	B	S	Lamb et al. (1983)
	Quercus virginiana	46	40	L	D	Geron et al. (2001)
	Quercus virginiana	30.9	NR	P	S	Tingey et al. (1979)
	Quercus virginiana	9.5	NR	B	S	Zimmerman (1979)
	Quercus wislizenii	12.5	NR	B	S	Arey et al. (1995)
	Quercus wislizenii	74	50	L	D	Geron et al. (2001)
Ginkgoaceae	*Ginkgo biloba*	0.34	NR	B	S	Chang et al. (2012)
	Ginkgo biloba	NED	NR	P	S	Corchonoy et al. (1992)
Juglandaceae	*Carya aquatica*	NED	NR	B	S	Zimmerman (1979)
	Juglans regia	NED	NR	B	S	Winer et al. (1992)
Lamiaceae	*Salvia mellifera*	0	NR	B	S	Arey et al. (1995)
	Salvia mellifera	BDL	NR	P	S	Winer et al. (1983)
Lauraceae	*Cinnamomum camphora*	4.31	NR	B	S	Chang et al. (2012)
	Cinnamomum camphora	NED	NR	P	S	Corchonoy et al. (1992)
	Cinnamomum camphora	NED	NR	B	S	Winer et al. (1983)
	Persea americana	BDL	NR	B	S	Winer et al. (1983)
	Persea borbonia	NED	NR	B	S	Zimmerman (1979)
Leguminosae	*Acacia farnesiana*	NED	NR	B	S	Zimmerman (1979)
	Cercis canadensis	0	NR	P	D	Evans et al. (1982)
	Glycine max	0	NR	P	D	Evans et al. (1982)
	Pueraria lobata	9.6	NR	P	D	Evans et al. (1982)
	Robinia pseudoacacia	13.5	NR	B	S	Lamb et al. (1983)
	Robinia pseudoacacia	10.1	NR	B	S	Winer et al. (1983)
Lythraceae	*Lagerstroemia indica*	NED	NR	P	S	Corchonoy et al. (1992)
	Lagerstroemia indica	NED	NR	B	S	Winer et al. (1983)
Magnoliaceae	*Liriodendron chinense*	0.11	NR	B	S	Chang et al. (2012)
	Liriodendron tulipifera	4.1	NR	B	S	Lamb et al. (1983)
	Magnolia grandiflora	0	NR	B	S	Chang et al. (2012)
	Magnolia grandiflora	BDL	NR	B	S	Winer et al. (1983)
Malvaceae	*Luehea seemanii*	NR	24	L	D	Keller and Lerdau (1999)

Table 1-1 (Continued)

Family	Species	Isoprene emission		*E*	*N*	Reference
		μg g^{-1} h^{-1}	nmol m^{-2} s^{-1}			
Malpighiaceae	*Stigmaphyllon hypargyreum*	NR	36	L	D	Keller and Lerdau (1999)
Menispermaceae	*Cissampelos pareira*	NR	28	L	D	Keller and Lerdau (1999)
Moraceae	*Brosimum utile*	NR	10.7	L	D	Lerdau and Throop (1999)
	Ficus fistulosa	27	NR	L	D	Cronn and Nutmagul (1982)
	Ficus insipida	NR	37	L	D	Keller and Lerdau (1999)
	Ficus nymphifolia	NR	3.9	L	D	Lerdau and Throop (1999)
	Ficus spp.	NR	16	L	D	Keller and Lerdau (1999)
	Morus rubra	NED	NR	B	S	Zimmerman (1979)
	Perebea xanthochyma	NR	14.7	L	D	Lerdau and Throop (1999)
Myristicaceae	*Virola spp.*	NR	13	L	D	Lerdau and Throop (1999)
Myrtaceae	*Callistemon citrinus*	16	NR	B	S	Winer et al. (1983)
	Eucalyptus botryoides	5.3	3.87	P	S	He et al. (2000)
	Eucalyptus calophylla	36.8	23.73	P	S	He et al. (2000)
	Eucalyptus camaldulensis	16.6	6.57	P	S	He et al. (2000)
	Eucalyptus citriodora	55.4	33.60	P	S	He et al. (2000)
	Eucalyptus cladocalyx	6.9	3.02	P	S	He et al. (2000)
	Eucalyptus forrestiana	40.6	35.23	P	S	He et al. (2000)
	Eucalyptus globulus	57	NR	P	D	Evans et al. (1982)
	Eucalyptus globulus	68.5	30.22	P	S	He et al. (2000)
	Eucalyptus gomphocephala	17.1	9.91	P	S	He et al. (2000)
	Eucalyptus grandis	61.1	22.71	P	S	He et al. (2000)
	Eucalyptus maculata	43	31.81	P	S	He et al. (2000)
	Eucalyptus marginata	29	26.30	P	S	He et al. (2000)
	Eucalyptus robusta	49.9	23.65	P	S	He et al. (2000)
	Eucalyptus rudis	61.4	38.78	P	S	He et al. (2000)
	Eucalyptus sargentii	28.5	25.89	P	S	He et al. (2000)
	Eucalyptus viminalis	8	NR	B	S	Winer et al. (1983)
	Eucalyptus wandoo	6	4.00	P	S	He et al. (2000)
	Eugenia grandis	12.1	NR	L	D	Cronn and Nutmagul (1982)
	Eugenia xerophytical	NR	45	L	D	Lerdau and Keller (1997)
	Myrtica cerifera	NED	NR	B	S	Zimmerman (1979)
	Myrtus communis	137	NR	B	S	Owen et al. (1997)
	Myrtus communis	25.2	NR	B	S	Hansen et al. (1997)
	Myrtus communis	34	NR	B	S	Winer et al. (1983)
	Rhamnus lycoides	22	NR	B	S	Owen et al. (1998)

Table 1-1 (Continued)

Family	Species	Isoprene emission		*E*	*N*	Reference
		μg g^{-1} h^{-1}	nmol m^{-2} s^{-1}			
Myrtaceae	*Ulex parvifolia*	22	NR	B	S	Owen et al. (1998)
Nyctaginaceae	*Pisonia albida*	NR	30	L	D	Lerdau and Keller (1997)
Nyssaceae	*Nyssa sylvatica*	77	30	L	D	Geron et al. (2001)
	Nyssa sylvatica	13	NR	L	S	Guenther et al. (1996a)
Oleaceae	*Fraxinus caroliniana*	NED	NR	B	S	Zimmerman (1979)
	Fraxinus uhdei	BDL	NR	B	S	Winer et al. (1983)
	Ligustrum lucidum	1.81	NR	B	S	Chang et al. (2012)
	Ligustrum lucidum	BDL	NR	B	S	Winer et al. (1983)
	Olea europaea	BDL	NR	B	S	Winer et al. (1983)
	Olea europaea	NED	NR	B	S	Winer et al. (1983)
	Osmanthus fragrans	0	NR	B	S	Chang et al. (2012)
Pinaceae	*Cedrus deodara*	NED	NR	P	S	Corchonoy et al. (1992)
	Cedrus deodara	BDL	NR	B	S	Winer et al. (1983)
	Picea engelmannii	16.3	NR	P	D	Evans et al. (1982)
	Picea sitchensis	4	NR	P	D	Evans et al. (1982)
	Pinus canariensis	NED	NR	P	S	Corchonoy et al. (1992)
	Pinus canariensis	BDL	NR	B	S	Winer et al. (1983)
	Pinus clausa	NED	NR	B	S	Zimmerman (1979)
	Pinus elliottii	0.11	NR	B	S	Chang et al. (2012)
	Pinus ellotii	NED	NR	P	D	Evans et al. (1982)
	Pinus ellotii	NED	NR	P	S	Tingey et al. (1979)
	Pinus ellotii	NED	NR	P	S	Tingey et al. (1980)
	Pinus ellotii	NED	NR	B	S	Zimmerman (1979)
	Pinus halepensis	NR	NR	P	S	Corchonoy et al. (1992)
	Pinus halepensis	BDL	NR	B	S	Winer et al. (1983)
	Pinus massoniana	0.45	NR	B	S	Chang et al. (2012)
	Pinus palustris	NED	NR	B	S	Zimmerman (1979)
	Pinus pinea	NED	NR	P	S	Corchonoy et al. (1992)
	Pinus pinea	BDL	NR	B	S	Winer et al. (1983)
	Pinus radiata	NED	NR	P	S	Corchonoy et al. (1992)
	Pinus radiata	BDL	NR	B	S	Winer et al. (1983)
	Pinus sylvestris	NED	NR	B	S	Isidorov et al. (1985)
	Pseudotsuga macrocarpa	0	NR	B	S	Arey et al. (1995)
Pittosporaceae	*Pittosporum tobira*	BDL	NR	B	S	Winer et al. (1983)
	Pittosporum undulatum	BDL	NR	B	S	Winer et al. (1983)

Table 1-1 (Continued)

Family	Species	Isoprene emission		*E*	*N*	Reference
		μg g^{-1} h^{-1}	nmol m^{-2} s^{-1}			
Platanaceae	*Platanus acerifolia*	10.1	NR	B	S	Chang et al. (2012)
	Platanus occidentalis	27.5	NR	P	D	Evans et al. (1982)
	Platanus occidentalis	71	22	L	D	Geron et al. (2001)
	Platanus orientalis	45	NR	B	S	Khedive et al. (2016)
	Platanus racemosa	10.9	NR	B	S	Winer et al. (1983)
Poaceae	*Arundo donax*	140	NR	B	S	Owen et al. (1998)
	Bambusa oldhamii	NR	99.1	L	S	Okumura et al. (2018)
	Bambusa multiplex	NR	62.4	L	S	Okumura et al. (2018)
	Chimonobambusa quadrangularis	NR	NED	L	S	Okumura et al. (2018)
	Phyllostachys pubescens	116.15	NR	B	S	Chang et al. (2012)
	Phyllostachys pubescens	NR	51.1	L	S	Okumura et al. (2018)
	Phyllostachys bambusoides	NR	48	L	S	Okumura et al. (2018)
	Phyllostachys nigra var. henonis	NR	11.6	L	S	Okumura et al. (2018)
	Phyllostachys aurea	NR	57.4	L	S	Okumura et al. (2018)
	Pleioblastus hindsii	36.64	NR	B	S	Chang et al. (2012)
	Pleioblastus simonii	NR	0.7	L	S	Okumura et al. (2018)
	Pseudosasa japonica	NR	1	L	S	Okumura et al. (2018)
	Sasa veitchii	NR	NED	L	S	Okumura et al. (2018)
	Sasa kurilensis	NR	24	L	S	Okumura et al. (2018)
	Semiarundinaria fastuosa	NR	57.8	L	S	Okumura et al. (2018)
	Semiarundinaria yashadake	NR	53.6	L	S	Okumura et al. (2018)
	Sinobambusa tootsik	NR	36.6	L	S	Okumura et al. (2018)
Podocarpaceae	*Podocarpus gracilior*	BDL	NR	B	S	Winer et al. (1983)
Polygonaceae	*Eriogonum fasciculatum*	BDL	NR	P	S	Winer et al. (1983)
Polypodiaceae	*Thelypteris decursivepinnata*	24.5	NR	P	D	Evans et al. (1982)
Rhamnaceae	*Ceanothus crassifolius*	BDL	NR	B	S	Winer et al. (1983)
	Ceanothus leucodermis	NED	NR	B	S	Winer et al. (1983)
	Ceanothus spinosus	0	NR	B	S	Arey et al. (1995)
	Krugiodendron ferreum	NR	30	L	D	Lerdau and Keller (1997)
	Reynosia guama	NR	100	L	D	Lerdau and Keller (1997)
	Rhamnus californica	29.3	NR	P	D	Evans et al. (1982)
	Rhamnus crocea	54.4	NR	B	S	Winer et al. (1983)

Table 1-1 (Continued)

Family	Species	Isoprene emission		*E*	*N*	Reference
		$\mu g\ g^{-1}\ h^{-1}$	$nmol\ m^{-2}\ s^{-1}$			
Rosaceae	*Adenostoma fasciculatum*	NED	NR	B	S	Arey et al. (1995)
	Adenostoma fasciculatum	NED	NR	B	S	Winer et al. (1983)
	Adenostoma fasciculatum	NED	NR	B	S	Winer et al. (1992)
	Cercocarpus betuloides	NED	NR	B	S	Arey et al. (1995)
	Cotoneaster pannosus	BDL	NR	B	S	Winer et al. (1992)
	Prunus armeniaca	NED	NR	B	S	Winer et al. (1992)
	Prunus avium	NED	NR	B	S	Winer et al. (1992)
	Prunus domestica	NED	NR	B	S	Winer et al. (1992)
	Prunus dulcis	NED	NR	B	S	Winer et al. (1992)
	Prunus persica	NED	NR	B	S	Winer et al. (1992)
	Pyrus kawakamii	BDL	NR	B	S	Winer et al. (1983)
	Rhaphiolepis indica	BDL	NR	B	S	Winer et al. (1983)
Rutaceae	*Citrus limon*	NED	NR	B	S	Winer et al. (1989)
	Citrus limon 'Meyer'	BDL	NR	B	S	Winer et al. (1983)
	Citrus sinensis	NED	NR	B	S	Winer et al. (1992)
	Citrus sinensis 'Valencia'	NED	NR	B	S	Winer et al. (1992)
Salicaceae	*Populus deltoides*	37	NR	P	D	Evans et al. (1982)
	Populus deltoides	97	43	L	D	Geron et al. (2001)
	Populus euroamericana	153	NR	L	S	Isebrands et al. (1999)
	Populus fremontii	NR	74	L	D	Fall and Monson (1992)
	Populus nigra	63	NR	B	S	Owen et al. (1998)
	Populus tremula	45	NR	B	S	Hakola et al. (1998)
	Populus tremuloides	50.2	NR	P	D	Evans et al. (1982)
	Populus tremuloides	78	NR	L	S	Isebrands et al. (1999)
	Populus tremuloides	165	59	L	D	Litvak et al. (1996)
	Populus tremuloides	NR	68	L	S	Sharkey et al. (1991)
	Populus trichocarpa	97	44	L	D	Geron et al. (2001)
	Salix babylonica	133.05	NR	B	S	Chang et al. (2012)
	Salix babylonica	115	NR	B	S	Winer et al. (1983)
	Salix caroliniana	12.5	NR	B	S	Zimmerman (1979)
	Salix discolor	91	NR	L	S	Isebrands et al. (1999)
	Salix humulis	41	NR	L	S	Isebrands et al. (1999)
	Salix petiolaris	102	NR	L	S	Isebrands et al. (1999)
	Salix phylicifolia	50	NR	B	S	Hakola et al. (1998)
	Salix nigra	25.2	NR	P	D	Evans et al. (1982)
	Salix nigra	93	37	L	D	Geron et al. (2001)
	Salix subsericea	57	NR	L	S	Isebrands et al. (1999)

Table 1-1 (Continued)

Family	Species	Isoprene emission		*E*	*N*	Reference
		$\mu g\ g^{-1}\ h^{-1}$	$nmol\ m^{-2}\ s^{-1}$			
Sapindaceae	*Cupaniopsis anacardioides*	50.9	NR	P	S	Corchonoy et al. (1992)
	Koelreuteria integrifolia	0.09	NR	B	S	Chang et al. (2012)
Taxodiaceae	*Taxodium sp.*	NED	NR	B	S	Zimmerman (1979)
Thymelaeaceae	*Edgeworthia chrysantha*	NR	7.3	L	S	Tani and Fushimi (2005)
Ulmaceae	*Ulmus americana*	BDL	NR	B	S	Winer et al. (1983)
	Ulmus americana	NED	NR	B	S	Zimmerman (1979)
	Ulmus parcifolia	BDL	NR	B	S	Winer et al. (1983)

1.3. Expansion of Bamboo Species in Eastern Asia

Bamboos belong to the Bambusoideae subfamily, comprising over 1500 species with highly diverse growth traits (Kleinhenz and Midmore, 2001; Clark et al., 2015). In Japan, bamboo includes two major subtribe classifications: Arundinariinae and Shibataeinae. Shibataeinae includes species with woody culms, and Arundinariinae is composed of both woody and dwarf bamboos. Shibataeinae is believed to have originated from tropical, subtropical, or warm-temperate climatic regions of China, later imported and adapted in Japan, while Arundinariinae originated from warm-temperate to temperate regions in Japan. Bamboos grow in diverse habitats; even different species within a genus might originate from different climates (e.g., *Pleioblastus hindsii* from subtropical regions; *Pleioblastus chino* from temperate regions), which implies different degrees of heat stress. Additionally, the two subtribes of bamboos grow in different niches, where dwarf bamboos usually grow in more shaded environments than woody species.

Bamboo forests are important components of ecosystems, accounting for 3.2 % (36.8 million hectares) of the global forest area, and occupy 23.6 million hectares in Asia (Lobovikov et al., 2007). Currently, several bamboo species, regardless of growth type, have invaded multiple regions (Okutomi et al., 1996; Torii, 2003; Chiou et al., 2009; Kudo et al., 2011; Takada et al., 2012). In Japan, a nonnative bamboo (i.e., *P. pubescens*) that is used for agriculture, has been reported to spread to the neighboring forests owing to mismanagement and abandonment (Torii, 2003; Song et al., 2011). The forest coverage of *P. pubescens* increased from 24 km^2 to 174 km^2 between 1953 and 1985 in Kyoto, Japan (Okutomi et al., 1996); *P. pubescens* forest area has been reported to increase from 21.6 hectare to 42.4 hectare between 1967 and 1985 in Mount Hachiman, Shiga Prefecture (Suzuki, 2015). Fast growth, shade tolerance of sprouts, and horizontally running rhizomes enable this bamboo to replace other forest trees (Wang and Kao, 1986; Yen et al., 2010; Wang et al., 2016). According to ecological niche simulations, bamboos, including *P. pubescens*, will expand greatly in the future owing to global warming, invading the northern or mountainous areas (Takano et al., 2017; Song et al., 2013). This rapid bamboo expansion has raised concerns on its impact on regional biodiversity and carbon and water cycles.

1.4. Objectives and Outline

Understanding isoprene emission dynamics can provide critical information on mitigating its negative effects. Regional isoprene emission patterns may be altered if the invading bamboo has isoprene emission characteristics different from the original vegetation. Since several bamboo species have been shown to have high potential isoprene emission rates, there is a critical need to evaluate their isoprene emission fluxes. However, to estimate isoprene emission from bamboo leaves, using the current empirical model, the dependence of isoprene emission flux on temperature and light intensity needs to be examined since there is a lack of observations with regard to bamboo species. Furthermore, owing to high heterogeneities in emission flux among the leaves of a single species, it becomes difficult to define a representative emission flux for the current empirical model. Although, traditionally, an empirical model can obtain a statistically representative value of isoprene emission flux by observing a certain number of samples, the current knowledge of isoprene emission controllers can help determine representative isoprene emission flux with more process-based senses. For example, the basal isoprene emission flux can be deemed as a function of controller variables such as electron transport rate (ETR). This will allow a more reliable and economical way to determine the emission flux, instead of conducting massive examination of the basal isoprene emissions. This study aims to observe isoprene emissions from bamboo species and verify the potential effects of morphology and physiological state, at leaf-scale, on isoprene biosynthesis in bamboo species.

In the following chapters, I describe my research on characterizing isoprene emission fluxes of bamboo species by field measurements of isoprene emission flux of bamboo leaves of different species and recording the meteorological, morphological, and physiological variables to verify their potential influences on isoprene emission fluxes.

Chapter 2 discusses the response of leaf isoprene emission flux to leaf temperature and light intensity, for a woody bamboo species (*Phyllostachys pubescens*), to validate the reproducibility of the isoprene emission model of Guenther et al. (1993) and to determine whether there is a need to formulate a parameter set for woody bamboo. Since the default parameters in the model were obtained from trees of North America, it might not be suitable for evaluating emissions from bamboo leaves.

From the isoprene emission data for bamboo leaves, I intend to find the potential factors controlling the isoprene emission capacity. In Chapter 3, I propose the hypothesis that leaf morphology (i.e., leaf mass per area; LMA) can influence isoprene emission capacity and cause inter-leaf variation. To test this hypothesis, I selected a hillslope, that had a high morphological diversity of *P. pubescens* culms, to measure isoprene emissions under constant environmental conditions and compare the results with those of other sites.

Chapter 4 documents the tests on the potential effects of the factors confirmed in the last two chapters and an additional factor (i.e., ETR) for 18 bamboo species within 5 genera in different niches to verify (1) whether there is a distinction of isoprene emission traits among bamboo species, and if so, (2) whether the differences could be explained by the potential factors.

Finally, Chapter 5 summarizes the results from each of the preceding chapters to present the conclusions of this study. With measurements for multiple sites and bamboo species, this study can provide useful data for expanding the database of BVOC emissions from bamboo leaves and enable a better understanding of the characteristics of isoprene emissions from bamboo species. This will help in the efforts to better estimate global BVOC emissions.

Reference

Archibald AT, Levine JG, Abraham NL, Cooke MC, Edwards PM, Heard DE, Jenkin ME, Karunaharan A, Pike RC, Monks PS, Shallcross DE, Telford PJ, Whalley LK, Pyle JA (2011) Impacts of HOx regeneration and recycling in the oxidation of isoprene: Consequences for the composition of past, present and future atmospheres. *Geophysical Research Letters* 38 (5):L05804. https://doi.org/10.1029/2010GL046520

Arey J, Crowley DE, Crowley M, Resketo M, Lester J (1995) Hydrocarbon emissions from natural vegetation in California's South Coast Air Basin. *Atmospheric Environment* 29 (21):2977-2988. https://doi.org/10.1016/1352-2310(95)00137-N

Behnke K, Kaiser A, Zimmer I, Brüggemann N, Janz D, Polle A, Hampp R, Hänsch R, Popko J, Schmitt-Kopplin P, Ehlting B, Rennenberg H, Barta C, Loreto F, Schnitzler J (2010) RNAi-mediated suppression of isoprene emission in poplar transiently impacts phenolic metabolism under high temperature and high light intensities: a transcriptomic and metabolomic analysis. *Plant Molecular Biology* 74 (1):61-75. https://doi.org/10.1007/s11103-010-9654-z

Biesenthal TA, Wu Q, Shepson PB, Wiebe HA, Anlauf KG, Mackay GI (1997) A study of relationships between isoprene, its oxidation products, and ozone, in the Lower Fraser Valley, BC. *Atmospheric Environment* 31 (14):2049-2058. https://doi.org/10.1016/S1352-2310(96)00318-4

Brüggemann N, Schnitzler J-P (2002) Diurnal variation of dimethylallyl diphosphate concentrations in oak (*Quercus robur*) leaves. *Physiologia Plantarum* 115 (2): 190-196. https://doi.org/10.1034/j.1399-3054.2002.1150203.x

Chang J, Ren Y, Shi Y, Zhu Y, Ge Y, Hong S, iao L, Lin F, Peng C, Mochizuki T, Tani A, Mu Y, Fu C (2012) An inventory of biogenic volatile organic compounds for a subtropical urban–rural complex. *Atmospheric Environment* 56:115-123. https://doi.org/10.1016/j.atmosenv.2012.03.053

Chapin FS, McFarland J, McGuire AD, Euskirchen ES, Ruess RW, Kielland K (2009) The changing global carbon cycle: Linking plant-soil carbon dynamics to global consequences. *Journal of Ecology* 97:840-850. https://doi.org/10.1111/j.1365-2745.2009.01529.x

Chiou C, Chen T, Lin Y, Yang Y, Lin S (2009) Distribution and Change Analysis of Bamboo Forest in Northern Taiwan. *Quarterly Journal of Chinese Forestry* 42 (1):89-105. http://dx.doi.org/10.30064%2fQJCF.200903.0006

Claeys M, Graham B, Vas G, Wang W, Vermeylen R, Pashynska V, Cafmeyer J. Guyon P, Andreae MO, Artaxo P, Maenhaut W, (2004a) Formation of Secondary Organic Aerosols Through Photooxidation of Isoprene. *Science* 303 (5661):1173-1176. https://doi.org/10.1126/science.1092805

Claeys M, Wang W, Ion AC, Kourtchev I, Gelencsér A, Maenhaut W (2004b) Formation of secondary organic aerosols from isoprene and its gas-phase oxidation products through reaction with hydrogen peroxide. *Atmospheric Environment* 38 (25):4093-4098. https://doi.org/10.1016/j.atmosenv.2004.06.001

Clark LG, Londoño X, Ruiz-Sanchez E (2015) Bamboo Taxonomy and Habitat. In Liese, Walter and Köhl, Michael, (Eds.)., Bamboo: The Plant and its Uses (1-30). *Springer International Publishing*. https://doi.org/10.1007/978-3-319-14133-6_1

Collins WJ, Derwent RG, Johnson CE, Stevenson DS (2002) The Oxidation of Organic Compounds in the Troposphere and their Global Warming Potentials. *Climatic Change* 52 (4):453-479. https://doi.org/10.1023/A:1014221225434

Corchnoy SB, Arey J, Atkinson R (1992) Hydrocarbon emissions from twelve urban shade trees of the Los Angeles, California, Air Basin. *Atmospheric Environment* 26 (3):339-348. https://doi.org/10.1016/0957-1272(92)90009-H

Cronn DR, Nutmagul W (1982) Analysis of atmospheric hydrocarbons during winter MONEX. *Tellus* 34 (2):159-165. https://doi.org/10.3402/tellusa.v34i2.10798

Dreyfus GB, Schade GW, Goldstein AH (2002) Observational constraints on the contribution of isoprene oxidation to ozone production on the western slope of the Sierra Nevada, California. *Journal of Geophysical Research* 107 (D19):4365. https://doi.org/10.1029/2001JD001490

Duane M, Poma B, Rembges D, Astorga C, Larsen BR (2002) Isoprene and its degradation products as strong ozone precursors in Insubria, Northern Italy. *Atmospheric Environment* 36 (24):3867-3879. https://doi.org/10.1016/S1352-2310(02)00359-X

Evans RC, Tingey DT, Gumpertz ML, Burns WF (1982) Estimates of Isoprene and Monoterpene Emission Rates in Plants. *Botanical Gazette* 143 (3):304-310. https://doi.org/10.1086/botanicalgazette.143.3.2474826

Fall R, Monson RK (1992) Isoprene emission rate and intercellular isoprene concentration as influenced by stomatal distribution and conductance. *Plant Physiology* 100 (2):987-992. https://doi.org/10.1104/pp.100.2.987

Fehsenfeld F, Calvert J, Fall R, Goldan P, Guenther AB, Hewitt CN, Lamb B, Liu S, Trainer M, Westberg H, Zimmerman P (1992) Emissions of volatile organic compounds from vegetation and the implications for atmospheric chemistry. *Global Biogeochemical Cycles* 6 (4):389-430. https://doi.org/10.1029/92GB02125

Fierravanti A, Fierravanti E, Cocozza C, Tognetti R, Rossi S (2017) Eligible reference cities in relation to BVOC-derived O_3 pollution. *Urban Forestry & Urban Greening* 28:73-80. https://doi.org/10.1016/j.ufug.2017.09.012

Flyckt DL (1979) Seasonal variation in the volatile hydrocarbon emissions from ponderosa pine and red oak. M.S.thesis, Washington State University, Pullman, Washington, U.S.A.

Geron C, Nie D, Arnts RR, Sharkey TD, Singsaas EL, Vanderveer PJ, Guenther A, Sickles JE, Kleindienst TE (1997) Biogenic isoprene emission: model evaluation in a southeastern United States bottomland deciduous forest. *Journal of Geophysical Research* 102 (D15):18889-18901. https://doi.org/10.1029/97JD00968

Geron C, Harley P, Guenther A (2001) Isoprene emission capacity for US tree species. *Atmospheric Environment* 35 (19):3341-3352. https://doi.org/10.1016/S1352-2310(00)00407-6

Geng F, Tie X, Guenther A, Li G, Cao J, Harley P (2011) Effect of isoprene emissions from major forests on ozone formation in the city of Shanghai, China. *Atmospheric Chemistry and Physics* 11 (20):10449-10459. https://doi.org/10.5194/acp-11-10449-2011

Guenther AB, Monson RK, Fall R (1991) Isoprene and monoterpene emission rate variability: Observations with eucalyptus and emission rate algorithm development. *Journal of Geophysical Research* 96 (D6):10799-10808. https://doi.org/10.1029/91JD00960

Guenther AB, Zimmerman PR, Harley PC, Monson RK, Fall R (1993) Isoprene and monoterpene emission rate variability: Model evaluations and sensitivity analyses. *Journal of Geophysical Research* 98 (D7):12609-12617. https://doi.org/10.1029/93JD00527

Guenther A, Zimmerman PR, Klinger L, Greenberg JP, Ennis C, Davis K, Pollock W, Westberg H, Allwine G, Geron CD (1996a) Estimates of regional natural volatile organic compound fluxes from enclosure and ambient measurements. *Journal of Geophysical Research* 101 (D1):1345-1359. https://doi.org/10.1029/95JD03006

Guenther A, Greenberg JP, Harley P, Helmig D, Klinger L, Vierling L, Zimmerman PR, Geron C (1996b) Leaf, branch, stand and landscape scale measurements of volatile organic compound fluxes from US woodlands. *Tree Physiology* 16 (1-2):17-24. https://doi.org/10.1093/treephys/16.1-2.17

Guenther A (2002) The contribution of reactive carbon emission from vegetation to the carbon balance of terrestrial ecosystems. *Chemosphere* 49 (8):837-844. https://doi.org/10.1016/S0045-6535(02)00384-3

Guenther A, Karl T, Harley P, Wiedinmyer C, Palmer PI, Geron C (2006) Estimates of global terrestrial isoprene emissions using MEGAN (Model of Emissions of Gases and Aerosols from Nature). *Atmospheric Chemistry and Physics* 6 (11):3181-3210. https://doi.org/10.5194/acp-6-3181-2006

Guenther AB. Jiang X. Heald Colette L, Sakulyanontvittaya T, Duhl T, Emmons LK, Wang X (2012) The Model of Emissions of Gases and Aerosols from Nature Version 2.1 (MEGAN2.1): An Extended and Updated Framework for Modeling Biogenic Emissions. *Geoscientific Model Development* 5 (6):1471–1492.

Hakola H, Rinne J, Laurila T (1998) The hydrocarbon emission rates of tea-leafed willow (*Salix phylicifolia*), silver birch (*Betula pendula*) and European aspen (*Populus tremula*). *Atmospheric Environment* 32:1825-1833. https://doi.org/10.1016/S1352-2310(97)00482-2

Harley P, Deem G, Flint S, Caldwell M (1996) Effects of growth under elevated UV-B on photosynthesis and isoprene emission in *Quercus gambelii* and *Mucuna pruriens*. *Global Change in Biosphere* 2 (2):101-106. https://doi.org/10.1111/j.1365-2486.1996.tb00060.x

Harley P, Guenther A, Zimmerman P (1997) Environmental controls over isoprene emission in deciduous oak canopies. *Tree Physiology* 17 (11):705-14. https://doi.org/10.1093/treephys/17.11.705

Harley PC, Monson RK, Lerdau MT (1999) Ecological and evolutionary aspects of isoprene emission from plants. *Oecologia* 118 (2):109-123. https://doi.org/10.1007/s004420050709

Harvey CM, Sharkey TD (2016) Exogenous isoprene modulates gene expression in unstressed Arabidopsis thaliana plants. *Plant, Cell & Environment* 39 (6):1251-1263. https://doi.org/10.1111/pce.12660

Hansen U, Van Eijk J, Bertin N, Staudt M, Kotzias D, Seufert G, Fugit JL, Torres L, Cecinato A, Brancaleoni E, Ciccioli P, Bomboi T (1997) Biogenic emissions and CO2 gas exchange investigated on four Mediterranean shrubs. *Atmospheric Environment* 31:157-166. https://doi.org/10.1016/S1352-2310(97)00082-4

He C, Murray F, Lyons T (2000) Monoterpene and isoprene emissions from 15 *Eucalyptus* species in Australia. *Atmospheric Environment* 34 (4):645-655. https://doi.org/10.1016/S1352-2310(99)00219-8

Isebrands JG, Guenther AB, Harley P, Helmig D, Klinger L, Vierling L, Zimmerman P, Geron C (1999) Volatile organic compound emission rates from mixed deciduous and coniferous forests in Northern Wisconsin, USA. *Atmospheric Environment* 33 (16):2527-2536. https://doi.org/10.1016/S1352-2310(98)00250-7

Isidorov VA, Zenkevich IG, Ioffe BV (1985) Volatile organic compounds in the atmosphere of forests. *Atmospheric Environment* 19 (1):1-8 https://doi.org/10.1016/0004-6981(85)90131-3

Jiang X, Guenther A, Potosnak M, Geron C, Seco R, Karl T (2018) Isoprene emission response to drought and the impact on global atmospheric chemistry. *Atmospheric Environment* 183:69-83. https://doi.org/10.1016/j.atmosenv.2018.01.026.

Kansal A (2009) Sources and reactivity of NMHCs and VOCs in the atmosphere: A review. *Journal of Hazardous Materials* 166 (1):17-26. https://doi.org/10.1016/j.jhazmat.2008.11.048

Kamens RM, Gery MW, Jeffries HE, Jackson M, Cole EI (1982) Ozone–isoprene reactions: Product formation and aerosol potential. *International Journal of Chemical Kinetics* 14:955-975. https://doi.org/10.1002/kin.550140902

Kanakidou M, Seinfeld JH, Pandis SN, Barnes I, Dentener FJ, Facchini MC, Van Dingenen R, Ervens B, Nenes A, Nielsen CJ, Swietlicki E, Putaud JP, Balkanski Y, Fuzzi S, Horth J, Moortgat GK, Winterhalter R, Myhre CEL, Tsigaridis K, Vignati E, Stephanou EG, Wilson J (2005) Organic aerosol and global climate modelling: a review. *Atmospheric Chemistry and Physics* 5 (4):1053-1123. https://doi.org/10.5194/acp-5-1053-2005

Keller M, Lerdau M (1999) Isoprene emission from tropical forest canopy leaves. *Global Biochemical Cycles* 13 (1):19-29. https://doi.org/10.1029/1998GB900007

Khedive E, Shirvany A, Assareh MH, Sharkey TD (2017) In situ emission of BVOCs by three urban woody species. *Urban Forestry & Urban Greening* 21:157-157. https://doi.org/10.1016/j.ufug.2016.11.018

Kleinhenz V, Midmore DJ (2001) Aspects of Bamboo Agronomy. *Advances in Agronomy* 74:99-153. https://doi.org/10.1016/S0065-2113(01)74032-1

Kroll JH, Ng NL, Murphy SM, Flagan RC, Seinfeld JH (2005) Secondary organic aerosol formation from isoprene photooxidation under high-NO_x conditions. *Geophysical Research Letters* 32:L18808. https://doi.org/10.1029/2005GL023637

Kroll JH, Ng NL, Murphy SM, Flagan RC, Seinfeld JH (2006) Secondary organic aerosol formation from isoprenephotooxidation. *Environmental Science & Technology* 40:1869-1877. https://doi.org/10.1021/es0524301

Kudo G, Amagai Y, Hoshino B, Kaneko M (2011) Invasion of dwarf bamboo into alpine snow-meadows in northern Japan: pattern of expansion and impact on species diversity. *Ecology and Evolution* 1:85-96. https://doi.org/10.1002/ece3.9

Lamb B, Westberg H, Quarles T, Flyckt D (1983) Natural hydrocarbon emission rate measurements from vegetation in Pennsylvania and Washington. Report PB84-124981, US. Environmental Protection Agency, National Technical Information Service. Springfield, Virginia, U.S.A.

Lamb B, Westberg H, Allwine G (1986) Isoprene emission fluxes determined by an atmospheric tracer techniquE. *Atmospheric Environment* 20 (1):1-8. https://doi.org/10.1016/0004-6981(86)90201-5

Lerdau M, Keller M (1997) Controls on isoprene emission from trees in a subtropical dry forest. *Plant, Cell and Environment* 20 (5):569-578. https://doi.org/10.1111/j.1365-3040.1997.00075.x

Lerdau M, Throop H (1999) Isoprene emission and photosynthesis in a tropical forest canopy: implications for model development. *Ecological Applications* 9 (4):1109-1117. https://doi.org/10.2307/2641381

Lichtenthaler HK (1999) The 1-deoxy-D-xylulose-5-phosphate pathway of isoprenoid biosynthesis in plants. *Annual Review of Plant Physiology and Plant Molecular Biology* J50:47-65. https://doi.org/10.1146/annurev.arplant.50.1.47

Litvak ME, Loreto F, Harley PC, Sharkey TD, Monson RK (1996) The response of isoprene emission rate and photosynthetic rate to photon flux and nitrogen supply in aspen and white oak trees. *Plant, Cell & Environment* 19 (5):549-559. https://doi.org/10.1111/j.1365-3040.1996.tb00388.x

Lobovikov M, Paudel S, Piazza M, Wu HR (2007) World Bamboo Resources - A Thematic Study Prepared in the Framework of the Global Forest Resources Assessment 2005. Food and Agriculture Organization of The United Nations, Rome. https://doi.org/10.13140/RG.2.1.1042.3764}

Loreto F, Sharkey TD (1990) A gas-exchange study of photosynthesis and isoprene emission in *Quercus rubra* L. *Planta* 182 (4):523-531. https://doi.org/10.1007/BF02341027

Loreto F, Velikova V (2001) Isoprene Produced by Leaves Protects the Photosynthetic Apparatus against Ozone Damage, Quenches Ozone Products, and Reduces Lipid Peroxidation of Cellular Membranes. *Plant Physiology* 127 (4):1781-1787. https://doi.org/10.1104/pp.010497

Loreto F, Mannozzi M, Maris C, Nascetti P, Ferranti F, Pasqualini S (2001) Ozone Quenching Properties of Isoprene and Its Antioxidant Role in Leaves. *Plant Physiology* 126 (3):993-1000. https://doi.org/10.1104/pp.126.3.993

Luyssaert S, Inglima I, Jung M, Richardson AD, Reichstein M, Papale D, Piao SL, Schulze D, Wingate L, Matteucci G, Aragao L, Aubinet M, Beer C, Bernhofer C, Black KG, Bonal D, Bonnefond J-M, Chambers J, Ciais P, Cook B, Davis KJ, Dolman AJ, Gielen B, Goulden M, Grace J, Granier A, Grelle A, Griffis T, Grünwald T, Guidolotti G, Hanson PJ, Harding R, Hollinger DY, Hutyra LR, Kolari P, Kruijt B, Kutsch W, Lagergren F, Laurila T, Law BE, Le Maire G, Lindroth A, Loustau D, Malhi Y, Mateus J, Migliavacca M, Misson L, Montagnani L, Moncrieff J, Moors E, Munger JW, Nikinmaa E, Ollinger SV, Pita G, Rebmann C, Roupsard O, Saigusa N, Sanz MJ, Seufert G, Sierra C, Smith ML, Tang J, Valentini R, Vesala T, Janssens IA (2007) CO_2 balance of boreal, temperate, and tropical forests derived from a global database. *Global Change Biology* 13 (12):2509-2537. https://doi.org/10.1111/j.1365-2486.2007.01439.x

Niinemets Ü, Reichstein M (2002) A model analysis of the effects of nonspecific monoterpenoid storage in leaf tissues on emission kinetics and composition in Mediterranean sclerophyllous *Quercus* species. *Global Biogeochemical Cycles* 16 (4):1110. https://doi.org/10.1029/2002GB001927

Martin MJ, Stirling CM, Humphries SW, Long SP (2000) A process-based model to predict the effects of climatic change on leaf isoprene emission rates. *Ecological Modelling* 131 (2–3):161-174. https://doi.org/10.1016/S0304-3800(00)00258-1.

Middleton P (1995) Sources of air pollutants. In: Singh HB (ed) Composition, Chemistry, and Climate of the Atmosphere. *Van Nostrand Reinhold*, New York, pp 88-119

Monson RK, Jones RT, Rosenstiel TN, Schnitzler J-P (2013) Why only some plants emit isoprene. *Plant, Cell & Environment* 36:503-516. https://doi.org/10.1111/pce.12015

Morfopoulos C, Sperlich D, Peñuelas J, Filella I, Llusià J, Medlyn BE, Niinemets Ü, Possell M, Sun Z, Prentice IC (2014) A model of plant isoprene emission based on available reducing power captures responses to atmospheric CO_2. *New Phytologist*, 203 (1): 125-139. https://doi.org/10.1111/nph.12770

Oku H, Inafuku M, Takamine T, Nagamine M, Saitoh S, Fukuta M (2014) Temperature threshold of isoprene emission from tropical trees, *Ficus virgata* and *Ficus septica*. *Chemosphere* 95:268-273. https://doi.org/10.1016/j.chemosphere.2013.09.003

Okumura M, Tani A, Kominami Y, Takanashi S, Kosugi Y, Miyama T, Tohno S (2008) Isoprene emission characteristics of *Quercus serrata* in a deciduous broad-leaved forest. *Journal Agricultural Meteorology* 64 (2):49-60. https://doi.org/10.2480/agrmet.64.49

Okumura M, Kosugi Y, Tani A (2018) Biogenic volatile organic compound emissions from bamboo species in Japan. *Journal of Agricultural Meteorology* 74 (1):40-44. https://doi.org/10.2480/agrmet.D-17-00017

Okutomi K, Shinoda S, Fukuda H (1996) Causal analysis of the invasion of broad-leaved forest by bamboo in Japan. *Journal of Vegetation Science* 7 (5):723-728. https://doi.org/10.2307/3236383

Owen S, Boissard C, Street RA, Duckham SC, Csiky O, Hewitt CN (1997) Screening of 18 Mediterranean plant species for volatile organic compound emissions. *Atmospheric Environment* 31:101-117. https://doi.org/10.1016/S1352-2310(97)00078-2

Owen SM, Hagenlocher BB, Hewitt CN (1998) Field studies of isoprene emissions from vegetation in the northwest Mediterranean region. *Journal of Geophysical Research: Atmospheres* 103 (D19):25499-25511. https://doi.org/10.1029/98JD01817

Pang X, Mu Y, Zhang Y, Lee X, Yuan J (2009) Contribution of isoprene to formaldehyde and ozone formation based on its oxidation products measurement in Beijing, China. *Atmospheric Environment* 43 (13):2142-2147. https://doi.org/10.1016/j.atmosenv.2009.01.022.

Paulson SE, Flagan RC, Seinfeld JH (1992) Atmospheric photooxidation of isoprene part I: The hydroxyl radical and ground state atomic oxygen reactions. *International Journal of Chemical Kinetics* 24:79-101. https://doi.org/10.1002/kin.550240109

Paulson SE, Seinfeld JH (1992) Development and evaluation of a photooxidation mechanism for isoprene. *Journal of Geophysical Research* 97 (D18):20703-20715. https://doi.org/10.1029/92JD01914

Pike RC, Young PJ (2009) How plants can influence tropospheric chemistry: the role of isoprene emissions from the biosphere. *Weather* 64 (12):332-336. https://doi.org/10.1002/wea.416

Pollastri S, Tsonev T, Loreto F (2014) Isoprene improves photochemical efficiency and enhances heat dissipation in plants at physiological temperatures. *Journal of Experimental Botany* 65 (6):1565-1570. https://doi.org/10.1093/jxb/eru033

Poisson N, Kanakidou M, Crutzen PJ (2000) Impact of non-methane hydrocarbons on tropospheric chemistry and the oxidizing power of the global troposphere: 3-dimensional modelling results. *Journal of Atmospheric Chemistry* 36 (2):157-230. http://dx.doi.org/10.1023/A:1006300616544

Rasmussen RA, Jones CA (1973) Emission of isoprene from leaf discs of *Hamamelis*. *Phytochemistry* 12 (1):15-19. https://doi.org/10.1016/S0031-9422(00)84618-X

Rasulov B, Hüve K, Välbe M, Laisk A, Niinemets U (2009) Evidence that light, carbon dioxide, and oxygen dependencies of leaf isoprene emission are driven by energy status in hybrid aspen. *Plant Physiology* 151 (1):448-60. https://doi.org/10.1104/pp.109.141978

Rasulov B, Hüve K, Bichele I, Laisk A, Niinemets Ü (2010) Temperature response of isoprene emission in vivo reflects a combined effect of substrate limitations and isoprene synthase activity: A kinetic analysis. *Plant Physiology* 154 (3):1558-1570. https://doi.org/10.1104/pp.110.162081

Rasulov B, Talts E, Bichele I, Niinemets Ü (2018) Evidence That Isoprene Emission Is Not Limited by Cytosolic Metabolites. Exogenous Malate Does Not Invert the Reverse Sensitivity of Isoprene Emission to High [CO_2]. *Plant Physiology* 176 (2):1573-1586. https://doi.org/10.1104/pp.17.01463

Rohmer M (1999) The discovery of a mevalonate-independent pathway for isoprenoid biosynthesis in bacteria, algae and higher plants. *Natural Product Reports* 16 (5):565-574. http://dx.doi.org/10.1039/A709175C

Rosenstiel TN, Fisher AJ, Fall R, Monson RK (2002) Differential accumulation of dimethylallyl diphosphate in leaves and needles of isoprene- and methylbutenol-emitting and nonemitting species. *Plant Physiology* 129 (3):1276-84. https://doi.org/10.1104/pp.002717

Sanadze GA (1957) The nature of gaseous substances emitted by leaves of *Robinia pseudoacacia*. *Soobscenija Akademii Nauk Gruzinskoj SSR* 19:83-86

Sanadze GA, Kalandaze AN (1966) Light and temperature curves of the evolution of C_5H_8. Soviet *Plant Physiology* 13 (3):458-461

Sasaki K, Ohara K, Yazaki K (2005) Gene expression and characterization of isoprene synthase from *Populus alba*. *FEBS Letters* 579 (11):2514-2518. https://doi.org/10.1016/j.febslet.2005.03.066

Saunois M, Stavert AR, Poulter B, Bousquet P, Canadell JG, Jackson RB, Raymond PA, Dlugokencky EJ, Houweling S, Patra PK, Ciais P, Arora VK, Bastviken D, Bergamaschi P, Blake DR, Brailsford G, Bruhwiler L, Carlson, KM, Carrol M, Castaldi S, Chandra N, Crevoisier C, Crill PM, Covey K, Curry CL, Etiope G, Frankenberg C, Gedney N, Hegglin MI, Höglund-Isaksson L, Hugelius G, Ishizawa M, Ito A, Janssens-Maenhout G, Jensen KM, Joos F, Kleinen T, Krummel PB, Langenfelds RL, Laruelle GG, Liu L, Machida T, Maksyutov S, McDonald KC, McNorton J, Miller PA, Melton JR, Morino I, Müller J, Murguia-Flores F, Naik V, Niwa Y, Noce S, O'Doherty S, Parker RJ, Peng C, Peng S, Peters GP, Prigent C, Prinn R, Ramonet M, Regnier P, Riley WJ, Rosentreter JA, Segers A, Simpson IJ, Shi H, Smith SJ, Steele LP, Thornton BF, Tian H, Tohjima Y, Tubiello FN, Tsuruta A, Viovy N, Voulgarakis A, Weber TS, van Weele M., van der Werf GR, Weiss RF, Worthy D, Wunch D, Yin Y, Yoshida Y, Zhang W, Zhang Z, Zhao Y, Zheng B, Zhu Q, Zhu Q, Zhuang Q (2020) The Global Methane Budget 2000–2017. *Earth System Science Data* 12 (3):1561-1623. https://doi.org/10.5194/essd-12-1561-2020

Schwender J, Zeidler J, Gröner R, Müller C, Focke M, Braun S, Lichtenthaler FW, Lichtenthaler HK (1997) Incorporation of 1-deoxy-D-xylulose into isoprene and phytol by higher plants and algae. *FEBS Letters* 414:129-134. https://doi.org/10.1016/S0014-5793(97)01002-8

Sharkey TD, Loreto F, Delwiche CF (1991) High carbon dioxide and sun/shade effects on isoprene emission from oak and aspen tree leaves. *Plant, Cell & Environment* 14 (3):333-338. https://doi.org/10.1111/j.1365-3040.1991.tb01509.x

Sharkey TD, Loreto F (1993) Water stress, temperature, and light effects on the capacity for isoprene emission and photosynthesis of kudzu leaves. *Oecologia* 95 (3):328-333. https://doi.org/10.1007/BF00320984

Sharkey TD, Singsaas EL (1995) Why plants emit isoprene. *Nature* 374 (6525):769-769. https://doi.org/10.1038/374769a0

Sharkey TD (1996) Isoprene synthesis by plants and animals. *Endeavour* 20 (2):74-78. https://doi.org/10.1016/0160-9327(96)10014-4

Sharkey TD, Singsaas EL, Vanderveer PJ, Geron C (1996) Field measurements of isoprene emission from trees in response to temperature and light. *Tree Physiology* 16 (7):649-654. https://doi.org/10.1093/treephys/16.7.649

Sharkey TD, Yeh S (2001) ISOPRENE EMISSION FROM PLANTS. *Annual Review of Plant Physiology and Plant Molecular Biology* 52 (1):407-436. https://doi.org/10.1146/annurev.arplant.52.1.407

Silver GM, Fall R (1991) Enzymatic synthesis of isoprene from dimethylallyl diphosphate in aspen leaf extracts. *Plant Physiology* 97 (4):1588-91. https://doi.org/10.1104/pp.97.4.1588

Sindelarova K, Granier C, Bouarar I, Guenther A, Tilmes S, Stavrakou T, Müller J-F, Kuhn U, Stefani P, Knorr W (2014) Global data set of biogenic VOC emissions calculated by the MEGAN model over the last 30 years. *Atmospheric Chemistry and Physics* 14 (17):9317-9341. https://doi.org/10.5194/acp-14-9317-2014

Siwko ME, Marrink SJ, Vries AH, Kozubek A, Uiterkamp AJ, Mark AE (2007) Does isoprene protect plant membranes from thermal shock? A molecular dynamics study. *Biochimica Et Biophysica Acta (BBA) - Biomembranes* 1768 (2):198-206. https://doi.org/10.1016/j.bbamem.2006.09.023

Song X, Zhou G, Jiang H, Yu S, Fu J, Li W, Wang W, Ma Z, Peng C (2011) Carbon sequestration by Chinese bamboo forests, and their ecological benefits: assessment of potential, problems, and future challenges. *Environmental Reviews* 19 (1):418-428. https://doi.org/10.1139/a11-015

Song X, Peng C, Zhou G, Jiang H, Wang, W, Xiang W (2013) Climate warming-induced upward shift of Moso bamboo population on Tianmu Mountain, China. *Journal of Mountain Science* 10 (3):363-369. https://doi.org/10.1007/s11629-013-2565-0

Spivakovsky CM, Logan JA, Montzka SA, Balkanski YJ, Foreman-Fowler M, Jones DBA, Horowitz LW, Fusco AC, Brenninkmeijer CAM, Prather MJ, Wofsy SC, McElroy MB (2000) Three-dimensional climatological distribution of tropospheric OH: Update and evaluation. *Journal of Geophysical Research* 105 (D7):8931-8980. https://doi.org/10.1029/1999JD901006

Steinbrecher R, Hauff K, Rabong R, Steinbrecher J (1997) Isoprenoid emission of oak species typical for the Mediterranean area: Source strength and controlling variables. *Atmospheric Environment* 31:79-88. https://doi.org/10.1016/S1352-2310(97)00076-9

Suzuki S (2015) Chronological location analyses of giant bamboo (*Phyllostachys pubescens*) groves and their invasive expansion in a satoyama landscape area, western Japan. *Plant Species Biology* 30 (1):63-71. https://doi.org/10.1111/1442-1984.12067

Takano KT, Hibino K, Numata A, Oguro M, Aiba M, Shiogama H, Takayabu I, Nakashizuka T (2017) Detecting latitudinal and altitudinal expansion of invasive bamboo *Phyllostachys edulis* and *Phyllostachys bambusoides* (Poaceae) in Japan to project potential habitats under 1.5–4.0°C global warming. *Ecology and Evolution* 7 (23):9848-9859. https://doi.org/10.1002/ece3.3471

Takada M, Inoue T, Mishima Y, Fujita H, Hirano T, Fujimura Y (2012) Geographical Assessment of Factors for Sasa Expansion in the Sarobetsu Mire, Japan. *Journal of Landscape Ecology 5* (1):58-71. https://doi.org/10.2478/v10285-012-0049-5

Tani A, Fushimi K (2005) Effects of temperature and light intensity on isoprene emission of *Edgeworthia chrysantha*. *Journal of Agricultural Meteorology* 61 (2):113-122. https://doi.org/10.2480/agrmet.61.113

Tani A, Kawawata Y (2008) Isoprene emission from the major native *Quercus* spp. in Japan. *Atmospheric Environment* 42 (19):4540-4550. https://doi.org/10.1016/j.atmosenv.2008.01.059

Teng AP, Crounse JD, Wennberg PO (2017) Isoprene Peroxy Radical Dynamics. *Journal of the American Chemical Society* 139 (15):5367-5377. https://doi.org/10.1021/jacs.6b12838

Tingey DT, Manning M, Grothaus LC, Burns WF (1979) The influence of light and temperature on isoprene emission rates from live oak. *Physiologia Plantarum* 47 (2):112-118. https://doi.org/10.1111/j.1399-3054.1979.tb03200.x

Tingey DT, Manning M, Grothaus LC, Burns WF (1980) Influence of light and temperature on monoterpene emission rates from slash pine. *Plant Physiology* 65 (5):797-801. https://doi.org/10.1104/pp.65.5.797

Torii A (2003) Bamboo forests as invaders to surrounded secondary forests. *Journal of the Japanese Society of Revegetation Technology* 28:412-416.

Vickers CE, Gershenzon J, Lerdau MT, Loreto F (2009) A unified mechanism of action for volatile isoprenoids in plant abiotic stress. *Nature Chemical Biology* 5 (5):283-291. https://doi.org/10.1038/nchembio.158

Wang TD, Kao YB (1986) The growth and development of bamboo. *Modern Silviculture* 2(1):47-63

Wang Y, Bai S, Binkley D, Zhou G, Fang F (2016) The independence of clonal shoot's growth from light availability supports moso bamboo invasion of closed-canopy forest. *Forest Ecology and Management* 368:105-110. https://doi.org/10.1016/j.foreco.2016.02.037

Way DA, Schnitzler JP, Monson RK, Jackson RB (2011) Enhanced isoprene-related tolerance of heat- and light-stressed photosynthesis at low, but not high, CO_2 concentrations. *Oecologia* 166 (1):273-282. https://doi.org/10.1007/s00442-011-1947-7

Wildermuth MC, Fall R (1996) Light-Dependent Isoprene Emission (Characterization of a Thylakoid-Bound Isoprene Synthase in *Salix* discolor Chloroplasts). *Plant Physiology* 112 (1):171-182. https://doi.org/10.1104/pp.112.1.171

Wildermuth MC, Fall R. (1998) Biochemical characterization of stromal and thylakoid-bound isoforms of isoprene synthase in willow leaves. *Plant Physiology* 116 (3):1111-23. https://doi.org/10.1104/pp.116.3.11

Winer AM, Arey J, Aschmann SM, Atkinson R, Long WD, Morrison LC, Olszyk DM (1989) Hydrocarbon emissions from vegetation found in California's Central Valley. Contract No. A732-155, prepared for the California Air Resources Board, by the Statewide Air Pollution Research Center. Riverside, California, U.S.A.

Winer AM, Arey J, Atkinson R, Aschmann SM, Long WD, Morrison CL, Olszyk DM (1992) Emission rates of organics from vegetation in California's Central Valley. *Atmospheric Environment* 26 (14):2647-2659. https://doi.org/10.1016/0960-1686(92)90116-3

Winer AM, Fitz DR, Miller PR (1983) Investigation of the role of natural hydrocarbons in photochemical smog formation in California. Contract No. AO-056-32, prepared for the California Air Resources Board, by the Statewide Air Pollution Research Center, Riverside, California, U.S.A.

Yen T, Ji Y, Lee J (2010) Estimating biomass production and carbon storage for a fast-growing makino bamboo (*Phyllostachys makinoi*) plant based on the diameter distribution model. *Forest Ecology and Management* 260 (3):339-344. https://doi.org/10.1016/j.foreco.2010.04.021

Zimmerman PR (1979) Determination of emission rates of hydrocarbons from indigenous species of vegetation in the Tampa/St Petersburg, Florida Area. EPA Contract No. 904/9-77-0282, prepared by the Tampa Bay Area Photochemical Oxidant Study. Bai S, Zhou G, Wang Y, Liang Q, Chen J, Cheng Y, Shen R (2013) Plant species diversity and dynamics in forests invaded by Moso bamboo (*Phyllostachys edulis*) in Tianmu Mountain Nature Reserve. *Biodiversity Science* 21(3):288-295. https://doi.org/10.3724/SP.J.1003.2013.08258

Zuo Z, Weraduwage SM, Lantz AT, Sanchez LM, Weise SE, Wang J, Childs KL, Sharkey TD (2019) Isoprene Acts as a Signaling Molecule in Gene Networks Important for Stress Responses and Plant Growth. *Plant Physiology* 180 (1):124-152. https://doi.org/10.1104/pp.18.01391

Chapter 2

Temperature and light response of isoprene emission flux from leaves of moso bamboo (*Phyllostachys pubescens*)

2.1. Chapter introduction and objective

It has been reported that different plant species have different isoprene emission capabilities (Benjamin et al., 1996). For instance, *Eucalyptus* spp. and *Quercus* spp. have been recognized as significant isoprene emitters (Benjamin et al., 1996; He et al., 2000; Geron et al., 2001; Okumura et al., 2008), while part of *Quercus* spp. showed very low or no detectable isoprene emissions (e.g., Tani and Kawawata, 2008). In addition, several studies have reported that isoprene emission from plants can respond to environmental factors such as light and temperature (e.g., Sanadze and Kalandadze, 1966; Rasmussen and Jones, 1973). Light can activate substrate biosynthesis of isoprene, which is related to photosynthetic metabolism, enabling isoprene production in plant leaves (Li and Sharkey, 2013); temperature can both regulate the activity of isoprene synthase and the concentration of substrate for isoprene production in photosynthetic metabolism (Rasulov et al., 2010). These two factors are the most widely used environmental factors in model-based estimations of isoprene emission flux from plants (e.g., Tingey et al., 1979; Guenther et al., 1993; Niinemets et al., 2010). It should be noted that responses to light and temperature differ considerably among species (Oku et al., 2008; Mutanda et al., 2016).

Bamboos are a dominant forest type, accounting for 3.2% (36.8 million ha) of forest area all over the world, and most bamboo areas (23.6 million ha) are distributed throughout Asia (Lobovikov et al., 2007). It was recently reported that some bamboo species can emit isoprene (Crespo et al., 2013; Bai et al., 2016; Okumura et al., 2018). In particular, *Phyllostachys pubescens* (moso bamboo) can be a strong isoprene emitter, with basal isoprene emission fluxes of 51.1 ± 7.7 nmol m^{-2} s^{-1} in Kyoto, Japan (Okumura et al., 2018). Moso bamboos were originally distributed in the southern part of mainland China, covering approximately 3 million ha (Fu, 2001). Currently, moso bamboo is widely spreading throughout eastern Asia due to active plantation for agricultural purposes or natural extension of abandoned moso bamboo forests (Torii, 2003; Song et al., 2011). Its fast growth, the shade tolerance of its sprouts, and its horizontally extending rhizomes enable moso bamboo to expand and invade forest ecosystems (Wang and Kao, 1986; Yen et al., 2010; Wang et al., 2016). For instance, moso bamboo coverage increased from 24 km^2 to 174 km^2 from 1953 to 1985 in Kyoto, Japan (Okutomi et al., 1996); similar trends were also found in Taiwan (Chiou et al., 2009). An ecological niche modeling also showed that the expansion would be faster under the context of global warming in Japan (Takano et al., 2017). There is an urgent need to assess how moso bamboo expansions can alter regional isoprene emissions.

Modeling is a useful approach for assessing the potential impacts of moso bamboo expansion on total isoprene emissions at stand or regional scales. Many previous studies have worked on simulating isoprene emissions from plants (e.g., Tingey, 1981; Evans et al., 1985; Lamb et al., 1987; Guenther et al., 1993). Among them, the model established by Guenther et al. (1993), which includes light and temperature dependencies (known as the G93 algorithm), is widely used in simulating isoprene emission fluxes from leaves. Although the G93 algorithm with its suggested parameters has been reported with good reproducibility of isoprene emissions from tree species in North and South America (Harley et al., 2004), it has been seldom used on bamboo species. There are only few studies have quantified isoprene emission fluxes from moso bamboo leaves (e.g., Zhang et al., 2002; Okumura et al., 2018), and only investigated the emission for a short term (about one day) with limited light and temperature changes. Thus, the validity of the G93 algorithm, including responses to environmental factors such as light and temperature still needs to be tested. In brief, the characteristics of isoprene emission from moso bamboo leaves, particularly the isoprene emission ability of moso bamboo and its dependency on light and temperature, are still unclear for conducting estimations with modeling.

To understand how moso bamboo expansion might alter regional isoprene emissions, this chapter aimed to establish a better model description that can simulate isoprene emission from moso bamboo leaves based on field measurements. The model can be combined with one-dimensional biosphere-vegetation models (e.g., multi-layer models and big leaf models), enabling us to calculate total isoprene emissions from moso bamboo leaves at stand or regional scales. To this end, this chapter measured isoprene emissions from moso bamboo leaves under different light conditions from September 2015 (summer) to March 2016 (spring). And then, the measurements of isoprene emission fluxes were used for validating the G93 algorithm. This chapter also compared the calculations from the G93 algorithm using the original parameters with those from the G93 algorithm using species-specific parameters determined using the field data in this site.

2.2. Materials and methods

2.2.1. Site description

The test was conducted at two sites: a bamboo specimen garden and a pure moso bamboo forest in the National Taiwan University Experimental Forest, in Xitou, central Taiwan (23°40'N, 120°47'E, elevation 1120 m). According to data acquired from the meteorological station in Xitou from 1950 to 2008, the annual mean temperature was ~16.5°C; the highest and the lowest monthly mean temperatures occurred in July (20.5°C) and January (11.2°C), respectively. The annual mean precipitation was 2567 mm; most precipitation (~78% of annual precipitation) occurred from May to September, and the least precipitation occurred from October to January (Tseng et al., 2017).

2.2.2. Isoprene flux observation

Observation of isoprene emission fluxes and corresponding environmental conditions including light intensity and leaf temperature was conducted with a photosynthesis measuring system (LI-6400XT, Li-Cor Inc., Lincoln, NE, USA). A diagram of this measurement system is shown in Figure 2-1. To collect leaf-emitted isoprene, a modification was applied to the Li-Cor 6400XT following the assembly method described in Okumura et al. (2008) and Tani et al. (2017), which divides the outlet airflow from the leaf cuvette into two channels by adding a Teflon T-junction. This allowed the air to flow into both the built-in infrared gas analyzer through one channel and a stainless steel tube containing adsorbent through the other. The air supplied to the LI-6400XT system was drawn through a 30-L capacity buffering box and a granular activated charcoal filter to supply VOC-free air, and warm up for one hour to ensure VOC are flushed from the system before starting the isoprene observations. The adsorbent consisted of 200 mg Tenax TA (GL science Inc., Tokyo, Japan) and 100 mg Carbotrap b (Supelco Inc., Bellefonte, PA, USA) to trap VOCs emitted from the leaf. The adsorbent tubes were preconditioned at 280°C for 10 min with a thermal desorption system (ATD-400, Perkin Elmer Inc., Waltham, MA, USA) to remove any VOCs in the adsorbent. When sampling the air from a leaf in the leaf cuvette, one side of the adsorbent tube is connected to the Li-Cor 6400XT, while the other side is connected to a minipump (MP-∑30NII, Sibata Inc., Tokyo, Japan) with a flow rate set at 200 mL min^{-1}. The sampling period was 10 min. During sampling, the environmental conditions were automatically measured by the LI-6400XT once per minute (nine times during a single collection). After each sampling, the adsorbent tube was sealed with brass caps and stored at temperature lower than 5°C and sent to analysis within one month.

VOCs collected by absorbent tubes were analyzed using a gas chromatograph equipped with a flame ionization detector (GC-17A, Shimadzu Inc., Kyoto, Japan) coupled with the ATD-400 thermal desorption system. In the thermal deposition process, samples were desorbed at 250°C for 10 minutes. Desorbed VOCs were first captured in a Tenax-TA-filled cold trap at -5°C, then quickly heated to 280°C to introduce analytes to the GC. VOCs separated in an SPB-1 capillary column (length: 60 m, diameter: 0.25 mm, ID, 1 μm, Supelco Inc.) with helium (purity > 99.9995%) as the carrier gas. The temperature in the column was maintained at 35°C for 5 min, increased to 200°C at 5°C min^{-1}, and increased again to 250°C at 40°C min^{-1}. The carrier gas pressure, column flow rate, linear velocity, and split ratio were 108.5 kPa, 1.0 mL min^{-1}, 25.7 cm s^{-1}, and 8:1, respectively. An analytical curve was obtained by collecting and analyzing different volumes (10, 20, 40, 60, and 80 mL) of isoprene standard gas (1.03 ppmv) (R = 0.999). The retention time of the isoprene signal appears at ~7.7 min. As an acceptance criterion, the signal/noise ratio (S/N ratio) that is larger than 3 is acceptable; peak with S/N ratio ≤ 3 was deemed to be no detection (n.d.).

To convert the isoprene emission from quantity (nmol) to flux (nmol m^{-2} s^{-1}), the sampling period (set to 600 seconds) and the valid leaf area from the isoprene measurements are required. There were two conditions when determining the leaf area: in the first, the leaf area exceeded the cuvette area; in the second, the in-cuvette leaf area was smaller than the cuvette area. In the first situation, I used the in-cuvette area as the leaf area (0.0006 m^2); in the second, the in-cuvette leaf samples were taken back to laboratory where the in-cuvette leaf area was calculated using an image processing software (ImageJ, National Institutes of Health, Bethesda, MD, USA).

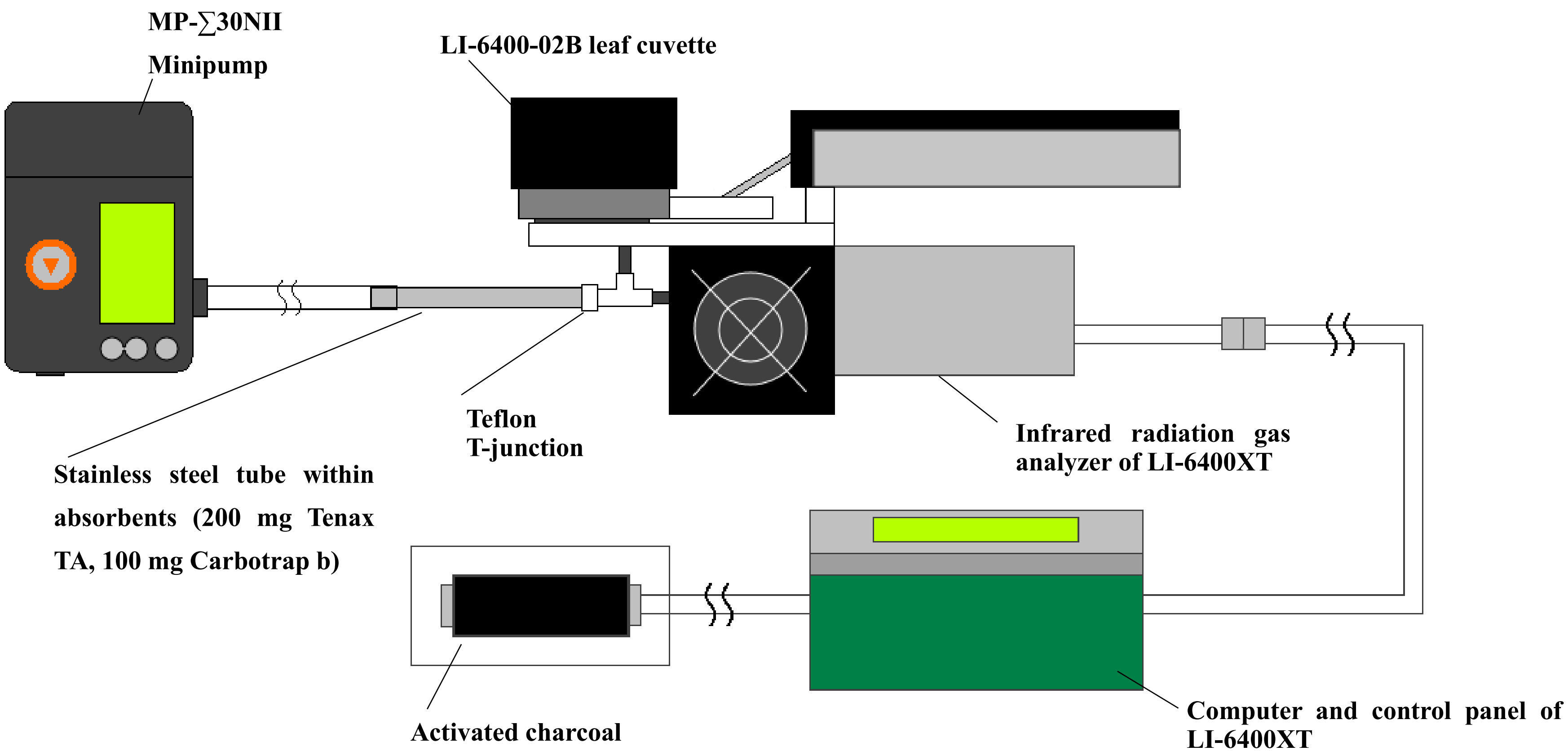

Figure 2-1 Diagram of isoprene measuring system including a photosynthesis measuring system (LI-6400XT), a minipump, an adsorbent tube, and a cylinder containing activated charcoal.

2.2.3. Sample selection and field sampling procedure

To investigate the variation in isoprene emission flux from moso bamboo, isoprene emission flux measurements under variable light conditions were conducted in the pure moso bamboo forest every month during the period from September 2015 to March 2016. At this site, culm density, mean diameter at breast height, and mean height were 6300 culms per hectare, 8.2 cm, and 15 m, respectively. In each measurement campaign, the isoprene emission fluxes were measured on three leaves from different individuals. The individuals for the measurements were selected near to the bordor of the stand. Although the leaves were collected from the lower part of the canopy, they were exposed to sunlight. Each measurement campaign was completed within two days (i.e., September 21 and 22; October 26; November 14; December 20 and 21; January 27 and 28; February 27 and 28; and March 15 and 16).

Light controls were performed during each leaf measurement with a LED light source leaf cuvette (LI-6400-02B, Li-Cor Inc.). For each leaf, the isoprene emission fluxes were measured under four to six different light levels with the LED light source. At each light level, the light condition was set at a stable photosynthetic photon flux density (PPFD; µmol m^{-2} s^{-1}), and the PPFD was adjusted within the range of 250–2500 µmol m^{-2} s^{-1}.

2.2.4. Modeling isoprene emission from P. pubescens leaves

The G93 algorithm established by Guenther et al. (1993) is a widely-use model for assessing isoprene emission fluxes from plant leaves (e.g., Benjamin et al., 1996; Geron et al., 2001; Okumura et al., 2018). This model considers light and leaf temperature dependencies of isoprene emission flux from plant leaves and is described as follows:

$$I = I_B \cdot L \cdot T \qquad \text{(Equation 2-1)},$$

where I is the isoprene emission flux at given light and leaf temperature conditions; I_B is the basal emission flux at a standard condition (PPFD = 1000 µmol m^{-2} s^{-1} and leaf temperature (T_L) = 30°C); L and T are calculated variables determined by functions linked to PPFD and T_L, respectively. L is defined as:

$$L = \alpha \cdot C_L \cdot \mathrm{PPFD} / \sqrt{1 + \alpha^2 \cdot \mathrm{PPFD}^2} \qquad \text{(Equation 2-2)},$$

where α and C_L are empirical coefficients related to light response. T is defined as:

$$T = \exp\,(C_{T1} \cdot [T_L - T_s]/[R \cdot T_s \cdot T_L])/(1 + \exp\,[C_{T2} \cdot \{T_L - T_M\}/\{R \cdot T_s \cdot T_L\}]) \qquad \text{(Equation 2-3)},$$

where R is the gas constant (= 8.314 J K^{-1} mol^{-1}); T_s is the leaf temperature under standard conditions (= 303.15 K); T_L is the leaf temperature (unit: K) at time of sampling; C_{T1} and C_{T2} are the empirical coefficients related to leaf temperature; T_M is an empirical coefficient relate to temperature of maximum isoprene emission. The values for α (= 0.0027), C_L (= 1.066), C_{T1}(= 95000 J mol^{-1}), C_{T2} (= 230000 J mol^{-1}), and T_M (= 314 K) were used in the original G93 algorithm, and were determined with data derived from eucalyptus, sweet gum, aspen, and velvet bean in Alabama, US (Guenther et al., 1993).

To confirm the reproducibility of the G93 algorithm for isoprene emission from moso bamboo leaves, the isoprene emission fluxes calculated from the G93 algorithm using original coefficients in Guenther et al. (1993) (the original G93 algorithm) were compared with those from the G93 algorithm using specific parameters for the moso bamboo leaves of this site (the G93 algorithm for moso bamboos). In here, I optimized I_B and the empirical coefficients in the G93 algorithm for moso bamboos; and optimized I_B only in the original G93 algorithm. The optimization was conducted by using a solver gram (Frontline Solver, Frontline Systems Inc., Incline Village, NV, USA). The parameters were determined by minimizing the root mean square deviation (RMSD) between the observed isoprene emission fluxes from moso bamboo leaves measured at PPFD ≥ 1000 μmol m^{-2} s^{-1} (O) and those calculated from the G93 algorithm (I). The RMSD is defined as:

$$\mathrm{RMSD} = \sqrt{\textstyle\sum_i^n (O_i - I_i)^2/n} \qquad \text{(Equation 2-4)},$$

where n is the total number of observed data, O_i is the i^{th} observed isoprene emission flux from moso bamboo leaves, and I_i is the i^{th} simulated isoprene emission at a given PPFD and T_L acquired using the G93 algorithm. To avoid the effects of outliers on the model performance, data from individuals that showed extreme fluxes were regarded as outliers and excluded from the optimization process. Outliers were determined using the boxplot-whisker method. First, the individual mean data were separated by leaf temperature into 2.5°C intervals; then, a boxplot analysis was applied to each interval. If the flux value of the datum > Q_3 + (IQR × 1.5) or < Q_1 – (IQR × 1.5), it was defined as an outlier, where Q_3, Q_1, and IQR represent the third quartile, the first quartile, and the interquartile range ($Q_3 - Q_1$) of the individual mean flux data set, respectively.

The coefficients in L were not parameterized because temperature was not controlled, thus the effect of leaf temperature on isoprene emission was not the same in each measurement campaign. In addition, C_{T2} and T_M were not parameterized as the decreasing tendency of the isoprene emission fluxes was not observed under conditions of high leaf temperature.

2.3. Results

2.3.1. Light response of isoprene emission flux

The isoprene emission fluxes from moso bamboo leaves generally increased with PPFD; responses to PPFD differed among individuals (Figure 2-2). Most emission fluxes saturated at approximately PPFD = 1000 μmol m^{-2} s^{-1}, but the emission fluxes of Individual I in November 2015 showed no saturation with PPFD. In addition, the emission fluxes at saturation differed among the months. The emission fluxes from September 2015 to November 2015 were larger than those from December 2015 to March 2016. The emission fluxes were even lower in February 2016 and March 2016.

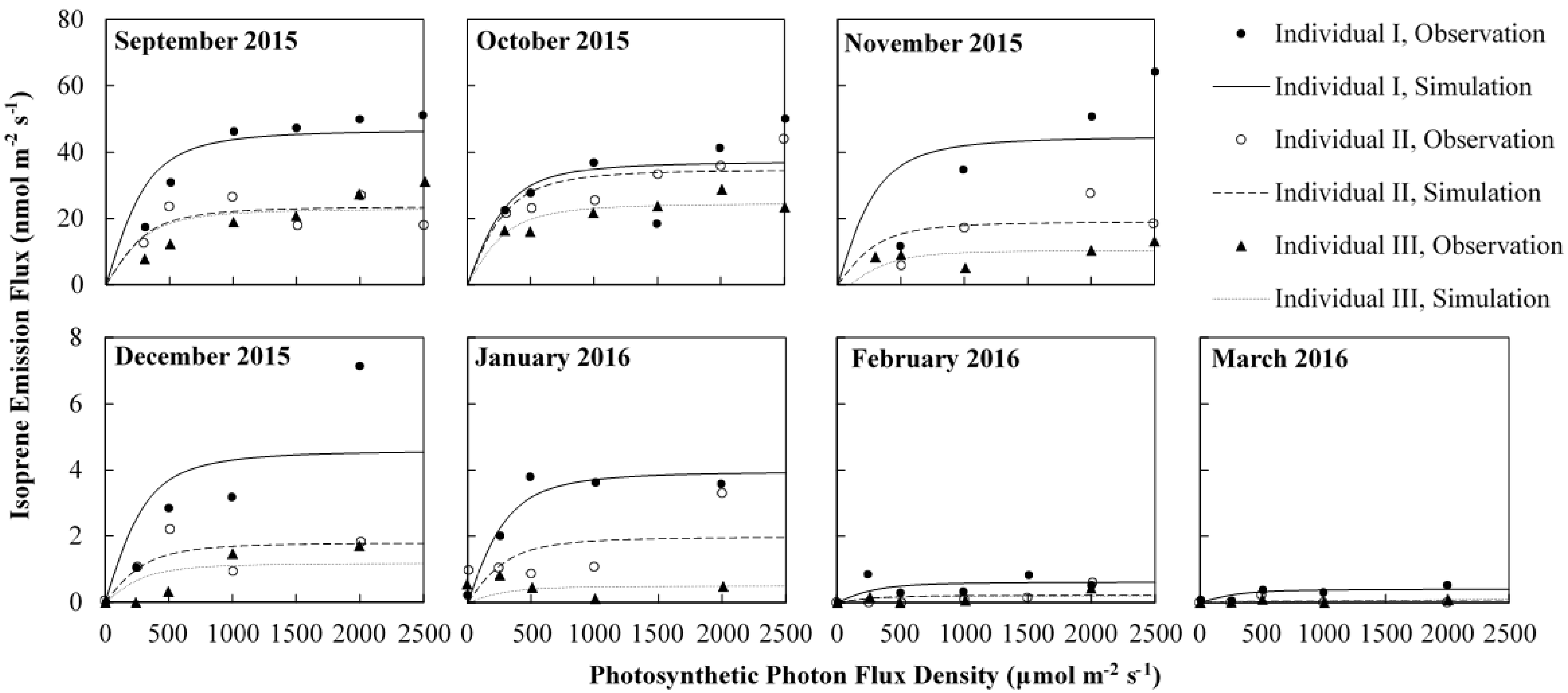

Figure 2-2 Observed isoprene emission fluxes (nmol m^{-2} s^{-1}) from moso bamboo leaves at different PPFDs (μmol m^{-2} s^{-1}) (dots) and the corresponding simulated light dependence curves (lines) using the G93 algorithm during the period from September 2015 to March 2016. In each panel, the data are differentiated by individual, using different symbols. The individuals were randomly selected from the research plot in each month.

2.3.2. Temperature response of isoprene emission flux

The measurements whose PPFD were set to larger than 1000 μmol m^{-2} s^{-1} (i.e. 1000, 1500, 2000 and 2500 μmol m^{-2} s^{-1}) demonstrate the isoprene emission fluxes increased with leaf temperature during the period from September 2015 to March 2016 (Figure 2-3). At high leaf temperature conditions (> 23°C), the emission fluxes showed larger divergence. Larger emission fluxes were observed from September 2015 to November 2015 with higher leaf temperatures (> 23°C), while low or zero emission fluxes were observed from December 2015 to March 2016 with lower leaf temperatures (< 23°C).

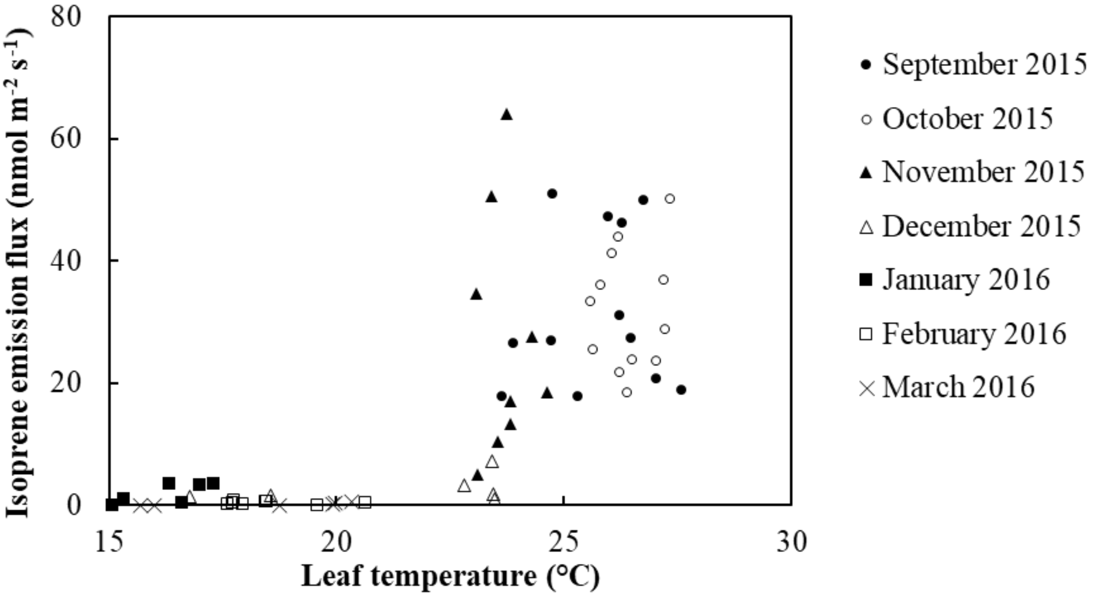

Figure 2-3 Observed isoprene emission fluxes (nmol m^{-2} s^{-1}) from moso bamboo leaves in relation to leaf temperature (°C) during the period from September 2015 to March 2016 with PPFD ≥1000 μmol m^{-2} s^{-1}. The data were differentiated by month, using different symbols (i.e., solid circles, open circles, solid triangles, open triangles, solid boxes, open boxes, and crosses).

2.3.3. Reproducibility of model estimation on isoprene emission

The original G93 algorithm overestimated the isoprene emission flux at lower leaf temperatures (< 23°C) (Figure 2-4). In the temperature dependence curves of the G93 algorithm for moso bamboos, C_{T1} and I_B became larger (C_{T1} = 192000 J mol^{-1} and I_B = 72.3 nmol m^{-2} s^{-1}) than in the original G93 algorithm (C_{T1} = 95000 J mol^{-1} and I_B = 39.8 nmol m^{-2} s^{-1}) (Table 2-1). Note that C_{T2} and T_M were not optimized in here, as the leaf temperatures in all measurement campaigns never exceeded T_M (= 314 K). According to Equation 2-1, 2-2 and 2-3, calculated isoprene emission flux (I) with the larger C_{T1} and I_B was increased when leaf temperature (T_L) larger than 23°C, and was decreased when T_L smaller than 23°C. As a result, the new C_{T1} and I_B reduced discrepancy between the observation and the simulation of the isoprene emission fluxes of moso bamboo in this site (Figure 2-5). The equation of the original G93 algorithm is defined as:

$$I = 39.8 \cdot 0.0027 \cdot 1.066 \cdot \mathrm{PPFD} \\ /\sqrt{1 + 0.0027^2 \cdot \mathrm{PPFD}^2} \cdot \exp\,(9.5 \cdot 10^4 \cdot [T_L - 303]/[8.314 \cdot 303 \cdot T_L]) \\ /(1 + \exp\,[2.3 \cdot 10^5 \cdot \{T_L - 314\}/\{8.314 \cdot 303 \cdot T_L\}]) \qquad \text{(Equation 2-5);}$$

the equation of optimized algorithm is defined as:

$$I = 72.3 \cdot 0.0027 \cdot 1.066 \cdot \mathrm{PPFD} \\ /\sqrt{1 + 0.0027^2 \cdot \mathrm{PPFD}^2} \cdot \exp\,(1.92 \cdot 10^5 \cdot [T_L - 303]/[8.314 \cdot 303 \cdot T_L]) \\ /(1 + \exp\,[2.3 \cdot 10^5 \cdot \{T_L - 314\}/\{8.314 \cdot 303 \cdot T_L\}]) \qquad \text{(Equation 2-6).}$$

The G93 algorithm for moso bamboos has higher reproducibility (slope of the linear regression = 0.823; R^2 = 0.724; RMSD = 7.542 nmol m^{-2} s^{-1}) than the G93 algorithm with the original coefficients (slope of the linear regression = 0.759; R^2 = 0.685; RMSD = 8.816 nmol m^{-2} s^{-1}) (Table 2-1).

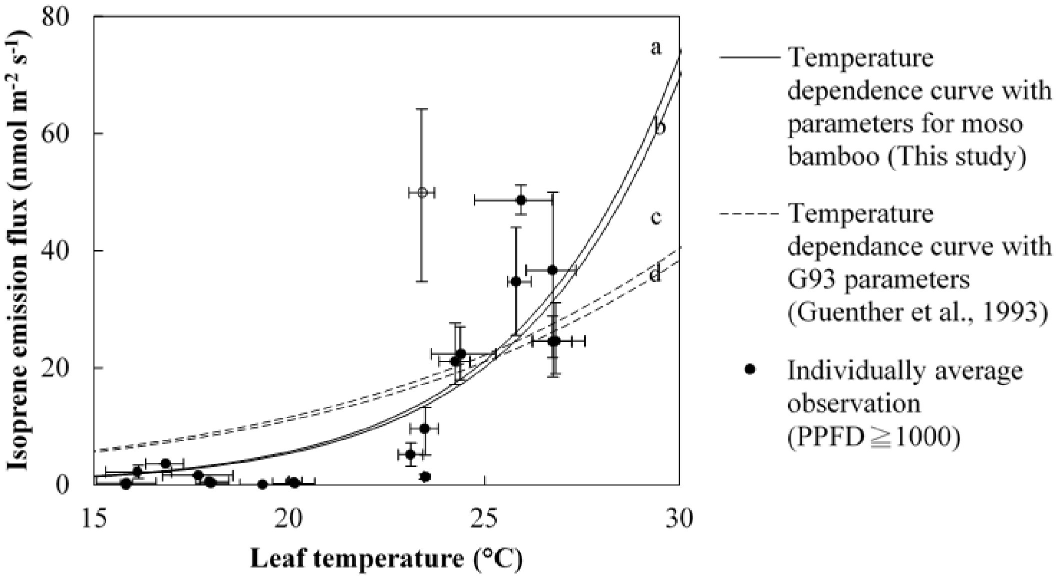

Figure 2-4 Isoprene emission fluxes in relation to leaf temperature. The solid circles represent the mean values of observed data measured at PPFD ≥ 1000 μmol m^{-2} s^{-1} for each individual; the opened circles (data from Individual I, November 2015) were excluded in the optimization procedure due to outlier classification based on the boxplot analysis (see main text). The vertical and horizontal error bars represent the highest and lowest measurements of isoprene emission fluxes and leaf temperature, respectively. The dashed lines represent the leaf temperature dependence curves of original G93 algorithm with PPFD values of 2500 μmol m^{-2} s^{-1} (c) and 1000 μmol m^{-2} s^{-1} (d). The solid lines represent leaf temperature dependence curves of the G93 algorithm for moso bamboos determined in here with PPFD values of 2500 μmol m^{-2} s^{-1} (a) and 1000 μmol m^{-2} s^{-1} (b).

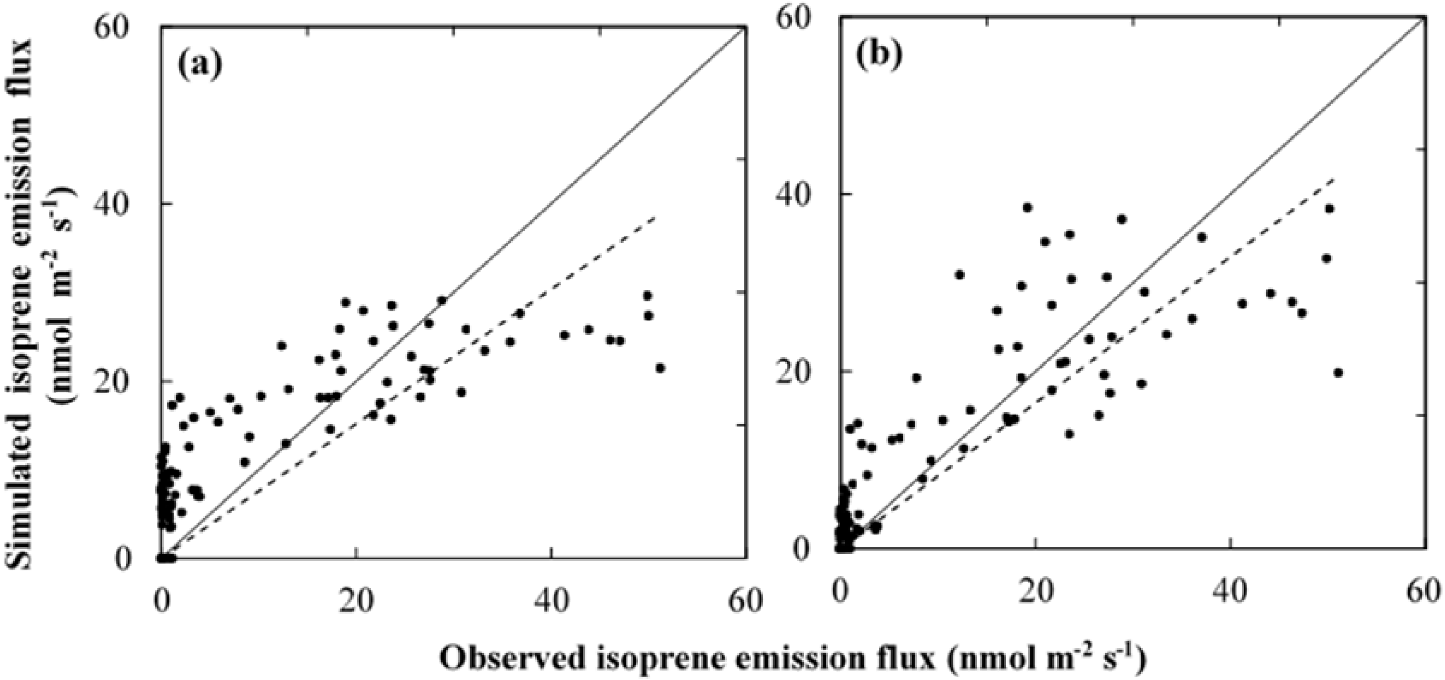

Figure 2-5 Comparison between observed and simulated isoprene emission fluxes (nmol m^{-2} s^{-1}) using (a) the original G93 algorithm and (b) the G93 algorithm for moso bamboos determined in this site. The solid lines represent the 1:1 line. The dotted lines represent the linear regression between observed and simulated isoprene emission fluxes.

Table 2-1 Parameters of temperature and light dependence curves used in this site. Reproducibility of the G93 algorithm with the original parameters in Guenther et al. (1993) and site-specific parameters for moso bamboo are shown using the slope of the linear regression with the coefficient of determination (R^2) and the root mean square deviation (RMSD) between the observed and calculated isoprene emission fluxes from moso bamboo leaves.

		The original G93 algorithm (Guenther et al., 1993)	The G93 algorithm for moso bamboo (This site)
	I_B	39.8 nmol m^{-2} s^{-1}	72.3 nmol m^{-2} s^{-1}
Parameters in temperature dependence	C_{T1}	95000 J mol^{-1}	192000 J mol^{-1}
	C_{T2}	230000 J mol^{-1}	230000 J mol^{-1}
	T_M	314 K	314 K
Parameters in light dependence	α	0.0027	0.0027
	C_L	1.066	1.066
Reproducibility	slope	0.759	0.823
	R^2	0.685	0.724
	RMSD	8.816 nmol m^{-2} s^{-1}	7.542 nmol m^{-2} s^{-1}

2.4. Discussion

The basal emission flux conducted from the moso bamboo stand during the period from September 2015 to March 2016 was significant (~39.8 nmol m^{-2} s^{-1}). Okumura et al. (2018) also showed moso bamboo species had large emissions, for instance, the basal isoprene emission fluxes from moso bamboo leaves were ~51.1 nmol m^{-2} s^{-1}, which is comparable to those of worldwide isoprene heavy emitter species in previous studies. For instance, Geron et al. (2001) reported basal isoprene emission fluxes of ~46 nmol m^{-2} s^{-1} in 18 *Quercus* spp. in North America; He et al. (2000) reported basal isoprene emission fluxes of 3 to 39 nmol m^{-2} s^{-1} in 15 *Eucalyptus* spp. in Australia. Benjamin et al. (1996) reported basal isoprene emission fluxes from 377 species, and the isoprene emission fluxes from moso bamboo in this site were the second largest (only *Elaeis guineensis* showed a larger emission flux than the bamboos). This suggests the isoprene emissions from moso bamboo in Taiwan might be significant.

In addition, the measurements here demonstrated that the isoprene emission fluxes with PPFD > 1000 μmol m^{-2} s^{-1} were related to leaf temperature, suggesting that the seasonal changes in isoprene emission fluxes could be regulated by not only light condition but also leaf temperature in moso bamboo. This was consistent with results from previous studies demonstrating that leaf temperature and light intensity strongly affects isoprene emission flux (e.g., Tingey et al., 1979; Sharkey and Loreto, 1993). Variation in isoprene emission flux was found among different leaves despite sharing the same environment, leading to large divergence at leaf temperature > 23°C. The discrepancies may be attributed to the different leaf development stage, which can cause different isoprene emission ability (Kuzma and Fall, 1993; Alves et al., 2014).

Generally, the light dependency in the G93 algorithm with the original coefficients, which is based on the light–photosynthesis curve, could reproduce the isoprene emission fluxes from moso bamboo leaves. This suggests the robustness of the G93 algorithm with the original coefficients for reproducing isoprene emission fluxes from moso bamboo leaves.

Guenther et al. (1993) defined the instant temperature dependency of isoprene emission in the algorithm based on the Arrhenius equation, showing the decreasing tendency of isoprene emission fluxes at high temperature conditions (i.e., temperature >

T_M). The isoprene emission from moso bamboo leaves did not show a decreasing tendency under high temperature conditions (Figure 2-3). During the measurement, the leaf temperature of moso bamboos ranged between 15°C and 27°C. According to previous studies, the temperature of maximum isoprene emission flux appeared above 35°C (e.g., Monson and Fall, 1989; Guenther et al., 1991; Monson et al., 1992; Guenther et al., 1993; Rasulov et al., 2010), which is much higher than the leaf temperatures measured in this site. Historical records also showed that air temperatures rarely exceed 30°C at this site, suggesting that leaf temperatures would not exceed 35°C. Further investigation including indoor-incubation or field measurements under episodic high temperature conditions are needed to clarify the isoprene emission characteristics at temperatures higher than the temperature of maximum emission.

A discrepancy between the measured and calculated isoprene emission fluxes by the original G93 algorithm (Guenther et al., 1993) was found (Figure 2-4). This discrepancy mainly originated from the overestimation of isoprene fluxes under low temperature conditions (< 23°C). The possible explanation for the low emissions from moso bamboo leaves at low temperatures might be the result of suppression of isoprene emission in isoprene-emitting species under colder conditions. Previous studies reported that plant leaves need a certain period of exposure to higher temperatures to break through the suppression (e.g., Sharkey and Loreto, 1993; Oku et al., 2014). It is reasonable for plants in tropical areas to suppress isoprene emission under cold conditions because plants produce isoprene to protect leaf cells from thermal damage. Suppressing the production of isoprene can strategically prevent the waste of energy and carbon.

Parameterization of the G93 algorithm using field observation data conducted from summer to spring could improve the reproducibility of the isoprene emission fluxes from moso bamboo leaves, implying that the seasonal variation of isoprene emission fluxes in moso bamboo can be reproduced by the G93 algorithm with site-specific parameters and that assessments for impacts of moso bamboo expansion on regional isoprene emissions should be performed with a parameterized G93 algorithm. However, when applying this approach for long-term assessment, it should be noted that previous studies indicated plant acclimation to temperature changes, leading to changes in isoprene emission ability (Sharkey et al., 1999; Pétron et al., 2001; Rasulov et al., 2015), and the responses of isoprene emission to light and leaf temperature (Monson et al., 1992; Harley et al., 1999; Rasulov et al., 2015). In addition, the highest temperature recorded during the measurements was quite low (< 27°C) because of that this site is under the influence of a cloud-forest-type climate in subtropical region, the air temperature beyond the canopy rarely exceed 30°C (Laplace et al., 2017; Tseng et al., 2017). This resulted in uncertainty of the characteristics of isoprene emission flux at high temperatures. Thus, further study including the isoprene emission response to long-term factors in moso bamboo is needed to improve the accuracy of models in response to marginal trends of climate change.

2.5. Chapter conclusion

This chapter was conducted to characterize the isoprene emission ability and responses to environmental variables of moso bamboo leaves for simulating isoprene emission fluxes from them. The result reveals that moso bamboo can be a significant isoprene emitter, and the emission ability of moso bamboo was equivalent to that of strong isoprene emitters reported in previous studies. The measurements conducted under variable environmental conditions showed that isoprene emission fluxes from moso bamboo leaves increased with light conditions with large individual variations in this site. The seasonal changes in isoprene emissions with PPFD > 1000 μmol m^{-2} s^{-1} were mainly regulated by leaf temperature, and low fluxes were observed under cold seasons. Because of the low emission fluxes at leaf temperatures < 23°C, overestimations were observed in the calculation by the original G93 algorithm under low temperature conditions. This problem was improved by optimizing the parameters in the G93 algorithm using measured isoprene emission fluxes. Further studies are needed to clarify the alteration to light and leaf temperature dependence of isoprene emission fluxes from moso bamboo caused by long-term effects. Also, researches on the responses of the isoprene emission fluxes to high leaf temperatures are needed in the context of global climate change.

Reference

Alves EG, Harley P, Gonçalves JFD, Moura CED, Jardine K (2014) Effects of light and temperature on isoprene emission at different leaf developmental stages of *Eschweilera coriacea* in central Amazon. *Acta Amazonica* 44 (1):9-18. https://dx.doi.org/10.1590/S0044-59672014000100002

Bai J, Guenther A, Turnipseed A, Duhl T, Yu S, Wang B (2016) Seasonal variations in whole-ecosystem BVOC emissions from a subtropical bamboo plantation in China. *Atmospheric Environment* 124:12-21. https://doi.org/10.1016/j.atmosenv.2015.11.008

Benjamin MT, Sudol M, Bloch L, Winer AM (1996) Low-emitting urban forests: a taxonomic methodology for assigning isoprene and monoterpenes emission rates. *Atmospheric Environment* 30 (9):1437-1452. https://doi.org/10.1016/1352-2310(95)00439-4

Chiou C, Chen T, Lin Y, Yang Y, Lin S (2009) Distribution and Change Analysis of Bamboo Forest in Northern Taiwan. *Quarterly Journal of Chinese Forestry* 42 (1):89-105. http://dx.doi.org/10.30064%2fQJCF.200903.0006

Crespo E, Graus M, Gilman JB, Lerner BM, Fall R, Harren FJM, Warneke C (2013) Volatile organic compound emissions from elephant grass and bamboo cultivars used as potential bioethanol crop. *Atmospheric Environment* 65:61-68. https://doi.org/10.1016/j.atmosenv.2012.10.009

Evans R, Tingey D, Gumpertz M (1985) Interspecies variation in terpenoid emissions from Engelmann and Sitka spruce seedlings. *Forest Science* 31 (1):132-142. https://doi.org/10.1093/forestscience/31.1.132

Fu J (2001) Chinese moso bamboo: its importance. *BAMBOO: Magazine of the American Bamboo Society* 22:5-7.

Geron C, Harley P, Guenther A (2001) Isoprene emission capacity for US tree species. *Atmospheric Environment* 35 (19):3341-3352. https://doi.org/10.1016/S1352-2310(00)00407-6

Guenther AB, Monson RK, Fall R (1991) Isoprene and monoterpene emission rate variability: Observations with eucalyptus and emission rate algorithm development. *Journal of Geophysical Research* 96 (D6):10799-10808. https://doi.org/10.1029/91JD00960

Guenther AB, Zimmerman PR, Harley PC, Monson RK, Fall R (1993) Isoprene and monoterpene emission rate variability: Model evaluations and sensitivity analyses. *Journal of Geophysical Research* 98 (D7):12609-12617. https://doi.org/10.1029/93JD00527

Harley PC, Monson RK, Lerdau MT (1999) Ecological and evolutionary aspects of isoprene emission from plants. *Oecologia* 118 (2):109-123. https://doi.org/10.1007/s004420050709

Harley P, Vasconcellos P, Vierling L, Pinheiros CC, Greenberg J, Guenther A, Klinger L, Almeida SS, Neill D, Baker T, Phillips O, Malhi Y (2004) Variation in potential for isoprene emissions among neotropical forest sites. *Global Change Biology* 10(5):1-21. https://doi.org/10.1111/j.1529-8817.2003.00760.x

He C, Murray F, Lyons T (2000) Monoterpene and isoprene emissions from 15 *Eucalyptus* species in Australia. *Atmospheric Environment* 34 (4):645-655. https://doi.org/10.1016/S1352-2310(99)00219-8

Kuzma J, Fall R (1993) Leaf Isoprene Emission Rate Is Dependent on Leaf Development and the Level of Isoprene Synthase. *Plant Physiology* 101 (2):435-440. https://doi.org/10.1104/pp.101.2.435

Lamb B, Guenther A, Gay D, Westberg H (1987) A national inventory of biogenic hydrocarbon emissions. *Atmospheric Environment* 21 (8):1695-1705. https://doi.org/10.1016/0004-6981(87)90108-9

Laplace S, Komatsu H, Tseng H, Kume T (2017) Difference between the transpiration rates of Moso bamboo (*Phyllostachys pubescens*) and Japanese cedar (*Cryptomeria japonica*) forests in a subtropical climate in Taiwan. *Ecological Research* 32 (6):835-843. https://doi.org/10.1007/s11284-017-1512-x

Li Z, Sharkey TD (2013) Molecular and pathway controls on biogenic volatile organic compound emissions. In: Niinemets Ü, Monson RK (ed) Biology, controls and models of tree volatile organic compound emissions. *Springer*, Berlin, pp 119-151. https://doi.org/10.1007/978-94-007-6606-8_5

Lobovikov M, Paudel S, Piazza M, Wu HR (2007) World Bamboo Resources - A Thematic Study Prepared in the Framework of the Global Forest Resources Assessment 2005. Food and Agriculture Organization of The United Nations, Rome. https://doi.org/10.13140/RG.2.1.1042.3764}

Monson RK, Fall R (1989) Isoprene emission from aspen leaves: Influence of environment and relation to photosynthesis and photorespiration. *Plant Physiology* 90 (1):267-274. https://doi.org/10.1104/pp.90.1.267

Monson RK, Jaeger CH, Adams WW, Driggers EM, Silver GM, Fall R (1992) Relationships among isoprene emission rate, photosynthesis, and isoprene synthase activity as influenced by temperature. *Plant Physiology* 98 (3):1175-1180. https://doi.org/10.1104/pp.98.3.1175

Mutanda I, Saitoh S, Inafuku M, Aoyama H, Takamine T, Satou K, Akutsu M, Teruya K, Tamotsu H, Shimoji M, Sunagawa H, Oku H (2016) Gene expression analysis of disabled and re-induced isoprene emission by the tropical tree *Ficus septica* before and after cold ambient temperature exposure. *Tree Physiology* 36 (7):873-882. https://doi.org/10.1093/treephys/tpw032

Niinemets Ü, Copolovici L, Hüve K (2010) High within-canopy variation in isoprene emission potentials in temperate trees: Implications for predicting canopy-scale isoprene fluxes. *Journal of Geophysical Research* 115 (G4):G04029. https://doi.org/10.1029/2010JG001436

Oku H, Fukuta M, Iwasaki H, Tambunan P, Baba S (2008) Modification of the isoprene emission model G93 for tropical tree *Ficus virgata*. *Atmospheric Environment* 42 (38):8747-8754. https://doi.org/10.1016/j.atmosenv.2008.08.036

Oku H, Inafuku M, Takamine T, Nagamine M, Saitoh S, Fukuta M (2014) Temperature threshold of isoprene emission from tropical trees, *Ficus virgata* and *Ficus septica*. *Chemosphere* 95:268-273. https://doi.org/10.1016/j.chemosphere.2013.09.003

Okumura M, Tani A, Kominami Y, Takanashi S, Kosugi Y, Miyama T, Tohno S (2008) Isoprene emission characteristics of *Quercus serrata* in a deciduous broad-leaved forest. *Journal Agricultural Meteorology* 64 (2):49-60. https://doi.org/10.2480/agrmet.64.49

Okumura M, Kosugi Y, Tani A (2018) Biogenic volatile organic compound emissions from bamboo species in Japan. *Journal of Agricultural Meteorology* 74 (1):40-44. https://doi.org/10.2480/agrmet.D-17-00017

Okutomi K, Shinoda S, Fukuda H (1996) Causal analysis of the invasion of broad-leaved forest by bamboo in Japan. *Journal of Vegetation Science* 7 (5):723-728. https://doi.org/10.2307/3236383

Pétron G, Harley P, Greenberg J, Guenther A (2001) Seasonal temperature variations influence isoprene emission. *Geophysical Research Letters* 28 (9):1707-1710. https://doi.org/10.1029/2000GL011583

Rasmussen RA, Jones CA (1973) Emission of isoprene from leaf discs of *Hamamelis*. *Phytochemistry* 12 (1):15-19. https://doi.org/10.1016/S0031-9422(00)84618-X

Rasulov B, Hüve K, Bichele I, Laisk A, Niinemets Ü (2010) Temperature response of isoprene emission in vivo reflects a combined effect of substrate limitations and isoprene synthase activity: A kinetic analysis. *Plant Physiology* 154 (3):1558-1570. https://doi.org/10.1104/pp.110.162081

Rasulov B, Bichele I, Hüve K, Vislap V, Niinemets Ü (2015) Acclimation of isoprene emission and photosynthesis to growth temperature in hybrid aspen: resolving structural and physiological controls. *Plant Cell and Environment* 38 (4):751-766. https://doi.org/10.1111/pce.12435

Sanadze GA, Kalandaze AN (1966) Light and temperature curves of the evolution of C_5H_8. Soviet *Plant Physiology* 13 (3):458-461

Sharkey TD, Loreto F (1993) Water stress, temperature, and light effects on the capacity for isoprene emission and photosynthesis of kudzu leaves. *Oecologia* 95 (3):328-333. https://doi.org/10.1007/BF00320984

Sharkey TD, Singsaas EL, Lerdau MT, Geron CD (1999) Weather effects on isoprene emission capacity and applications in emissions algorithms. *Ecological Applications* 9 (4):1132-1137. https://doi.org/10.1890/1051-0761(1999)009[1132:WEOIEC]2.0.CO;2

Song X, Zhou G, Jiang H, Yu S, Fu J, Li W, Wang W, Ma Z, Peng C (2011) Carbon sequestration by Chinese bamboo forests, and their ecological benefits: assessment of potential, problems, and future challenges. *Environmental Reviews* 19 (1):418-428. https://doi.org/10.1139/a11-015

Takano KT, Hibino K, Numata A, Oguro M, Aiba M, Shiogama H, Takayabu I, Nakashizuka T (2017) Detecting latitudinal and altitudinal expansion of invasive bamboo *Phyllostachys edulis* and *Phyllostachys bambusoides* (Poaceae) in Japan to project potential habitats under 1.5–4.0°C global warming. *Ecology and Evolution* 7 (23):9848-9859. https://doi.org/10.1002/ece3.3471

Tani A, Kawawata Y (2008) Isoprene emission from the major native *Quercus* spp. in Japan. *Atmospheric Environment* 42 (19):4540-4550. https://doi.org/10.1016/j.atmosenv.2008.01.059

Tani A, Ohno T, Saito T, Ito S, Yonekura T, Miwa M (2017) Effects of ozone on isoprene emission from two major Quercus species native to East Asia. *Journal of Agricultural Meteorology* 73 (4):195-202. https://doi.org/10.2480/agrmet.D-17-00022

Tingey DT, Manning M, Grothaus LC, Burns WF (1979) The influence of light and temperature on isoprene emission rates from live oak. *Physiologia Plantarum* 47 (2):112-118. https://doi.org/10.1111/j.1399-3054.1979.tb03200.x

Tingey D (1981) The effect of environmental factors on the emission of biogenic hydrocarbons from live oak and slash pine. In: Bufalini J and Arnts R Atmospheric Biogenic Hydrocarbons. *Butterworth*, Stoneham, Massachusetts, pp. 53-72.

Torii A (2003) Bamboo forests as invaders to surrounded secondary forests. *Journal of the Japanese Society of Revegetation Technology* 28:412-416.

Tseng H, Chiu CW, Laplace S, Kume T (2017) Can we assume insignificant temporal changes in spatial variations of sap flux for year-round individual tree transpiration estimates? A case study on *Cryptomeria japonica* in central Taiwan. *Trees* 31(4):1239-1251. https://doi.org/10.1007/s00468-017-1542-6

Wang TD, Kao YB (1986) The growth and development of bamboo. *Modern Silviculture* 2(1):47-63

Wang Y, Bai S, Binkley D, Zhou G, Fang F (2016) The independence of clonal shoot's growth from light availability supports moso bamboo invasion of closed-canopy forest. *Forest Ecology and Management* 368:105-110. https://doi.org/10.1016/j.foreco.2016.02.037

Yen T, Ji Y, Lee J (2010) Estimating biomass production and carbon storage for a fast-growing makino bamboo (*Phyllostachys makinoi*) plant based on the diameter distribution model. *Forest Ecology and Management* 260 (3):339-344. https://doi.org/10.1016/j.foreco.2010.04.021

Zhang L, Bai Y, Wang X, Ouyang Z, Mu Y, Miao Q (2002) Isoprene Emission of Bamboo and its Implication to Ozone Level in Region. *Acta Ecologica Sinica* 22 (8):1333-1338.

Chapter 3

Dependency of isoprene emission capacity of *P. pubescens* leaves on leaf mass per area

3.1. Chapter introduction and objectives

The current global estimation of isoprene emissions, such as the Model of Emissions of Gases and Aerosols from Nature (MEGAN, Guenther et al., 1995; 2006; 2012) combines meteorological data, land use maps, emission inventories (i.e. basal isoprene emission, the isoprene emission capacity under a specific light and leaf temperature), activity factors including responses to light, temperature, leaf age, soil moisture, leaf area index, and CO_2 inhibition. It has been shown that estimation results are highly sensitive to emission inventory (Henrot et al., 2017). Since isoprene emission capacity could change among different species and have intraspecific variation, determination of emission inventory should be carefully obtained from field observations or scientific estimations.

Physiology-linked factors (e.g., temperature, leaf nitrogen concentration, photosynthetic limitations) of isoprene emission capacity of the plant leaves have been well shown by previous studies (e.g., Oku et al., 2014; Litvak et al., 1996; Rosenstiel et al., 2004; Niinemets et al., 1999; Beckett et al., 2008). Currently, however, knowledge of the relationship between morphologic effect and isoprene emission is limited, only Harley et al. (1997) reported that sunlit leaves with higher leaf mass per area (LMA) showed higher area-based isoprene emission flux than shaded leaves for deciduous oak species. It has been showed that the LMA of moso bamboo leaves could vary largely, from 25 to 70 g m^{-2} (Lin et al., 2020), but only isoprene emission from leaves with higher LMA (> 55 g m^{-2}) has been observed. Because the area-based isoprene emission flux is often used for model estimation, leaf morphology could play a critical role in determining isoprene emission capacity. Therefore, by clarifying the relationship between LMA and isoprene emission, a better determination of the emission factor for isoprene could be achieved.

This chapter aims to determine the relationship between isoprene emission capacity and LMA. Here I hypothesize a linkage between area-based isoprene emission flux and LMA to explain the variation in isoprene emission capacity for moso bamboo. To test this hypothesis, this chapter conducted isoprene emission measurements in constant environmental conditions on a hillslope that demonstrates a high morphological diversity for moso bamboo culms. Due to the lack of isoprene emission observations of moso bamboo leaves with LMA of < 55 g m^{-2}, this chapter conducted measurements on leaves of overtopped moso bamboo culms to fill the gap in isoprene emission traits with lower LMA. Because the photosynthetic rate and nitrogen concentration could also influence isoprene emission capacity (Niinemets et al., 1999; Rasulov et al., 2009; Harley et al., 1994; Litvak et al., 1996; Rosenstiel et al., 2004), these factors were also recorded in this chapter to help in determining the attribution of LMA.

3.2. Materials and methods

3.2.1. Site description and sample selection

The field work of this chapter was conducted in an unmanaged pure moso bamboo stand on a hillslope in Fukuoka Prefecture, Japan (33°38' N, 130°33' E) with a slope angle of 42.8°. This site has a subtropical monsoon climate with an average annual temperature of 15.9 °C and annual precipitation of 1833 mm. Average culm density, diameter at breast height (DBH), and height of 8000±480 culms per hectare, 9.5±0.7 cm, and 11.1±0.7 m were recorded, respectively. Previous investigations of vegetation and soil indicated large spatial variations in culm density, culm height, DBH, biomass distribution, soil nitrogen content, and soil moisture at this site (Ichihashi et al., 2015; Shimono et al., 2021). Eight moso bamboo culms (Culm A to Culm H) were chosen for measurement at the site, each of which demonstrated different DBH and culm height values (Table 3-1). Note that the chosen culms demonstrated lower culm height (4.2–7.9 m), DBH (2.0–5.2 cm), and weaker light exposures to their neighboring culms. For each culm, four leaves near the top of the crown were measured for isoprene emission flux, photosynthetic rate, nitrogen concentration, and LMA.

3.2.2. Observations and sampling process

The culm height and DBH were measured for each of the selected culms, and the isoprene emission flux, photosynthetic rate, LMA, and nitrogen concentration were measured for each of the chosen leaves from the selected culms.

The measurement period of isoprene emission flux and photosynthetic rate was August 14–17, 2019. A portable photosynthesis measuring system (LI-6400, Li-Cor Inc., Lincoln, NE, USA) equipped with an LED cuvette (LI-6400-02B, Li-Cor Inc.) was used to conduct the measurements. To capture isoprene, a T-junction (made of Teflon to avoid adsorption of VOCs) was added to replace the original tube between the leaf cuvette of LI-6400 and its embedded infrared gas analyzer (IRGA), adding another channel that can be plugged to an adsorbent tube; a granular filter filled with activated charcoal was connected to the air inlet of the LI-6400 system to supply VOC-free air. The adsorbent tube used for isoprene collection is made of glass and filled with 250 mg Tenax-TA 60/80 mesh (GL Science Inc., Tokyo, Japan), based on the method tested and verified by Chang (2009).

During sampling, the light and leaf temperatures in the cuvette were set at a photosynthetic photon density flux (PPFD) of 1000 μmol m^{-2} s^{-1} and a temperature of 30 °C. Leaves were clapped by the leaf cuvette for approximately 5 min to record the photosynthetic rate and stabilize the isoprene concentration in the cuvette. Then, an adsorbent tube was plugged into the T-junction channel on one side and a micropump (MP-Σ30NII, SIBATA Inc., Tokyo, Japan) on the other side. The pumping rate was set at 150 mL min^{-1} to draw out the air from the leaf cuvette for 400 s. Air (1 L) was passed through the adsorbent tube to trap the isoprene component. The collected adsorbents were stored at a temperature of approximately 5 °C for less than 14 days until isoprene levels were quantified. The area-based photosynthetic rate (A_{Area}, μmol m^{-2} s^{-1}) and mass-based photosynthetic rate (A_{Mass}, mg g^{-1} hr^{-1}) were determined as follows:

$$A_{Area} = A_{Origin} \cdot R_{Cuvette} / R_{Origin} \quad \text{(Equation 3-1)},$$

$$A_{Mass} = A_{Area} \cdot M_{CO_2} \cdot R_{Leaf} / M_{Leaf} \quad \text{(Equation 3-2)},$$

where A_{Origin} (μmol m^{-2} s^{-1}) is the measured value of the photosynthetic rate with the default leaf area (R_{Origin}) set at 6 cm^2, $R_{Cuvette}$ (cm^2) is the actual in-cuvette leaf area,

M_{CO2} is the molecular mass of CO_2 (44.01 g mol^{-1}), R_{Leaf} (cm^2) and M_{Leaf} (g) are the whole leaf area and dry mass of the measured leaf, respectively.

The LMA (g m^{-2}) of the leaves was determined using R_{Leaf} and M_{Leaf}. To obtain R_{Leaf}, the leaves were scanned quickly after excision with a scanner (GT-S650, Seiko Epson Corporation, Nagano, Japan) before deformation due to dehydration, and measured using an image processing software (ImageJ, National Institutes of Health, Bethesda, MD, USA). The scanned leaves were then dried in an oven at 60 °C for 72 h for M_{Leaf} measurement with a microbalance (accuracy: 0.1 mg).

The quantification of isoprene emissions was determined by gas chromatography-mass spectrometry. The isoprene content in the adsorbent tube was first desorbed and re-trapped with a preconcentrator (Model 7100A, Entech Instruments Inc., CA, USA), and then introduced into a gas chromatography system with a mass spectrometer (HP6890, Agilent Technologies Inc., CA, USA) for identification and quantification. A calibration line ($R^2 > 0.995$) was obtained by testing standard samples at different isoprene concentrations (5, 10, 20, 50, and 100 ppb) with the same air flow as the actual field measurements. The obtained isoprene concentration ($C_{Isoprene}$) was then used to calculate the area-based isoprene emission flux (I_{Area}, nmol m^{-2} s^{-1}) and mass-based isoprene emission flux (I_{Mass}, µg g^{-1} hr^{-1}) using the following equation:

$$I_{Area} = C_{Isoprene} \cdot V / R_{Cuvette} \qquad \text{(Equation 3-3),}$$

$$I_{Mass} = I_{Area} \cdot M_{isoprene} \cdot R_{Leaf} / M_{Leaf} \qquad \text{(Equation 3-4),}$$

where V (µmol s^{-1}) is the flow velocity of the LI-6400 air inflow, and $M_{isoprene}$ is the molecular mass of isoprene (68.12 g mol^{-1}).

The whole leaf nitrogen content ($N_{Content}$, mg) was determined using an element analyzer (JM1000 system, J-SCIENCE LAB, Co., Ltd., Japan) based on the Pregl-Dumas method. A calibration line ($R^2 > 0.999$) was established by testing the standard material (hippuric acid, $C_9H_9NO_3$) in different masses (3, 6, 9, 20, 30, and 50 mg). Area-based nitrogen concentration (N_{Area}, g m^{-2}) and mass-based nitrogen concentration (N_{Mass}, %) are defined as follows:

$$N_{Area} = N_{Content} / R_{Leaf} \qquad \text{(Equation 3-5),}$$

$$N_{Mass} = N_{Content} / M_{Leaf} \qquad \text{(Equation 3-6),}$$

3.3. Results

3.3.1. Observation result of isoprene emission flux and its related factors

The moso bamboo culms selected for measurement exhibited various morphologies, with differing DBH and culm height measured; observations including I_{Area}, I_{Mass}, LMA, A_{Area}, A_{Mass}, N_{Area}, and N_{Mass} also demonstrated variations among culms (Table 3-1). Even under the same irradiance (PPFD = 1000 μmol m^{-2} s^{-1}) and leaf temperature (~30 °C), large variations in isoprene emission fluxes were recorded (I_{Area}: 1.4–32.2 nmol m^{-2} s^{-1}; I_{Mass}: 12.4–164.8 μg g^{-1} hr^{-1}). The observed factors also demonstrated variations among leaves, where LMA exhibited a range of 27.5–47.9 g m^{-2}; A_{Area} and A_{Mass} exhibited ranges of 0.6–7.7 μmol m^{-2} s^{-1} and 3.5–31.4 mg g^{-1} hr^{-1}, respectively; N_{Area} and N_{Mass} exhibited ranges of 0.7–1.4 g m^{-2} and 2.3–3.3 %.

Table 3-1 DBH, culm height, leaf mass per area (LMA), area-based isoprene emission flux (I_{Area}), mass-based isoprene emission flux (I_{Mass}), area-based photosynthetic rate (A_{Area}), mass-based photosynthetic rate (A_{Mass}), area-based leaf nitrogen concentration (N_{Area}), and mass-based leaf nitrogen concentration (N_{Mass}) of each moso bamboo culm. (Mean ± standard deviation)

Culm	I_{Area} (nmol m^{-2} s^{-1})	I_{Mass} (μg g^{-1} hr^{-1})	LMA (g m^{-2})	A_{Area} (μmol m^{-2} s^{-1})	A_{Mass} (mg g^{-1} hr^{-1})	N_{Area} (g m^{-2})	N_{Mass} (%)	DBH (cm)	Height (m)
A	24.1±6.0	135.4±28.8	43.6±4.6	4.8±2.1	17.3±6.9	1.2±0.2	2.7±0.2	2.7	5.9
B	16.4±6.2	104.3±42.6	39.5±5.0	5.3±2.7	22.0±11.6	1.0±0.1	2.5±0.1	3.9	6.8
C	14.5±3.8	95.3±24.8	37.3±1.3	4.7±1.4	20.0±5.6	1.0±0.1	2.6±0.1	5.0	7.9
D	11.7±5.2	90.6±45.3	32.4±2.6	3.9±2.2	18.6±10.2	0.8±0.1	2.6±0.2	2.0	4.7
E	11.4±3.0	87.1±18.1	31.8±2.3	2.2±1.2	11.2±5.8	0.9±0.1	2.8±0.1	3.0	4.2
F	10.1±2.3	83.9±18.5	32.2±1.0	3.3±1.2	15.9±5.7	0.9±0.1	2.8±0.3	3.3	6.9
G	8.6±7.5	59.2±48.3	34.7±2.7	4.6±1.6	20.9±6.4	0.9±0.1	2.5±0.2	5.2	7.9
H	5.3±5.0	43.6±40.3	29.2±1.2	2.2±1.4	11.6±7.6	0.9±0.0	3.1±0.0	2.6	6.7

I_{Area} and I_{Mass} were more likely to be associated with varying leaf morphology instead with DBH or culm height though the culms exhibited a large variety in these culm morphologies (Table 3-1). As shown in Figure 3-1, I_{Area} significantly increased with LMA. Statistical tests showed a strong correlation between I_{Area} and LMA ($P < 0.001$; $R = 0.666$), and LMA was determined to be the most significant factor influencing I_{Area}; the effect of LMA on I_{Mass} was less, but still significant (Table 3-2).

Both A_{Area} and N_{Area} exhibited significant positive correlations with I_{Area} (Table 3-2). No relationship was detected, however, between N_{Mass} and I_{Mass} or between A_{Mass} and I_{Mass}. Note that all three observations in the area-based units demonstrated strong correlations with LMA, which explained most of the variation in them (Table 3-2).

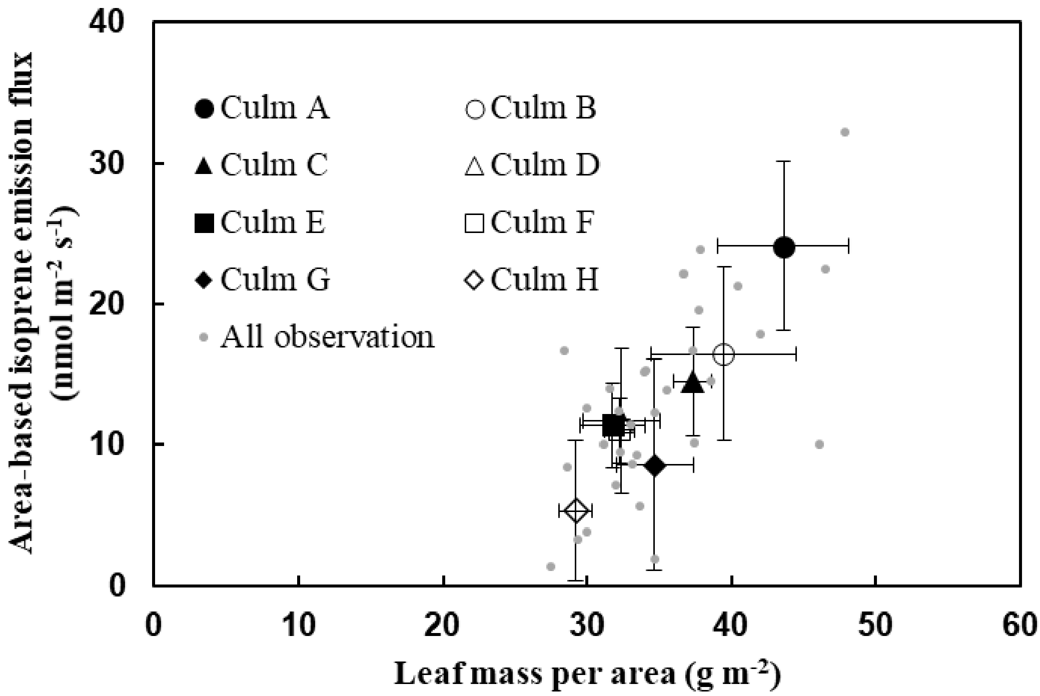

Figure 3-1 Relationship between area-based isoprene emission flux and leaf mass per area. Gray dots represent all the observations. Solid and open circle, triangle, square, and diamond represent observation averages with standard deviation error bars (N = 4) from different culm.

Table 3-2 Correlation coefficient (R) and significance determined by p-value of each pair between area-based isoprene emission flux (I_{Area}), mass-based isoprene emission flux (I_{Mass}), leaf mass per area (*LMA*), area-based photosynthetic rate (A_{Area}), mass-based photosynthetic rate (A_{Mass}), area-based leaf nitrogen concentration (N_{Area}), and mass-based nitrogen concentration (N_{Mass}).

	LMA		A_{Area}		A_{Mass}		N_{Area}		N_{Mass}	
	R	p-value	R	p-value	R	p-value	R	p-value	R	p-value
I_{Area}	0.666	***	0.432	*	0.255		0.586	***	-0.227	
I_{Mass}	0.437	*	0.315		0.190		0.352		-0.227	
LMA			0.507	**	0.292		0.816	***	-0.364	*

*: statistically significant correlation (p-value ≤ 0.05) **: strong correlation (p-value ≤ 0.01) ***: very strong correlation (p-value ≤ 0.001)

3.3.2. Relationship between isoprene emission flux and leaf mass per area across sites

By comparing the results with other studies on isoprene emission from moso bamboo (Chang et al., 2019; under submission), it demonstrates that I_{Area} in here was remarkably lower than those in the other sites (Figure 3-2a). These three sites had different stand characteristics. The site of Chang et al. (2019) was in a pure moso bamboo stand in central Taiwan under an influence of humid subtropical climates. This site keeps well-grown culms with a height of 15 m, and the measured leaf demonstrated the largest LMA among the sites (77.7±16.3 g m^{-2}). The data selected for comparison of this site were recorded in September 2015 with a leaf temperature of 25.7±1.6 °C and PPFD of 1000 μmol m^{-2} s^{-1}. The site of Chang et al. (under submission) was in a specimen garden in Kyoto, Japan. Although the height of the measured culm was relatively low (6.5 m), the leaves were well exposed to sunlight due to a far distribution between each culm at this site and demonstrated a moderate LMA among the sites (52.7±2.3 g m^{-2}). The data collected from this site were recorded in August 2019 with a leaf temperature of 31.4±1.0 °C and a PPFD of 1000 μmol m^{-2} s^{-1}. With I_{Area} adjusted by the G93 model (Guenther et al., 1993) to simulate a temperature of 30 °C, a generally consistent pattern across the different sites could be seen between the adjusted I_{Area} and LMA (R^2 = 0.830) (Figure 3-2).

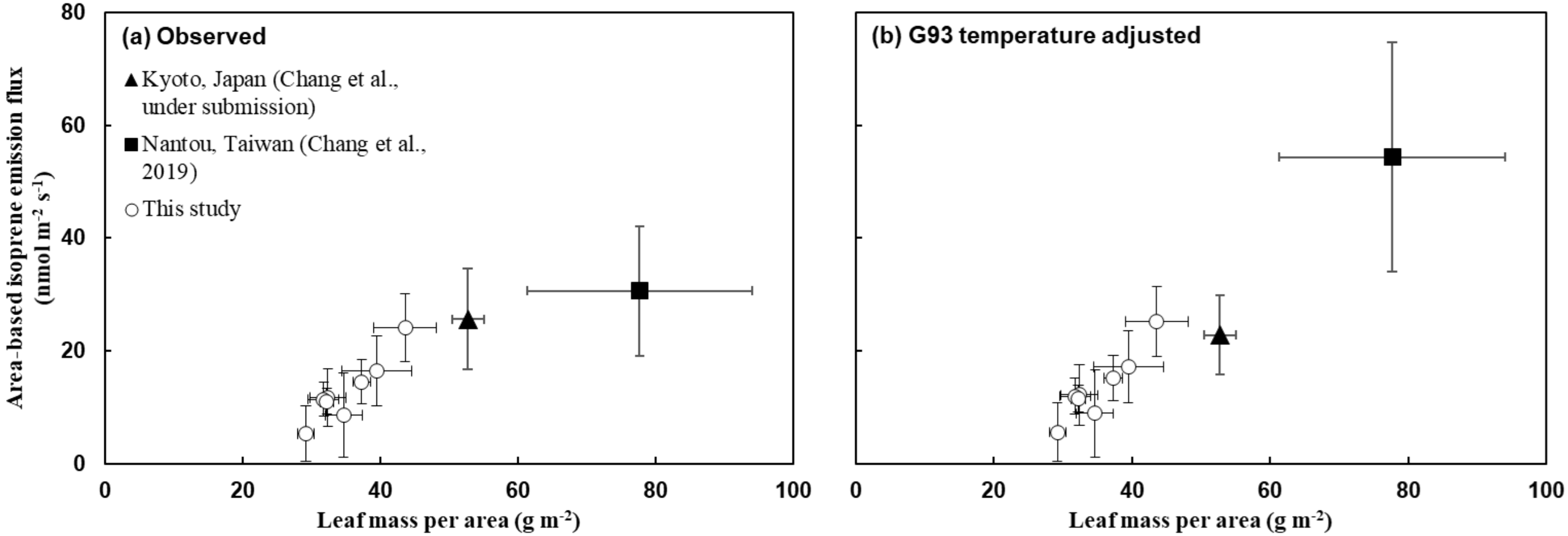

Figure 3-2 Relationship between (a) area-based isoprene emission flux and leaf mass per area, and (b) area-isoprene emission flux adjusted by G93 algorithm (Guenther et al., 1993) and leaf mass per area in different sites (This chapter, Chapter 2, and Chapter 4). Open circles represent the observation averaged by each selected culm in this site (N = 4 per culm, leaf temperature = 29.9±0.0°C); solid square represents the averaged observation from a newly abandoned moso bamboo stand in Taiwan (N = 4, leaf temperature = 25.7±1.6 °C); solid triangle represents the averaged observation from a moso bamboo plot in a specimen garden in Kyoto (N = 3; leaf temperature = 31.4±1.0 °C).

3.4. Discussion

There is no direct evidence of the effect of growth light on LMA for woody bamboos, yet, according to Poorter et al. (2009), LMA is strongly related to light of growth environment in most vegetation. Therefore, a lower LMA would be expected in the overtopped moso bamboo culms in this site. These overtopped leaves demonstrated lower LMA (27.5–47.9 g m^{-2}) when compared to recorded averages according to Lin et al. (2020). The large range of LMA recorded in here could be due to the consequently various canopy gap sizes to the large spatial variation in culm density in this site. Even under the same incident light and temperature, isoprene emission fluxes demonstrated large variance among the selected leaves in this site. By plotting the isoprene emission fluxes and LMA, it could be found that LMA explained most of the variation in I_{Area} and part of the variation in I_{Mass}. Considering the measurements in a previous study on moso bamboos (i.e., Chang et al., 2019; under submission) conducted under similar incident light and season, a consistent pattern was observed between the I_{Area} and LMA across these sites. The linkage between I_{Area} and LMA could be explained by the higher quantity of chloroplasts per unit leaf area for leaves with higher LMA. Assuming that the leaf density is consistent for all leaves, a higher LMA implies thicker mesophylls, which tend to have larger chloroplasts per area (Hanba et al., 1999; Liakoura et al., 2009; Ivanova et al., 2018); isoprene is produced only by chloroplasts in leaves (Wildermuth and Fall, 1996; 1998; Sasaki et al., 2005), meaning a larger quantity of chloroplasts per area could induce larger I_{Area} at the leaf scale.

The positive correlation between I_{Mass} and LMA (Table 3-2) could be partially explained by an increased proportion of mesophyll in leaves with larger LMA. By analyzing the effect from nitrogen concentration and photosynthetic rate on isoprene emission capacity, correlations between I_{Area}, N_{Area}, and A_{Area} were detected. However, since I_{Area}, N_{Area}, and A_{Area} were all demonstrated strong correlations with LMA, LMA could be a confounding variable and lead to spurious correlations between N_{Area} and I_{Area} and between A_{Area} and I_{Area}. To exclude this effect, I analyzed the mass-based form and found no correlation between A_{Mass} and I_{Mass}, nor between N_{Mass} and I_{Mass}. Since nitrogen in ammonium form could potentially enhance isoprene production by enlarging the substrate (i.e., DMAPP) pool of isoprene synthesis (Rosenstiel et al., 2004), no correlation between I_{Mass} and N_{Mass} implies a possibility that the substrate for isoprene production was not constrained by nitrogen status of leaf during the measurement. The dependency of isoprene production on photosynthesis mainly comes from the energetic and reductive agents produced in light-dependent reactions. Previous studies have revealed that this dependency is more likely to relate to the electron transport chain rather than the whole photosynthesis process since photosynthetic rate could be limited by other factors such as stomatal conductance (Rodrigues et al., 2020). Although A_{Mass} did not explain I_{Mass}, the effect of electron transport rate could not be excluded, which has been reported to have a significant influence on isoprene emissions (Rasulov et al., 2009).

3.5. Chapter conclusion

In this chapter, I measured isoprene emission flux from low-LMA moso bamboo leaves under a constant light of 1000 μmol m^{-2} s^{-1} and leaf temperature of ~30 °C. By combining the observations of moso bamboo with higher LMA conducted in previous studies, this chapter filled the knowledge gap in the relationship between isoprene emission capacity and LMA. Because area-based isoprene emission capacity is a critical factor in current global-scale isoprene emission estimation methods, the detection of LMA can provide a better way to determine the isoprene emission capacity of plant leaves.

Reference

Beckett M, Loreto F, Velikova V, Brunetti C, Di Ferdinando M, Tattini M, Calfapietra C, Farrant JM (2012) Photosynthetic limitations and volatile and non-volatile isoprenoids in the poikilochlorophyllous resurrection plant *Xerophyta humilis* during dehydration and rehydration. *Plant, Cell & Environment* 35 (12):2061-2074. https://doi.org/10.1111/j.1365-3040.2012.02536.x

Chang M (2009) Seasonal variations of *C. Sinensis* BVOCs flux measurements and its environmental factors at middle altitude in Taiwan (Master's thesis, National Yunlin University of Science and Technology, Yunlin, Taiwan) Retrived from https://hdl.handle.net/11296/cfx6en

Chang T, Kume T, Okumura M, Kosugi Y (2019) Characteristics of isoprene emission from moso bamboo leaves in a forest in central Taiwan. *Atmospheric Environment* 211:288-295. https://doi.org/10.1016/j.atmosenv.2019.05.026

Guenther AB, Zimmerman PR, Harley PC, Monson RK, Fall R (1993) Isoprene and monoterpene emission rate variability: Model evaluations and sensitivity analyses. *Journal of Geophysical Research* 98 (D7):12609-12617. https://doi.org/10.1029/93JD00527

Guenther A, Hewitt CN, Erickson D, Fall R, Geron C, Graedel T, Harley P, Klinger L, Lerdau M, Mckay WA, Pierce T, Scholes B, Steinbrecher R, Tallamraju R, Taylor J, Zimmerman P (1995) A global model of natural volatile organic compound emissions. *Journal of Geophysical Research: Atmospheres* 100 (D5):8873-8892. https://doi.org/10.1029/94JD02950

Guenther A, Karl T, Harley P, Wiedinmyer C, Palmer PI, Geron C (2006) Estimates of global terrestrial isoprene emissions using MEGAN (Model of Emissions of Gases and Aerosols from Nature). *Atmospheric Chemistry and Physics* 6 (11):3181-3210. https://doi.org/10.5194/acp-6-3181-2006

Guenther AB. Jiang X. Heald Colette L, Sakulyanontvittaya T, Duhl T, Emmons LK, Wang X (2012) The Model of Emissions of Gases and Aerosols from Nature Version 2.1 (MEGAN2.1): An Extended and Updated Framework for Modeling Biogenic Emissions. *Geoscientific Model Development* 5 (6):1471–1492.

Hanba YT, Miyazawa SI, Terashima I (1999) The influence of leaf thickness on the CO_2 transfer conductance and leaf stable carbon isotope ratio for some evergreen tree species in Japanese warm-temperate forests. *Functional Ecology* 13 (5):632-639. https://doi.org/10.1046/j.1365-2435.1999.00364.x

Harley PC, Litvak ME, Sharkey TD, Monson RK (1994) Isoprene Emission from Velvet Bean Leaves (Interactions among Nitrogen Availability, Growth Photon Flux Density, and Leaf Development). *Plant Physiology* 105 (1):279-285. https://doi.org/10.1104/pp.105.1.279

Harley P, Guenther A, Zimmerman P (1997) Environmental controls over isoprene emission in deciduous oak canopies. *Tree Physiology* 17 (11):705-14. https://doi.org/10.1093/treephys/17.11.705

Henrot AJ, Stanelle T, Schröder S, Siegenthaler C, Taraborrelli D, Schultz MG (2017) Implementation of the MEGAN (v2.1) biogenic emission model in the ECHAM6-HAMMOZ chemistry climate model. Geoscientific Model Development 10 (2):903-926. https://doi.org/10.5194/gmd-10-903-2017

Ichihashi R, Komatsu H, Kume T, Onozawa Y, Shinohara Y, Tsuruta K, Otsuki K (2015) Stand-scale transpiration of two Moso bamboo stands with different culm densities. Ecohydrology 8 (3): 450-459. https://doi.org/10.1002/eco.1515

Ivanova LA, Yudina PK, Ronzhina DA, Ivanov LA, Hölzel N (2018) Quantitative mesophyll parameters rather than whole-leaf traits predict response of C3 steppe plants to aridity. New Phytologist 217 (2):558-570. https://doi.org/10.1111/nph.14840

Liakoura V, Fotelli MN, Rennenberg H, Karabourniotis G (2009) Should structure–function relations be considered separately for homobaric vs. heterobaric leaves?. *American Journal of Botany* 96:612-619. https://doi.org/10.3732/ajb.0800166

Lin S, Niklas KJ, Wan Y, Hölscher D, Hui C, Ding Y, Shi P (2020) Leaf shape influences the scaling of leaf dry mass vs. area: a test case using bamboos. Annals of Forest Science 77 (1):[11]. https://doi.org/10.1007/s13595-019-0911-2

Litvak ME, Loreto F, Harley PC, Sharkey TD, Monson RK (1996) The response of isoprene emission rate and photosynthetic rate to photon flux and nitrogen supply in aspen and white oak trees. *Plant, Cell & Environment* 19 (5):549-559. https://doi.org/10.1111/j.1365-3040.1996.tb00388.x

Niinemets Ü, Tenhunen JD, Harley PC, Steinbrecher R (1999) A model of isoprene emission based on energetic requirements for isoprene synthesis and leaf photosynthetic properties for *Liquidambar* and *Quercus*. *Plant, Cell & Environment* 22 (11):1319-1335. https://doi.org/10.1046/j.1365-3040.1999.00505.x

Oku H, Inafuku M, Takamine T, Nagamine M, Saitoh S, Fukuta M (2014) Temperature threshold of isoprene emission from tropical trees, *Ficus virgata* and *Ficus septica*. *Chemosphere* 95:268-273. https://doi.org/10.1016/j.chemosphere.2013.09.003

Poorter H, Niinemets Ü, Poorter L, Wright IJ, Villar R (2009) Causes and consequences of variation in leaf mass per area (LMA): a meta-analysis. *New Phytologist* 182 (3): 565-588. https://doi.org/10.1111/j.1469-8137.2009.02830.x

Rasulov B, Hüve K, Välbe M, Laisk A, Niinemets U (2009) Evidence that light, carbon dioxide, and oxygen dependencies of leaf isoprene emission are driven by energy status in hybrid aspen. *Plant Physiology* 151 (1):448-60. https://doi.org/10.1104/pp.109.141978

Rodrigues TB, Baker CR, Walker AP, McDowell N, Rogers A, Higuchi N, Chambers JQ, Jardine KJ (2020) Stimulation of isoprene emissions and electron transport rates as key mechanisms of thermal tolerance in the tropical species *Vismia guianensis*. *Global Change Biology* 26 (10):5928– 5941. https://doi.org/10.1111/gcb.15213

Rosenstiel TN, Ebbets AL, Khatri WC, Fall R, Monson RK (2004) Induction of Poplar Leaf Nitrate Reductase: A Test of Extrachloroplastic Control of Isoprene Emission Rate. *Plant Biology* 6 (1):12-21. https://doi.org/10.1055/s-2003-44722

Sasaki K, Ohara K, Yazaki K (2005) Gene expression and characterization of isoprene synthase from *Populus alba*. *FEBS Letters* 579 (11):2514-2518. https://doi.org/10.1016/j.febslet.2005.03.066.

Shimono K, Katayama A, Abe H, Enoki T (2021) Carbon and nitrogen storage of dead woody debris in an abandoned Moso bamboo forest. *Bulletin of Kyushu University Forest* 102:9-14. https://doi.org/10.15017/4377826

Wildermuth MC, Fall R (1996) Light-Dependent Isoprene Emission (Characterization of a Thylakoid-Bound Isoprene Synthase in Salix discolor Chloroplasts). *Plant Physiology* 112 (1):171-182. https://doi.org/10.1104/pp.112.1.171

Wildermuth MC, Fall R. (1998) Biochemical characterization of stromal and thylakoid-bound isoforms of isoprene synthase in willow leaves. *Plant Physiology* 116 (3):1111-23. https://doi.org/10.1104/pp.116.3.1111

Chapter 4

Characteristics of isoprene emission flux from leaves of 18 bamboo species

4.1. Chapter introduction

Bamboos are important components of ecosystems, accounting for 3.2 % (36.8 million hectares) of global forest area and occupy 23.6 million hectares in Asia (Lobovikov et al., 2007). Several bamboo species, regardless of growth type, have been reported to expand and invade multiple regions (Okutomi et al., 1996; Torii, 2003; Chiou et al., 2009; Kudo et al., 2011; Takada et al., 2012; Akutsu et al., 2012). Bamboos are plant species under the *Bambusoideae* subfamily, comprising over 1500 species with highly diverse growing traits (Kleinhenz and Midmore, 2001; Clark et al., 2015). In Japan, bamboos include two major subtribe classifications: *Arundinariinae* and *Shibataeinae* subtribes. *Shibataeinae* includes species with woody culms, and *Arundinariinae* is composed of both woody and dwarf bamboos. *Shibataeinae* is believed to have originated from tropical, subtropical or warm-temperate climate regions in China, then imported and adapted in Japan, and *Arundinariinae* originated from warm-temperate to temperate regions in Japan. Nevertheless, bamboo species exhibit a diversity in distribution of habitats; furthermore, even within the same genus, different species might originate from different climates (e.g., *Pleioblastus hindsii*, originated from subtropical regions; *Pleioblastus chino*, originated from temperate regions), which could imply different degrees of heat stress. In addition to climate, a major difference in niche can be observed between the two growth types of bamboos, where dwarf bamboos usually grow in more shaded environments than woody bamboos.

Evidence has shown that isoprene production in plants can promote tolerance to multiple stresses, such as heat, oxidation, and over-irradiance, which can damage cellular membranes or chloroplast membranes in leaves (Siwko et al., 2007; Loreto and Velikova, 2001; Way et al., 2011). However, isoprene emission can also be a cost to the plant in terms of both carbon and energy loss, which is a disadvantage in plant growth (Sharkey and Loreto, 1993). This implies and manifests in different isoprene emission traits of different plant species for fitness to environmental conditions (Sharkey and Loreto, 1993; Monson et al., 2013). Previous studies have revealed that plants produce dimethylallyl pyrophosphate (DMAPP) through 2-C-methyl-D-erythritol 4-phosphate/1-deoxy-D-xylulose 5-phosphate (MEP/DOXP) pathways and convert it to isoprene in the cells of the thylakoid membrane on the stromal side of chloroplasts (Wildermuth and Fall, 1996, 1998; Sasaki et al., 2005). The catalytic reaction of the isoprene synthesis enzyme, isoprene synthase (IspS), which converts DMAPP to isoprene, is required and plays a role in regulating the production rate of isoprene (Silver and Fall, 1991; Sasaki et al., 2005; Oku et al., 2014). The IspS gene is absent in several plant species and this causes non-emission of isoprene from these species (Monson et al., 2013). A previous study demonstrated that isoprene emission ability could vary among species within a genus (e.g., *Quercus* spp., Tani and Kawawata, 2008).

Although the increasing numbers in the area of bamboos, only 2 out of 17 species (i.e., *Phyllostachys pubescens* and *Pleioblastus hindsii*; Chang et al., 2012) are assigned emission flux values based on the observations available in "MEGAN2019b vegetation type EF" (https://bai.ess.uci.edu/megan/data-and-code#h.p_UD2ckP0JM58D), the current default database of MEGANv3.1, while the remaining 15 species were assigned assumed values. Other studies on isoprene emission flux from bamboo leaves (i.e., Okumura et al., 2018) recorded the emission fluxes for a limited number of leaves. However, isoprene emission could also be highly diverse among bamboo species (Okumura et al., 2018). Therefore, it is necessary to observe isoprene emissions from multiple bamboo species for providing realistic emission inventory for better estimation of BVOCs emissions from bamboo species.

At the leaf scale, the concentration of chloroplasts could affect the isoprene emission flux because isoprene is produced in chloroplasts; higher isoprene emission fluxes could be expected in thicker leaves. As a related factor to leaf thickness (Liakoura et al., 2009), Harley et al. (1997) reported a relationship between isoprene emission flux and leaf mass per area (LMA) while using area-based units of isoprene emission flux. In addition, according to the process base of isoprene production, the isoprene product is constrained to the DMAPP pool size, which incorporates pyruvate and glyceraldehyde 3-phosphate into the 5-carbon skeleton to form DMAPP (Wiberley et al., 2009; Vickers et al., 2011; Monson et al., 2012; Schwender et al., 1997; Rohmer, 1999; Lichtenthaler, 1999). The pool size of DMAPP is highly related to photosynthetic chemistry, where the substrate, reducing equivalent, and energy equivalent are acquired and limited by the electron transport rate (ETR) (Brüggemann and Schnitzler, 2002; Rosenstiel et al., 2002; Rasulov et al., 2009; Rasulov et al., 2018). Thus, there is a need to discriminate between the effect of LMA and photosynthetic traits when comparing isoprene emission genotypes across multiple species.

To clarify (1) whether there is a distinction of isoprene emission traits among bamboo species and if so, (2) whether the differences could be explained by differences in LMA or caused by photosynthetic traits such as the photosynthetic rate or ETR, this chapter measured isoprene emission fluxes and other factors of 18 species of bamboos within five genera, including dwarf and woody bamboo types; part of the genera includes species originating from different climates.

4.2. Materials and methods

4.2.1. Site description and selected bamboo species

The field work was conducted in bamboo specimen plots located at Kamigamo experimental station, Kyoto, Japan (35° 04’ N, 135° 46’ E), with an annual temperature of 14.6 °C and annual precipitation of 1582 mm. The bamboos were grown by species, separately in concrete plots. I selected the following 18 species within five genera as measuring subjects: *Phyllostachys makinoi*, *Phyllostachys aurea*, *Phyllostachys bambusoides*, *Phyllostachys pubescens*, *Phyllostachys nigra* f. henonis, *Semiarundinaria fastuosa*, *Semiarundinaria yashadake*, *Semiarundinaria fortis*, *Semiarundinaria kagamiana*, *Pleioblastus hindsii*, *Pleioblastus linearis*, *Pleioblastus simonii*, *Pleioblastus chino*, *Sasa tsuboiana*, *Sasa veitchii*, *Sasa chartacea*, *Sasaella ramosa*, *Sasaella hortensis* *(Phyllostachys*, *Semiarundinaria*, *Pleioblastus*, *Sasa*, and *Sasaella* are hereinafter abbreviated as *P.*, *Se.*, *Pl.*, *S.*, and *Sa.*, respectively). Among them, *Phyllostachys* spp., *Semiarundinaria* spp., and *Pleioblastus* spp. are woody species, whereas *Sasa* spp. and *Sasaella* spp. are dwarf species. Basing on the distribution region described in Ohrnberger (1999), Suzuki (1996), and Kobayashi (2017), I categorize the 18 species into three classifications corresponding to their climate of origins: temperate area (TE) includes *Se. kagamiana*, *Pl. chino* and *S. chartacea*; warm-temperate area (WT) includes *P. bambusoides*, *P. pubescens*, *P. nigra* f. *henonis*, *Se. fastuosa*, *Se. yashadake*, *Se. fortis*, *Pl. simonii*, *S. tsuboiana*, *S. veitchii*, *Sa. ramosa* and *Sa. hortensis*; subtropical area (ST) includes *P. mokinoi*, *P. aurea*, *Pl. hindsii* and *Pl. linearis*. Noted that bamboos gradually defoliate at around January and begins to emerge leaf sprouts at around April and May. Isoprene measurements for some of the species (i.e., *Pl. chino*, *S. chartacea* and *Sa. ramosa*) in May 2020 were observed from new leaves due to die out of old leaf. For other species, old leaves of the 2019 season were observed until May 2020. Basing on our observations made from April 2019 to June 2020, most of the species used in this study share a similar leaf life cycle, whereby leaves usually emerge in April or May and fall after approximately 12 to 14 months. Only two species showed exceptions; one was *P. nigra* f. *henonis*, where the species underwent a synchronous flowering event in October 2019 then died out at about June 2020. The other was *P. pubescens*, which did not emerge any new leaf in 2020 spring and kept most of the leaves to second year. This two-year leaf lifespan of *P. pubescens* was also reported by previous study (Li et al., 1998a,b).

4.2.2. Field sampling

The measurements were conducted monthly from August 2019 to May 2020 (August 2–5, 2019; September 12–18, 2019; October 15–20, 2019; November 13–17, 2019; December 14–16, 2019; January 11–13, 2020; February 24–26, 2020; March 15–20, 2020; April 19–25, 2020; May 17–24, 2020). Each month, measurements were conducted on three leaves of each species. Leaves at or near the top of the culm, which was exposed to full sunlight with no obvious damage or least damage, were chosen for the measurements. The measurements of isoprene observations were conducted using the same procedure and described in Section 3.2.2. In addition to Section 3.2.2., a fluorescence cuvette (LI-6400-40) was used during the ETR measurement. Three steps were performed during each measurement of every leaf. First, the leaf was clapped by the leaf cuvette with controls on irradiance (1000 μmol m^{-2} s^{-1} of photosynthetic photon density flux, PPFD), and also on T_L for each monthly measurement campaigns from September to December 2019, where stable T_L were supplied to 30, 25, 20, and 10 °C respectively from September to December 2019 which were close to the ambient temperature corresponding to each month with an LED cuvette (LI-6400-02B, Li-Cor Inc.). Manipulating T_L into 30 °C was attempted in August 2019, however, the strong heat from sunlight caused a major influence to cause different T_L among measurements. According to the meteorological data in Kyoto City, daily average and maximum air temperature during overavation days in August were 31.7±0.3 and 37.6±0.6, respevtively. T_L of the measurements from January to May 2020 was not controlled and were close to ambient temperatures. During this step, the photosynthetic rate was measured without connecting the adsorbent tubes into the system. The photosynthetic rates here were calculated in area-based form (A_{Area}, μmol m^{-2} s^{-1}) and mass-based form (A_{Mass}, μmol g^{-1} s^{-1}) using the following equations:

$$A_{Area} = A_{Origin} \cdot R_{Cuvette} / R_{Origin} \quad \text{(Equation 4-1)},$$

$$A_{Mass} = A_{Area} \cdot R_{Leaf} / M_{Leaf} \quad \text{(Equation 4-2)},$$

where A_{Origin} (μmol m^{-2} s^{-1}) is the measured value of the photosynthetic rate with the default leaf area (R_{Origin}) set at 6 cm^2, $R_{Cuvette}$ (cm^2) is the actual in-cuvette leaf area,

R_{Leaf} (cm^2) and M_{Leaf} (g) is the whole leaf area and dry mass of the measured leaf, respectively.

After approximately 5 min to stabilize the isoprene concentration in the cuvette in the first step, next, an adsorbent tube was plugged into the T-junction channel on one side, and a micropump (MP-Σ30NII, SIBATA Inc., Tokyo, Japan) on the other side. The micropump was set at a rate of 150 mL min^{-1} to draw out the air from the cuvette for 400 s. Air (1 L) was passed through the adsorbent tube to trap the VOC component, including isoprene. After VOC collection, the adsorbent tube was immediately stored at a temperature of approximately 5 °C.

The final step of field sampling was to measure the ETR of the leaf using the fluorescence method. During this step, a standard light set at 1500 μmol m^{-2} s^{-1} of PPFD with 10 % blue light was supplied to the leaf, and the steady state fluorescence (F_S, μmol m^{-2} s^{-1}) was recorded when it stabilized. A one-second light pulse with over 7000 μmol m^{-2} s^{-1} was then applied to acquire the maximum fluorescence (F_m, μmol m^{-2} s^{-1}). Area- and mass-based ETR (ETR_{Area}, μmol m^{-2} s^{-1}; ETR_{Mass}, μmol g^{-1} s^{-1}) were calculated using the following equations:

$$ETR_{Area} = ((F_m - F_S)/F_m) \cdot L \cdot Q \cdot \alpha_{Leaf} \qquad \text{(Equation 4-3)},$$

$$ETR_{Mass} = E_{Area} \cdot R_{Leaf}/M_{Leaf} \qquad \text{(Equation 4-4)},$$

where L is the PPFD of standard light (1500 μmol m^{-2} s^{-1}), Q is the fraction of absorbed quanta used by photosystem II (assumed to be 0.5), and α_{Leaf} is the leaf absorptance (assumed to be 0.84).

4.2.3. Isoprene flux observation

After the field measurements, the measured leaves and the adsorbent tubes were collected in the laboratory for analysis. The leaves were scanned before deformation then dried at 60 °C for 72 h to acquire R_{Leaf}, $R_{Cuvette}$, M_{Leaf}, and LMA.

To determine the isoprene concentration ($C_{Isoprene}$), isoprene content in the adsorbent tube was desorbed and re-trapped with a preconcentrator (Model 7100A, Entech Instruments Inc., CA, USA), and then introduced into a gas chromatography system with a mass spectrometer (HP6890, Agilent Technologies Inc., CA, USA) for identification and quantification. Area-based isoprene emission flux (I_{Area}, nmol m^{-2} s^{-1})

and mass-based isoprene emission flux (I_{Mass}, nmol g^{-1} s^{-1}) were calculated as follows:

$$I_{Area} = C_{Isoprene} \cdot V / R_{Cuvette} \qquad \text{(Equation 4-5),}$$

$$I_{Mass} = I_{Area} \cdot R_{Leaf} / M_{Leaf} \qquad \text{Equation (4-6),}$$

where V (μmol s^{-1}) is the flow velocity of LI-6400 air inflow.

4.3. Results

4.3.1. Isoprene emission fluxes of 18 species of bamboo from August 2019 to May 2020

The results of the measurement of isoprene emission from the subject bamboo species indicated a large range of I_{Area} (from 0 to 50.21 nmol m^{-2} s^{-1}). All species were found to emit isoprene in August 2019 and the emission gradually decreased or ceased from September 2019 to February 2020, before slowly increasing from March to May 2020. Noted that isoprene measurements for *Pl. chino*, *S. chartacea* and *Sa. ramosa* in May 2020 were observed from new leaves. The variation in isoprene emission fluxes generally corresponded with the fluctuation of leaf temperature; August 2019 had the highest leaf temperatures (30–35 °C) and January 2020 had the lowest leaf temperatures (~5 °C) (Table 4-1; 4-2).

A large discrepancy in the relationship between isoprene emission and leaf temperature in each genus was recorded between the woody species (*Phyllostachys*, *Semiarundinaria,* and *Pleioblastus* spp.) and the dwarf species (*Sasa* and *Sasaella* spp.). The woody species exhibited large isoprene emission fluxes, which were mainly distributed in a leaf temperature range of 25–35 °C; whereas the dwarf species exhibited very low or no isoprene emission at all leaf temperatures (Figure 4-1).

Table 4-1 Area-based isoprene emission flux and leaf temperature in each month from August 2019 to December 2020 of 18 bamboo species. The values are represented in mean ± standard deviation with three measurements.

pecies	August 2019		September 2019		October 2019		November 2019		December 2019	
	I_{Area} (nmol m^{-2} s^{-1})	T_L (°C)	I_{Area} (nmol m^{-2} s^{-1})	T_L (°C)	I_{Area} (nmol m^{-2} s^{-1})	T_L (°C)	I_{Area} (nmol m^{-2} s^{-1})	T_L (°C)	I_{Area} (nmol m^{-2} s^{-1})	T_L (°C)
P. makinoi	36.8±12.3	30.3±0.5	13.3±6.4	30.0±0.1	3.3±0.5	24.9±0.0	7.7±1.5	19.9±0.0	3.8±0.4	10.0±0.1
P. aurea	14.9±5.7	30.7±0.7	11.3±2.6	29.9±0.0	4.0±1.2	25.0±0.0	7.7±1.1	19.9±0.0	3.9±0.2	9.9±0.0
P. bambusoides	17.5±2.1	30.2±0.5	6.3±1.2	30.0±0.0	1.5±0.3	24.9±0.0	5.7±2.6	20.0±0.0	10.0±2.8	10.0±0.0
P. pubescens	25.6±8.9	31.4±1.0	12.1±3.2	30.0±0.0	1.4±1.1	25.0±0.0	2.2±0.3	20.0±0.1	4.3±0.2	10.0±0.0
P. nigra f. henonis	4.9±3.7	30.2±0.3	6.9±1.7	30.0±0.0	0.9±0.1	24.7±0.1	0.4±0.6	20.0±0.1	n.d.	10.0±0.0
Se. fastuosa	14.2±3.6	30.8±0.2	6.2±0.8	30.0±0.0	0.8±0.1	24.8±0.1	1.5±0.3	19.8±0.1	n.d.	10.0±0.0
Se. yashadake	29.5±15.9	31.6±0.3	10.3±1.4	30.0±0.0	1.6±0.5	24.9±0.0	1.0±0.4	19.9±0.0	n.d.	10.0±0.0
Se. fortis	21.6±5.5	31.5±0.3	14.0±3.7	29.9±0.0	1.8±0.6	24.8±0.0	1.5±0.2	19.6±0.2	2.2±1.9	10.0±0.0
Se. kagamiana	23.5±5.8	31.7±0.3	9.8±3.1	30.0±0.0	1.2±0.2	24.8±0.1	0.9±0.1	19.9±0.0	0.7±1.2	10.0±0.0
Pl. hindsii	30.0±2.2	32.0±1.0	16.7±1.4	30.0±0.1	1.0±0.9	24.8±0.0	n.d.	19.3±0.2	n.d.	9.9±0.0
Pl. linearis	42.7±6.1	34.0±0.6	7.9±4.6	30.0±0.0	0.3±0.5	23.8±0.6	n.d.	19.8±0.2	n.d.	9.7±0.0
Pl. simonii	43.0±8.8	33.2±0.5	15.7±1.4	29.9±0.0	2.3±0.3	24.9±0.1	n.d.	19.9±0.0	n.d.	10.0±0.0
Pl. chino	24.0±7.9	33.5±0.2	18.3±2.4	29.9±0.0	2.6±0.3	24.9±0.0	n.d.	20.0±0.0	n.d.	9.9±0.0
S. tsuboiana	7.0±3.1	32.4±1.3	0.7±0.7	29.9±0.0	0.3±0.3	25.0±0.2	n.d.	19.7±0.2	n.d.	9.9±0.0
S. veitchii	0.2±0.2	30.4±0.4	n.d.	30.0±0.0	n.d.	25.0±0.2	n.d.	19.9±0.0	n.d.	9.7±0.0
S. chartacea	1.4±0.2	32.5±1.5	1.0±0.9	30.1±0.3	0.1±0.1	24.9±0.0	n.d.	19.9±0.0	n.d.	9.9±0.0
Sa. ramosa	0.6±0.2	31.1±0.2	n.d.	29.8±0.2	n.d.	24.7±0.0	n.d.	20.0±0.0	n.d.	9.9±0.0
Sa. hortensis	0.5±0.2	34.1±1.0	n.d.	30.0±0.1	n.d.	24.7±0.0	n.d.	20.0±0.0	n.d.	9.9±0.0

n.d.: No detection

Table 4-2 Area-based isoprene emission flux and leaf temperature in each month from January to May 2020 of 18 bamboo species. The values are represented in mean ± standard deviation with three measurements.

Species	January 2020		February 2020		March 2020		April 2020		May 2020	
	I_{Area} (nmol m^{-2} s^{-1})	T_L (°C)	I_{Area} (nmol m^{-2} s^{-1})	T_L (°C)	I_{Area} (nmol m^{-2} s^{-1})	T_L (°C)	I_{Area} (nmol m^{-2} s^{-1})	T_L (°C)	I_{Area} (nmol m^{-2} s^{-1})	T_L (°C)
P. makinoi	0.4±0.7	5.2±0.2	0.1±0.1	10.9±0.0	0.1±0.1	15.4±0.3	0.0±0.0	12.9±0.4	0.0±0.0	25.9±0.9
P. aurea	n.d.	5.2±0.1	0.1±0.0	11.0±0.0	0.1±0.0	12.9±0.5	0.1±0.1	14.3±0.3	1.8±3.1	30.0±1.0
P. bambusoides	1.0±0.0	5.5±0.5	0.1±0.0	11.0±0.0	0.4±0.2	14.8±0.1	1.0±0.1	14.5±0.5	6.2±3.5	26.8±1.6
P. pubescens	n.d.	6.1±0.0	0.03±0.03	11.0±0.0	0.1±0.0	10.7±1.3	0.2±0.1	15.6±1.5	2.4±0.4	31.2±0.5
P. nigra f. henonis	n.d.	5.3±0.0	n.d.	11.0±0.0	0.1±0.1	14.5±0.1	n.d.	15.7±0.1	1.2±2.2	25.1±0.8
Se. fastuosa	n.d.	5.6±0.0	n.d.	10.0±0.0	0.04±0.01	12.6±0.5	0.1±0.0	20.5±0.0	1.9±0.3	30.9±0.3
Se. yashadake	n.d.	5.2±0.0	n.d.	11.0±0.0	0.04±0.01	13.0±0.5	0.5±0.1	20.1±0.2	10.5±4.9	34.1±0.4
Se. fortis	n.d.	5.6±0.2	n.d.	11.0±0.0	0.05±0.00	12.8±0.6	1.0±0.1	22.4±1.1	7.0±2.5	31.9±0.3
Se. kagamiana	n.d.	5.2±0.0	n.d.	11.0±0.0	0.1±0.0	12.4±0.2	1.0±0.4	22.0±0.9	8.8±3.6	31.8±0.3
Pl. hindsii	n.d.	7.4±0.0	n.d.	11.7±0.0	0.1±0.0	16.8±0.9	0.1±0.0	22.1±0.1	0.2±0.2	29.7±1.2
Pl. linearis	n.d.	7.6±0.0	n.d.	11.3±0.0	0.2±0.1	13.9±0.6	0.1±0.1	20.7±0.4	1.8±1.5	27.6±1.7
Pl. simonii	n.d.	7.3±0.0	n.d.	10.6±0.0	0.1±0.1	12.0±0.6	0.1±0.0	19.5±1.6	0.1±0.1	24.4±0.3
Pl. chino	n.d.	4.8±0.0	n.d.	9.9±0.0	0.1±0.0	12.0±0.9	0.1±0.0	19.7±1.4	3.0±1.7	24.7±0.9
S. tsuboiana	n.d.	5.5±0.0	n.d.	9.9±0.0	n.d.	12.0±0.0	0.1±0.0	20.1±0.3	n.d.	24.4±0.3
S. veitchii	n.d.	7.2±0.0	n.d.	9.8±0.0	n.d.	12.5±0.0	0.1±0.0	23.6±0.2	n.d.	27.3±1.7
S. chartacea	n.d.	6.7±0.0	n.d.	10.0±0.0	n.d.	12.1±0.0	0.1±0.0	21.8±0.4	0.1±0.2	28.3±0.7
Sa. ramosa	n.d.	4.9±0.0	n.d.	9.8±0.0	n.d.	12.0±0.0	n.d.	23.2±0.2	n.d.	25.8±0.7
Sa. hortensis	n.d.	4.9±0.0	n.d.	9.8±0.0	n.d.	12.0±0.0	n.d.	23.2±0.0	n.d.	25.8±0.0

n.d.: No detection

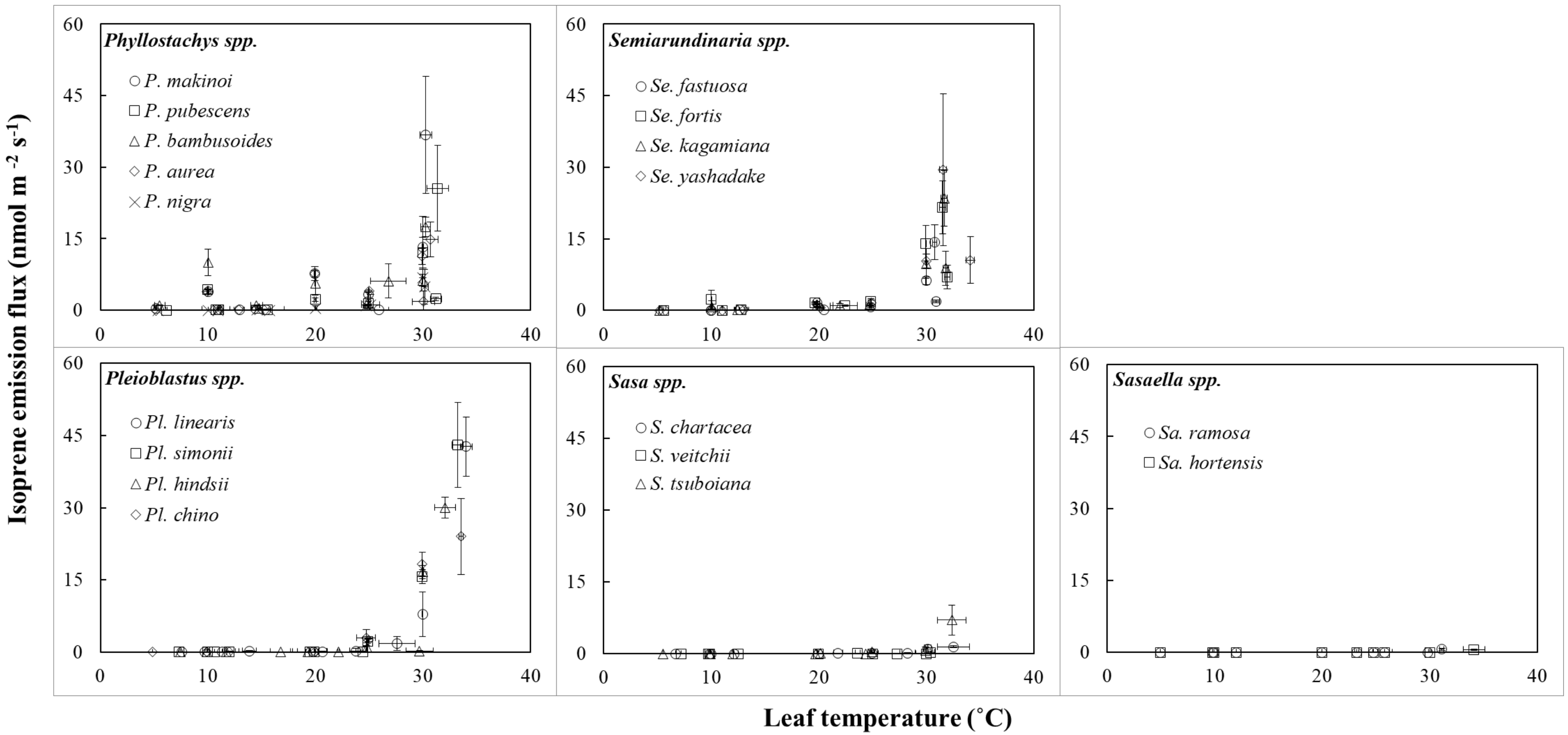

Figure 4-1 Isoprene emission flux in response to leaf temperature for 18 species of bamboo within five genera from August 2019 to May 2020. The open circles are averaged observations of each species in each month (three measurements). The vertical and horizontal error bars represent standard deviation of isoprene emission flux and leaf temperature, respectively.

Since the major difference in isoprene emissions among the bamboo species was recorded in August and September 2019, the averaged I_{Area} and T_L of each species in August and September 2019 are plotted in Figure 4-2. In August 2019, nine out of thirteen woody bamboo species exhibited isoprene emission fluxes larger than 20 nmol m^{-2} s^{-1} regardless of subtribe (*P. makinoi*, *P. pubescens*, *Se. yashadake*, *Se. fortis*, *Se. kagamiana*, *Pl. hindsii*, *Pl. linearis*, *Pl. simonii* and *Pl. chino*), however, none of the dwarf species demonstrated area-based emission fluxes larger than 10 nmol m^{-2} s^{-1}. On average, woody species demonstrated higher isoprene emission fluxes (August 2019: 25.24±12.71 nmol m^{-2} s^{-1}; September 2019: 11.37±4.66 nmol m^{-2} s^{-1}) compared to those of the dwarf species (August 2019: 1.96±2.80 nmol m^{-2} s^{-1}; September 2019: 0.34±0.60 nmol m^{-2} s^{-1}).

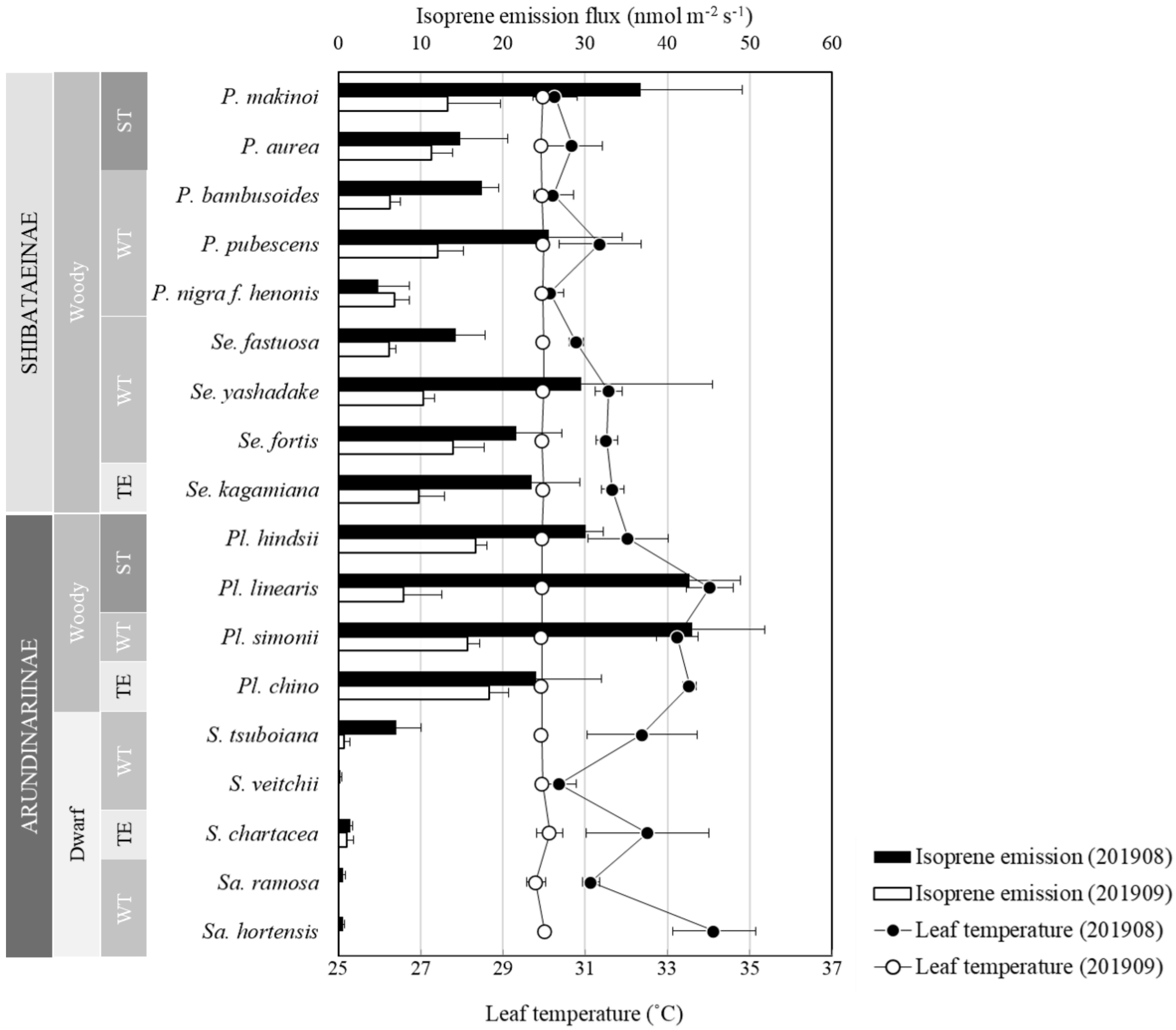

Figure 4-2 Isoprene emission flux and leaf temperature of 18 bamboo species observed in August and September 2019. Solid bars and open bars represent mean isoprene emission flux with error bars representing standard deviation during August and September 2019, respectively; Solid circles and open circles represent mean leaf temperature with error bars representing standard deviation during August and September 2019, respectively. TE, WT, and ST are the climate of the region of origin of the species, which stand for temperate, warm temperate, and subtropical, respectively. *Arundinariinae* and *Shibataeinae* are subtribes under *Arundinarieae* tribe. Woody and dwarf represent two different growth types in bamboo stem.

Moreover, when the isoprene emission fluxes were compared based on the climate of the region of origin, no significant difference in I_{Area} was observed among different climatic origins for both woody and dwarf species during August and September (Table 4-3).

A decrease in both isoprene emission and leaf temperature was observed in most of the species from August to September. However, this decrease was not proportional to the change in leaf temperature. For instance, *P. makinoi* demonstrated a 64 % decrease in isoprene emission flux without a large difference in leaf temperature; in contrast, *Pl. chino* exhibited no significant change in isoprene emission flux, while a large difference in leaf temperature was observed.

Table 4-3 One-way ANOVA of the effect from climatic origins on isoprene emission fluxes for the woody and dwarf species in August and September 2019. A p-value ≤ 0.05 is needed to discard the null hypothesis that no significant difference in isoprene emission flux among the climatic origins.

	Sum of squared error	Degree of freedom	Mean squared error	F-ratio	p-value
Woody, August 2019					
Between Climates	601.64	2	300.82	1.96	0.16
Within Climates	5539.17	36	153.87		
Total	6140.81	38			
Woody, September 2019					
Between Climates	89.29	2	44.65	2.19	0.13
Within Climates	714.30	35	20.41		
Total	803.59	37			
Dwarf, August 2019					
Between Climates	1.08	1	1.08	0.12	0.73
Within Climates	116.14	13	8.93		
Total	117.22	14			
Dwarf, September 2019					
Between Climates	1.62	1	1.62	0.18	0.68
Within Climates	3.71	13	0.29		
Total	5.33	14			

4.3.2. Relationship between LMA and isoprene emission flux

Positive relationships were observed between area-based isoprene emission flux and LMA of the woody species when the monthly linear relationship was evaluated separately (Table 4-4). The woody species exhibited slopes of 0.574 and 0.238 in August and September 2019, respectively; no linear relationship between area-based isoprene emission flux and LMA was observed in the dwarf species (Figure 4-3). Although there was no significant difference in LMA between the dwarf species and the woody species (Table 4-5), the isoprene emission of the dwarf species was lower than that of the woody species under any degree of LMA.

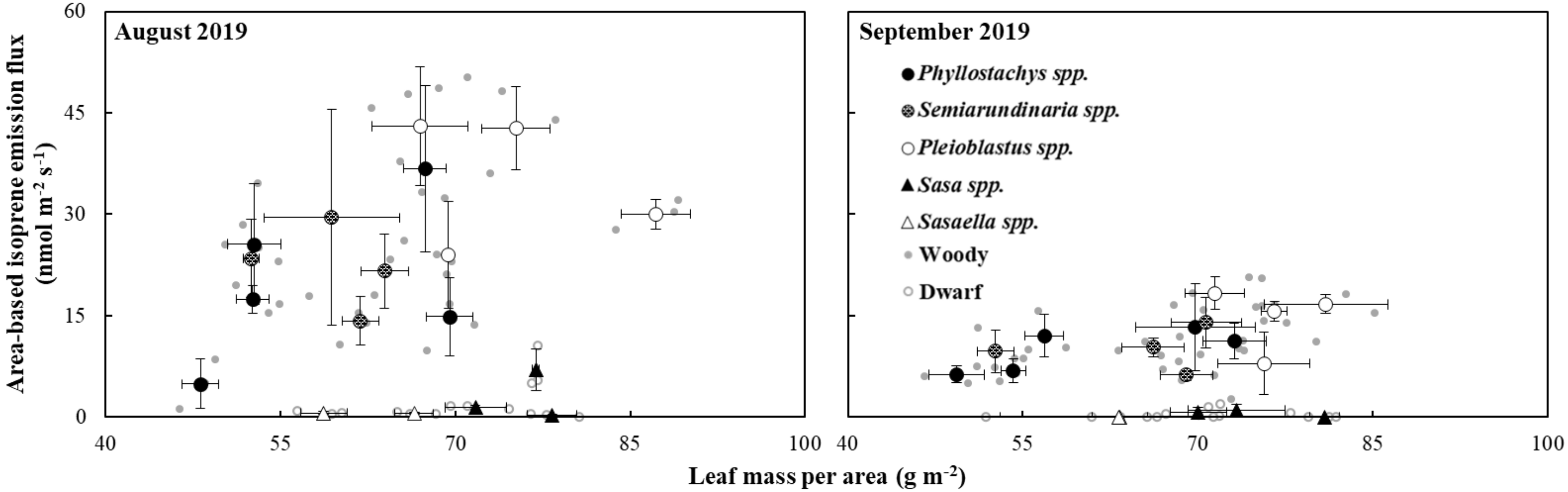

Figure 4-3 Area-based isoprene emission flux in response to leaf mass per area for 18 species of bamboo within five genera observed in August and September 2019. Solid circles, dot-pattern circles, and diagonal-pattern circles, with error bars representing standard deviations, indicate averaged observations of each species in *Phyllostachys*, *Semiarundinaria,* and *Pleioblastus*, respectively; open triangles and dot-pattern triangles, with error bars representing standard deviations, indicate averaged observations of each species in *Sasa* and *Sasaella*, respectively.

Table 4-4 Coefficient of determination (R^2) and p-value of each pair between area-based isoprene emission flux (I_{Area}), mass-based isoprene emission flux (I_{Mass}), leaf mass per area (*LMA*), area-based electron transport rate (ETR_{Area}), mass-based electron transport rate (ETR_{Mass}), area-based photosynthetic rate (A_{Area}), and mass-based photosynthetic rate (A_{Mass}) for 13 species of woody bamboos.

Aug 2019, Woody species	I_{Mass}		*LMA*		ETR_{Area}		ETR_{Mass}		A_{Area}		A_{Mass}	
	R^2	p-value	R^2	p-value	R^2	p-value	R^2	p-value	R^2	p-value	R^2	p-value
I_{Area}	0.896	***	0.237	**	0.378	***	0.168	**	0.257	***	0.099	
I_{Mass}			0.043		0.338	***	0.287	***	0.233	**	0.165	*
LMA					0.157	*	0.011		0.057		0.018	
ETR_{Area}							0.741	***	0.406	***	0.285	***
ETR_{Mass}									0.315	***	0.436	***
A_{Area}											0.843	***
Sep 2019, Woody species												
I_{Area}	0.853	***	0.277	***	0.542	***	0.418	***	0.472	***	0.355	***
I_{Mass}			0.032		0.434	***	0.448	***	0.242	**	0.277	***
LMA					0.177	**	0.030		0.463	***	0.137	*
ETR_{Area}							0.926	***	0.428	***	0.369	***
ETR_{Mass}									0.259	***	0.302	***
A_{Area}											0.856	***

*: statistically significant correlation (p-value ≤ 0.05) **: strong correlation (p-value ≤ 0.01) ***: very strong correlation (p-value ≤ 0.001)

Table 4-5 Coefficient of determination (R^2) and p-value of each pair between area-based isoprene emission flux (I_{Area}), mass-based isoprene emission flux (I_{Mass}), leaf mass per area (*LMA*), area-based electron transport rate (ETR_{Area}), mass-based electron transport rate (ETR_{Mass}), area-based photosynthetic rate (A_{Area}), and mass-based photosynthetic rate (A_{Mass}) for 5 species of dwarf bamboos.

	I_{Mass}		*LMA*		ETR_{Area}		ETR_{Mass}		A_{Area}		A_{Mass}	
	R^2	p-value	R^2	p-value	R^2	p-value	R^2	p-value	R^2	p-value	R^2	p-value
Aug 2019, Dwarf species												
I_{Area}	0.999	***	0.145		0.207		0.012		0.028		0.069	
I_{Mass}			0.128		0.222		0.018		0.027		0.063	
LMA					0.058		0.466	**	0.028		0.049	
ETR_{Area}							0.749	***	0.123		0.234	
ETR_{Mass}									0.054		0.282	*
A_{Area}											0.839	***
Sep 2019, Dwarf species												
I_{Area}	0.999	**	0.014		0.544	**	0.486	**	0.047		0.037	
I_{Mass}			0.013		0.538	**	0.485	**	0.047		0.036	
LMA					0.073		0.023		0.108		0.022	
ETR_{Area}							0.827	***	0.447	**	0.404	*
ETR_{Mass}									0.324	*	0.379	*
A_{Area}											0.958	***

*: statistically significant correlation (p-value ≤ 0.05)   **: strong correlation (p-value ≤ 0.01)   ***: very strong correlation (p-value ≤ 0.001)

4.3.3. Relationship between photosynthetic traits and isoprene emission flux

In August and September 2019, the range of ETR_{Area} observation for the woody species and dwarf species were 30–160 μmol m^{-2} s^{-1} and 60–150 μmol m^{-2} s^{-1}, respectively, and most of the species demonstrated lower ETR_{Area} in September 2019 regardless of their growth types (Table 4-6; 4-7). No significant differences were recorded between the woody species and dwarf species. Linear relationships between isoprene emission flux and ETR_{Area} were shown in the observations including those during August and September 2019 for the woody species; even more definitive relationships could be recorded if monthly observations were separately evaluated for the woody species, where R^2 in August and September 2019 were up to 0.378 and 0.525, respectively, and both of the correlations were significant according to the analysis of T-test (p-value < 0.01) (Table 4-4).

Since both the measurement of I_{Area} and ETR_{Area} in the area-based form demonstrated a correlation with LMA, a spurious correlation might exist between them. To exclude the effect of the potential spurious correlation, the isoprene emission flux against ETR in mass-based units was also tested. The results show that I_{Mass} increased with ETR_{Mass} in August and September 2019 for the woody species but was less definitive compared to those in area-base units and no correlation was seen when the observations during August and September 2019 for the woody species were included (Figure 4-4).

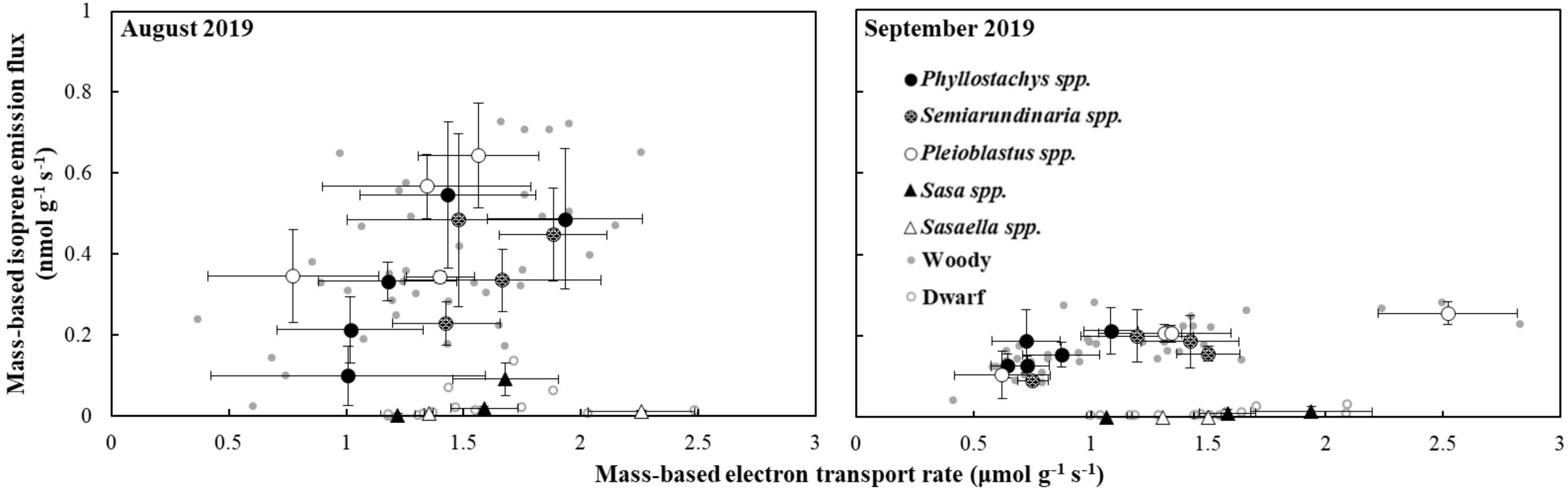

Figure 4-4 Mass-based isoprene emission flux in response to mass-based electron transport rate for 18 species of bamboo within five genera observed in August and September 2019. Solid circles, dot-pattern circles, and diagonal-pattern circles, with error bars representing standard deviations, indicate averaged observations of each species in *Phyllostachys*, *Semiarundinaria,* and *Pleioblastus*, respectively; open triangles and dot-pattern triangles, with error bars representing standard deviations, indicate averaged observations of each species in *Sasa* and *Sasaella*, respectively. Solid gray dots and open gray dots represent observations in the woody species (*Phyllostachys*, *Semiarundinaria,* and *Pleioblastus* spp.) and the dwarf species (*Sasa* and *Sasaella* spp.), respectively.

The woody species exhibited extremely positive correlations between I_{Area} and A_{Area} in August and September 2019 (Table 4-4); no correlation was exhibited by the dwarf species (Table 4-5). Part of the correlation between I_{Area} and ETR_{Area} might be due to the spurious correlation from the LMA. I_{Mass} also increased with A_{Mass} in August and September 2019 for the woody species (Figure 4-5), but with a lower correlation compared to I_{Area} and A_{Area} (Table 4-4).

The photosynthetic rate did not show a large difference between the woody species and dwarf species. Due to the discrepancy in isoprene emission, the ratio of carbon emitted as isoprene to carbon fixed by net photosynthesis ($\mathrm{Carbon\ ratio}\ (\%) = I_{Area}(\mu mol\ m^{-2}s^{-1}) \div A_{Area}(\mu mol\ m^{-2}s^{-1})$ indicated a large variation. Woody species in August and September 2019 exhibited average carbon ratios of 1.6 % and 0.6 %, respectively; carbon ratios observed in the dwarf species in August and September 2019 were much lower, at approximately 0.1 % and 0.0 %, respectively (Table 4-6; Table 4-7).

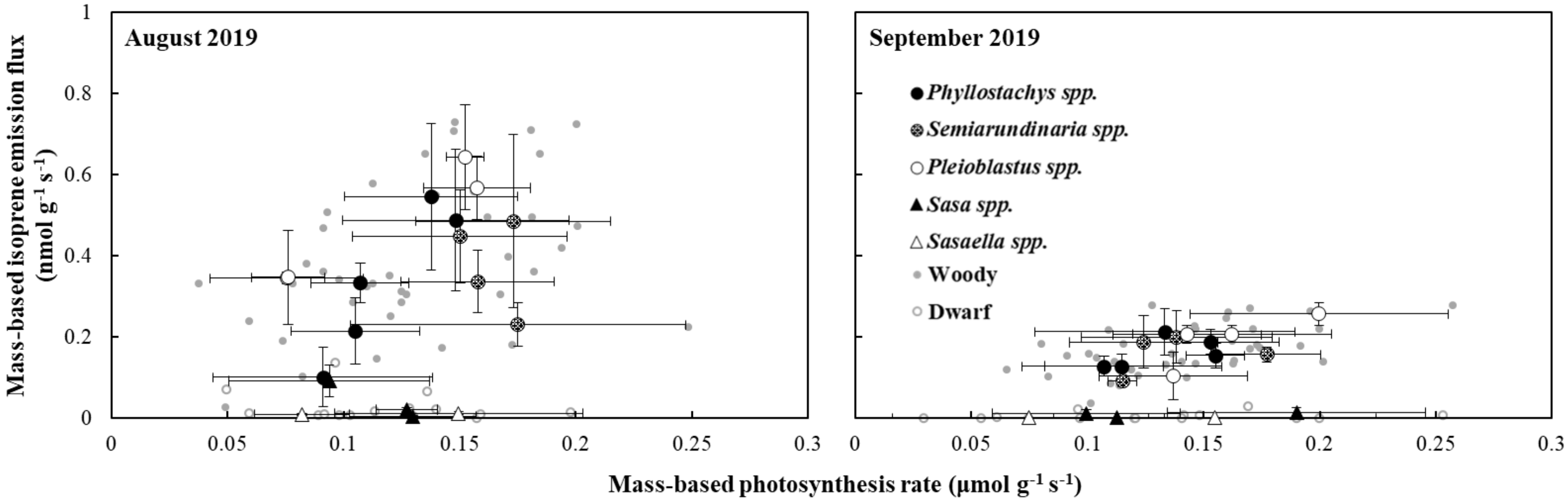

Figure 4-5 Mass-based isoprene emission flux in response to mass-based photosynthetic rate for 18 species of bamboo within five genera observed in August and September 2019. Solid circles, dot-pattern circles, and diagonal-pattern circles, with error bars representing standard deviations, indicate averaged observations of each species in *Phyllostachys*, *Semiarundinaria,* and *Pleioblastus*, respectively; open triangles and dot-pattern triangles, with error bars representing standard deviations, indicate averaged observations of each species in *Sasa* and *Sasaella*, respectively. Solid gray dots and open gray dots represent each observation in the woody species (*Phyllostachys*, *Semiarundinaria,* and *Pleioblastus* spp.) and the dwarf species (*Sasa* and *Sasaella* spp.), respectively.

Table 4-6 Area-based isoprene emission (I_{Area}), area-based photosynthetic rate (A_{Area}), carbon ration, leaf temperature (T_L), and area-based electron transport rate (ETR_{Area}) in August and September 2019 for 13 species of woody bamboos. The values are represented in mean ± standard deviation.

Genus	Species	I_{Area} (nmol m^{-2} s^{-1})		A_{Area} (μmol m^{-2} s^{-1})		Carbon ratio (%)		T_L (°C)		ETR_{Area} (μmol m^{-2} s^{-1})	
		Aug 2019	Sep 2019	Aug 2019	Sep 2019	Aug 2019	Sep 2019	Aug 2019	Sep 2019	Aug 2019	Sep 2019
Phyllostachys	*P. makinoi*	36.8±12.3	13.3±6.4	9.3±2.7	10.7±2.4	2.0±0.6	0.6±0.2	30.3±0.5	30.0±0.1	96.9±26.8	51.0±13.8
	P. aurea	14.9±5.7	11.3±2.6	7.3±1.8	11.3±1.0	1.0±0.4	0.5±0.1	30.7±0.7	29.9±0.0	70.9±22.5	63.9±12.3
	P. bambusoides	17.5±2.1	6.3±1.2	5.7±1.2	5.2±1.0	1.6±0.6	0.6±0.1	30.2±0.5	30.0±0.0	62.2±17.1	35.9±5.2
	P. pubescens	25.6±8.9	12.1±3.2	7.9±2.8	7.6±3.4	1.8±0.9	0.9±0.4	31.4±1.0	30.0±0.0	101.7±16.4	61.6±5.4
	P. nigra f. henonis	4.9±3.7	6.9±1.7	4.4±2.4	6.2±2.3	0.5±0.2	0.6±0.3	30.2±0.3	30.0±0.0	49.0±29.6	34.9±3.3
	Average	19.9±12.8	10.0±4.2	6.9±2.6	8.2±3.1	1.4±0.7	0.6±0.2	30.5±0.7	30.0±0.0	76.1±28.6	49.5±14.8
Semiarundinaria	*Se. fastuosa*	14.2±3.6	6.2±0.8	10.8±4.5	7.9±0.2	0.8±0.5	0.4±0.0	30.8±0.2	30.0±0.0	88.2±13.9	51.9±3.0
	Se. yashadake	29.5±15.9	10.3±1.4	10.3±3.0	11.8±1.8	1.4±0.4	0.4±0.1	31.6±0.3	30.0±0.0	89.1±36.1	99.4±11.5
	Se. fortis	21.6±5.5	14.0±3.7	10.1±2.4	9.7±2.6	1.1±0.1	0.8±0.1	31.5±0.3	29.9±0.0	107.1±29.9	84.2±13.5
	Se. kagamiana	23.5±5.8	9.8±3.1	7.9±2.5	6.5±1.5	1.5±0.4	0.7±0.1	31.7±0.3	30.0±0.0	98.8±13.1	74.8±9.2
	Average	22.2±9.6	9.7±3.4	9.8±3.0	9.0±2.5	1.2±0.4	0.6±0.2	31.4±0.4	30.0±0.0	95.8±23.1	77.6±20.0
Pleioblastus	*Pl. hindsii*	30.0±2.2	16.7±1.4	6.6±3.0	13.1±3.4	2.7±1.5	0.7±0.1	32.0±1.0	30.0±0.1	121.8±9.1	105.7±18.5
	Pl. linearis	42.7±6.1	7.9±4.6	11.8±1.7	10.4±2.9	1.9±0.5	0.4±0.2	34.0±0.6	30.0±0.0	100.7±31.2	47.6±17.8
	Pl. simonii	43.0±8.8	15.7±1.4	10.2±0.8	10.9±2.5	2.1±0.5	0.8±0.2	33.2±0.5	29.9±0.0	104.9±19.7	102.8±2.1
	Pl. chino	24.0±7.9	18.3±2.4	5.3±1.1	14.4±4.5	2.2±0.3	0.7±0.1	33.5±0.2	29.9±0.0	53.7±25.2	180.3±22.3
	Average	34.9±10.3	14.6±4.8	8.5±3.2	12.2±3.3	2.2±0.8	0.6±0.2	33.2±0.9	29.9±0.0	95.3±32.8	109.1±51.4
Average		25.2±12.7	11.4±4.7	8.3±3.1	9.7±3.4	1.6±0.8	0.6±0.2	31.6±1.3	30.0±0.0	88.1±29.3	76.5±39.8

Table 4-7 Area-based isoprene emission (I_{Area}), area-based photosynthetic rate (A_{Area}), carbon ration, leaf temperature (T_L), and area-based electron transport rate (ETR_{Area}) in August and September 2019 for 5 species of dwarf bamboos. The values are represented in mean ± standard deviation.

Genus	Species	I_{Area} (nmol m^{-2} s^{-1})		A_{Area} (μmol m^{-2} s^{-1})		Carbon ratio (%)		T_L (°C)		ETR_{Area} (μmol m^{-2} s^{-1})	
		Aug 2019	Sep 2019	Aug 2019	Sep 2019	Aug 2019	Sep 2019	Aug 2019	Sep 2019	Aug 2019	Sep 2019
Sasa	*S. tsuboiana*	7.0±3.1	0.7±0.7	7.2±3.3	6.9±2.6	0.6±0.3	0.1±0.1	32.4±1.3	29.9±0.0	129.1±16.9	110.8±8.8
	S. veitchii	0.2±0.2	n.d.	10.2±2.4	9.1±1.0	0.0±0.0	0.0±0.0	30.4±0.4	30.0±0.0	95.5±5.8	86.3±5.6
	S. chartacea	1.4±0.2	1.0±0.9	9.1±0.7	13.8±3.4	0.1±0.0	0.0±0.0	32.5±1.5	30.1±0.3	113.9±11.1	141.5±12.0
	Average	2.9±3.5	0.6±0.7	8.8±2.5	9.9±3.8	0.2±0.3	0.0±0.0	31.8±1.5	30.0±0.2	112.8±18.0	112.9±25.3
Sasaella	*Sa. Ramosa*	0.6±0.2	n.d.	8.7±2.9	9.8±4.4	0.0±0.0	0.0±0.0	31.1±0.2	29.8±0.2	132.3±9.1	94.9±6.0
	Sa. Hortensis	0.5±0.2	n.d.	5.5±1.5	5.1±4.4	0.1±0.0	0.0±0.0	34.1±1.0	30.0±0.1	89.9±0.9	83.6±20.9
	Average	0.6±0.2	n.d.	7.1±2.7	7.4±4.7	0.0±0.0	0.0±0.0	32.6±1.8	29.9±0.2	111.1±23.9	89.2±15.1
Average		2.0±2.9	0.3±0.6	8.1±2.6	8.9±4.2	0.1±0.2	0.0±0.0	32.1±1.6	30.0±0.2	112.1±19.7	103.4±24.3

4.4. Discussion

The results obtained from isoprene emission measurements of bamboo from August 2019 to May 2020 indicate a clear variation in isoprene emission flux from the bamboo species under higher temperatures; all the species exhibited very low or no isoprene emissions during the measurement from October 2019 to April 2020. The isoprene emissions from certain species indicated a threshold-like dependence on leaf temperature, where larger fluxes were observed when the leaf temperature was > 25 °C. Under the condition of lower leaf temperature, all the species exhibited very low or no emission of isoprene, and thus no significant difference was observed between isoprene emission fluxes among the species. This temperature dependency on seasonality could be explained by long-term control of the genetic expression of IspS with temperature (Oku et al., 2014; Mutanda et al., 2016). A similar phenomenon was previously reported by Chang et al. (2019), whereby isoprene emission measurements of *P. pubescens* in Taiwan demonstrated a temperature threshold of approximately 23 °C. Although the temperature during the measurements in May 2020 was also higher than the threshold temperature, low isoprene emissions even from high emitter species were reported on average, which might be due to the aging of the leaves, as indicated in previous studies (Niinemets et al., 2015; Funk et al., 1999) or due to just-expanded leaves for *Pl. chino*.

To focus on the definitive variation in isoprene emission flux that occurs in the warmer season and to exclude the temperature dependence and other possible fluctuations in leaf phenology, here I select the data measured in August and September 2019 to be discussed in next. I first hypothesized that the isoprene emission trait from bamboo species could be distinct either by growth type or by the climate of the region of origin of each species. As a result, a major difference was observed between the isoprene emission fluxes of the two different growth types (i.e., woody and dwarf), where the isoprene emission flux of woody bamboos ranged from 4.9 to 43.0 nmol m^{-2} s^{-1} in area-based unit and 24.6 to 157.8 μg g^{-1} h^{-1} in mass-based unit, while that of dwarf bamboos ranged from 0.2 to 7.0 nmol m^{-2} s^{-1} and 0.7 to 22.3 μg g^{-1} h^{-1}, respectively, in August. Okumura et al. (2018) recorded isoprene emission fluxes of 0.7 to 99.1 nmol m^{-2} s^{-1} of 14 bamboo species (*Phyllostachys* spp., *Tetragonocalamus* sp., *Sinobambusa* sp., *Bambusa* spp., *Semiarundinaria* spp., *Pseudosasa* sp., P*leioblastus* sp., and *Sasa* spp.). The high emitter genera reported by Okumura et al. (2018) were generally consistent with the results here, however, a dwarf species (*Sasa kurilensis*) was observed with considerable emission (24.0 nmol m^{-2} s^{-1}). Comparing to the result in this site, Okumura et al. (2018) demonstrated generally higher isoprene emission fluxes of *Phyllostachys* spp. (6.8 to 68.6 nmol m^{-2} s^{-1}) and *Semiarundinaria* spp. (53.6 to 57.8 nmol m^{-2} s^{-1}) under similar temperature in August of this site. The isoprene emission flux under light intensity of 1000 µmol m^{-2} s^{-1} and leaf temperature of 30 °C of woody bamboos is comparable to that of the highest emitter species, such as *Populus* sp. (59 nmol m^{-2} s^{-1}; 165 µg g^{-1} h^{-1}), *Quercus* spp. (79 nmol m^{-2} s^{-1}; 157 µg g^{-1} h^{-1}), and *Salix* spp. (37; 133 µg g^{-1} h^{-1}) (Litvak et al., 1996; Geron et al., 2001; Chang et al., 2012). However, there is no evidence that isoprene emission fluxes differ among the origin climates. Species in the same genus tend to exhibit similar isoprene emission fluxes despite the fact that they might have different origin climates.

A previous study indicated that the area-based isoprene emission flux could vary with LMA (Harley et al., 1997). Indeed, results in this chapter indicated a positive correlation between area-based isoprene emission flux and LMA across the woody species. Variation in LMA is usually related to acclimation to light environments, in which the leaves exposed to sunlight tend to exhibit higher LMA (Poorter et al., 2009). However, the light environments of all the species were unshaded and shared similar light profiles, regardless of growth types. Furthermore, the actual observation of LMA in August and September 2019 for the bamboo species exhibited no significant difference between the woody species and dwarf species. Therefore, the possibility that the difference in isoprene emission flux between the two growth types was caused by variations in LMA can be excluded. Indeed, higher isoprene fluxes were observed in the bamboo species with higher LMA, as the leaf thickness, and thus the concentration of chloroplasts where isoprene is produced, could affect the isoprene; nevertheless, it is only valid in the woody species.

Although major dependencies were recorded in leaf temperature and LMA, variation among leaves was still large. Previous studies have indicated the critical role of energetic and reducing agents in isoprene emission; the correlation between ETR and isoprene emission from multiple plant species (e.g., *Quercus spp.*, *Eucalyptus spp.*, and

Vismia guianensis) has also been reported in several studies (Niinemets and Reichstein, 2002; Rapparini et al., 2004; Dani et al., 2015; Rodrigues et al., 2020). Furthermore, according to Farquhar et al. (1980), the photosynthetic rate is regulated by both intercellular CO_2 concentration, which is correlated to stomatal conductance, and electron transport. While the emission of isoprene is not limited to stomatal conductance (Sharkey, 1991), a much greater increase in isoprene emission flux could be expected under extremely high temperatures because photosynthesis reaches a maximum at lower temperatures (Niinemets et al., 1999; Rodrigues et al., 2020). The results in this chapter demonstrated definitive correlations among isoprene emission, photosynthetic rate, and ETR, which is consistent with previous results; even more definitive correlation was found with ETR_{Mass} than that with A_{Mass}. The relationship between isoprene emission flux and ETR could explain part of the discrepancy in isoprene emission flux across the woody species. This evidence suggests a dependence of isoprene emission on ETR. However, this is only adequate for the woody species. Moreover, despite a low total isoprene emission, the photosynthetic traits of the dwarf species were not significantly different from those of the woody species.

August and September 2019 showed obviously different isoprene emission traits to each other for the woody species, where September 2019 generally showed much lower isoprene emission rates and carbon ratios. One of the reasons of this discrepancy might be attributed to a change in temperature. Larger isoprene emission fluxes were found in August with higher leaf temperature, especially for *Pleioblastus* spp., which were consistent with the temperature dependence curve in Figure 4-1; *P. nigra* f. *henonis* demonstrated a smaller difference in I_{Area} between August and September since almost no difference in T_L (Figure 4-2). However, other reasons should be counted because some of the genera (i.e., *Phyllostachys* spp. and *Semiarundinaria* spp.) showed large decrease in isoprene emissions even under similar T_L between the two months. This might be partially attributed to the influence of ETR, where several species (e.g., *P. makinoi*, *P. bambusoides*, *P. pubescens*, *Se. fastuosa*, *Se. fortis*, *Se. kagamiana* and *Pl. linearis*) also showed a large decrease in ETR September (Table 4-6). The other possibility is the previous exposure of higher ambient temperature in August, as an attemption to manipulate T_L into 30 °C, lower T_L were recorded than that in ambient. Previous studies also indicated that leaf in different growth stage demonstrates different capacity of isoprene emission rate (Kuzma and Fall, 1993; Monson et al., 1994). Thus, leaf phenological change could also influence the isoprene emission rate from August to September. According to the meteorological data in Kyoto City, both August and September 2019 had remarkable monthly precipitation though August had much more precipitation than September 2019 (August: 355.0 mm; September: 84.5 mm). Also, based on the gas exchange results in A_{Area}, there were no clear evidence of drought stress both in August and September 2019 (Table 4-6; 4-7). Since the effects of previous exposure to ambient temperature and leaf phenology on isoprene emission were not directly observed in this site, further investigation is suggested for bamboo species.

Typically, carbon loss from isoprene emission in assimilation usually accounts for approximately 1–2 % at 30 °C and depends on the photosynthetic rate; under extremely high temperatures, the isoprene emission could account for more than 50 % of carbon loss (Tingey et al., 1979; Harley et al., 1994; Tani and Kawawata, 2008; Morfopoulos et al., 2014). Okumura et al. (2018) reported a range of 0–1.5 % of carbon loss from isoprene emissions in multiple bamboo species during summer. It was observed that the average carbon ratio for woody bamboo species was 1.6 % and 0.6 % in August and September 2019, respectively; certain species can reach a carbon ratio of 2.7 % during *a* T_L of 32 °C. In contrast, the dwarf bamboo species used very low carbon for isoprene emissions, which was usually less than 0.2 %. Since evidence has shown that isoprene production in plants majorly for enhancing tolerance to heat or light stresses (Sharkey and Singsaas, 1995; Loreto and Velikova, 2001, Siwko et al., 2007; Way et al., 2011), this difference is very reasonable because dwarf bamboos usually grow in the understory of forest areas, where heat stress is less due to indirect sunlight. Moreover, to adapt to low light conditions, preventing loss of carbon could be a critical life strategy by dwarf bamboos. On the other hand, mid-size and tall-size Sasa/Bamboo are not suitable to grow under shaded environment and have to encounter heat and over-light stresses. Nonetheless, in this chapter, the dwarf species was exposed to direct sunlight, which is unnatural. This implies that the low isoprene emission capacity is genetically determined in case of the dwarf species, as plants lacking the IspS gene are unable to produce isoprene (Behnke et al., 2007).

4.5. Chapter conclusion

Based on observations in isoprene emission flux and related factors such as LMA, ETR, and photosynthetic rate of 18 bamboo species, the study suggests a distinction in isoprene emissions between the woody and dwarf bamboos, which is genetically determined. This difference in genotype causes different dependencies of isoprene emission on leaf temperature, LMA, photosynthetic rate, and ETR.

Reference

Behnke K, Ehlting B, Teuber M, Bauerfeind M, Louis S, Hänsch R, Polle A, Bohlmann J, Schnitzler JP (2007) Transgenic, non-isoprene emitting poplars don't like it hot. *The Plant Journal* 51 (3):485-99. https://doi.org/10.1111/j.1365-313x.2007.03157.x

Brüggemann N, Schnitzler J-P (2002) Diurnal variation of dimethylallyl diphosphate concentrations in oak (*Quercus robur*) leaves. *Physiologia Plantarum* 115 (2): 190-196. https://doi.org/10.1034/j.1399-3054.2002.1150203.x

Chang J, Ren Y, Shi Y, Zhu Y, Ge Y, Hong S, iao L, Lin F, Peng C, Mochizuki T, Tani A, Mu Y, Fu C (2012) An inventory of biogenic volatile organic compounds for a subtropical urban–rural complex. *Atmospheric Environment* 56:115-123. https://doi.org/10.1016/j.atmosenv.2012.03.053

Chang M (2009) Seasonal variations of *C. Sinensis* BVOCs flux measurements and its environmental factors at middle altitude in Taiwan (Master's thesis, National Yunlin University of Science and Technology, Yunlin, Taiwan) Retrived from https://hdl.handle.net/11296/cfx6en

Chang T, Kume T, Okumura M, Kosugi Y (2019) Characteristics of isoprene emission from moso bamboo leaves in a forest in central Taiwan. *Atmospheric Environment* 211:288-295. https://doi.org/10.1016/j.atmosenv.2019.05.026

Dani KGS, Jamie IM, Prentice IC, Atwell BJ (2015) Species-specific photorespiratory rate, drought tolerance and isoprene emission rate in plants. *Plant Signaling & Behavior* 10 (3):e990830. https://doi.org/10.4161/15592324.2014.990830

Farquhar GD, von Caemmerer S, Berry JA (1980) A biochemical model of photosynthetic CO_2 assimilation in leaves of C_3 species. *Planta* 149 (1):78-90. https://doi.org/10.1007/BF00386231

Funk JL, Jones CG, Lerdau MT (1999) Defoliation effects on isoprene emission from *Populus deltoides*. *Oecologia* 118 (3):333-339. https://doi.org/10.1007/s004420050734

Geron C, Harley P, Guenther A (2001) Isoprene emission capacity for US tree species. *Atmospheric Environment* 35 (19):3341-3352. https://doi.org/10.1016/S1352-2310(00)00407-6

Harley PC, Litvak ME, Sharkey TD, Monson RK (1994) Isoprene Emission from Velvet Bean Leaves (Interactions among Nitrogen Availability, Growth Photon Flux Density, and Leaf Development). *Plant Physiology* 105 (1):279-285. https://doi.org/10.1104/pp.105.1.279

Harley P, Guenther A, Zimmerman P (1997) Environmental controls over isoprene emission in deciduous oak canopies. *Tree Physiology* 17 (11):705-14. https://doi.org/10.1093/treephys/17.11.705

Kobayashi M (2017) The illustrated book of plant systematics in color: *Bambusoideae* in Japan. *Horyukan*.

Kuzma J, Fall R (1993) Leaf Isoprene Emission Rate Is Dependent on Leaf Development and the Level of Isoprene Synthase. *Plant Physiology* 101 (2):435-440. https://doi.org/10.1104/pp.101.2.435

Li R, During HJ, Werger MJA, Zhong ZC (1998a) Positioning of new shoots relative to adult shoots in groves of giant bamboo, *Phyllostachys pubescens*. *Flora* 193 (3):315-321. https://doi.org/10.1016/S0367-2530(17)30852-6

Li R, Werger MJA, During HJ, Zhong ZC (1998b) Biennial variation in production of new shoots in groves of the giant bamboo *Phyllostachys pubescens* in Sichuan, China. *Plant Ecology* 135 (1):103-112. https://doi.org/10.1023/A:1009761428401

Liakoura V, Fotelli MN, Rennenberg H, Karabourniotis G (2009) Should structure-function relations be considered separately for homobaric vs. heterobaric leaves?. *American Journal of Botany* 96:612-619. https://doi.org/10.3732/ajb.0800166

Lichtenthaler HK (1999) The 1-deoxy-D-xylulose-5-phosphate pathway of isoprenoid biosynthesis in plants. *Annual Review of Plant Physiology and Plant Molecular Biology* J50:47-65. https://doi.org/10.1146/annurev.arplant.50.1.47

Litvak ME, Loreto F, Harley PC, Sharkey TD, Monson RK (1996) The response of isoprene emission rate and photosynthetic rate to photon flux and nitrogen supply in aspen and white oak trees. *Plant, Cell & Environment* 19 (5):549-559. https://doi.org/10.1111/j.1365-3040.1996.tb00388.x

Loreto F, Velikova V (2001) Isoprene produced by leaves protects the photosynthetic apparatus against ozone damage, quenches ozone products, and reduces lipid peroxidation of cellular membranes. *Plant Physiology 127* (4):1781-7. https://doi.org/10.1104/pp.010497

Monson RK, Harley PC, Litvak ME, Wildermuth M, Guenther AB, Zimmerman PR, Fall R (1994) Environmental and developmental controls over the seasonal pattern of isoprene emission from aspen leaves. *Oecologia* 99 (3):260-270. https://doi.org/10.1007/BF00627738

Monson RK, Grote R, Niinemets Ü, Schnitzler J-P (2012) Modeling the isoprene emission rate from leaves. *New Phytologist* 195 (3):541-559. https://doi.org/10.1111/j.1469-8137.2012.04204.x

Monson RK, Jones RT, Rosenstiel TN, Schnitzler J-P (2013) Why only some plants emit isoprene. *Plant, Cell & Environment* 36:503-516. https://doi.org/10.1111/pce.12015

Morfopoulos C, Sperlich D, Peñuelas J, Filella I, Llusià J, Medlyn BE, Niinemets Ü, Possell M, Sun Z, Prentice IC (2014) A model of plant isoprene emission based on available reducing power captures responses to atmospheric CO_2. *New Phytologist*, 203 (1): 125-139. https://doi.org/10.1111/nph.12770

Mutanda I, Saitoh S, Inafuku M, Aoyama H, Takamine T, Satou K, Akutsu M, Teruya K, Tamotsu H, Shimoji M, Sunagawa H, Oku H (2016) Gene expression analysis of disabled and re-induced isoprene emission by the tropical tree *Ficus septica* before and after cold ambient temperature exposure. *Tree Physiology* 36 (7):873-882. https://doi.org/10.1093/treephys/tpw032

Sharkey TD, Loreto F (1993) Water stress, temperature, and light effects on the capacity for isoprene emission and photosynthesis of kudzu leaves. *Oecologia* 95 (3):328-333. https://doi.org/10.1007/BF00320984

Niinemets Ü, Tenhunen JD, Harley PC, Steinbrecher R (1999) A model of isoprene emission based on energetic requirements for isoprene synthesis and leaf photosynthetic properties for *Liquidambar* and *Quercus*. *Plant, Cell & Environment* 22 (11):1319-1335. https://doi.org/10.1046/j.1365-3040.1999.00505.x

Niinemets Ü, Reichstein M (2002) A model analysis of the effects of nonspecific monoterpenoid storage in leaf tissues on emission kinetics and composition in Mediterranean sclerophyllous *Quercus* species. *Global Biogeochemical Cycles* 16 (4):1110. https://doi.org/10.1029/2002GB001927

Niinemets Ü, Keenan TF, Hallik L (2015) A worldwide analysis of within-canopy variations in leaf structural, chemical and physiological traits across plant functional types. *New Phytologist* 205 (3): 973-993. https://doi.org/10.1111/nph.13096

Ohrnberger D (1999) The Bamboos of the World. *Elsevier*. https://doi.org/10.1016/B978-0-444-50020-5.50021-6

Oku H, Inafuku M, Takamine T, Nagamine M, Saitoh S, Fukuta M (2014) Temperature threshold of isoprene emission from tropical trees, *Ficus virgata* and *Ficus septica*. *Chemosphere* 95:268-273. https://doi.org/10.1016/j.chemosphere.2013.09.003

Okumura M, Kosugi Y, Tani A (2018) Biogenic volatile organic compound emissions from bamboo species in Japan. *Journal of Agricultural Meteorology* 74 (1):40-44. https://doi.org/10.2480/agrmet.D-17-00017

Poorter H, Niinemets Ü, Poorter L, Wright IJ, Villar R (2009) Causes and consequences of variation in leaf mass per area (LMA): a meta-analysis. *New Phytologist* 182 (3): 565-588. https://doi.org/10.1111/j.1469-8137.2009.02830.x

Rapparini F, Baraldi R, Miglietta F, Loreto F (2004) Isoprenoid emission in trees of *Quercus pubescens* and *Quercus ilex* with lifetime exposure to naturally high CO_2 environment†. *Plant, Cell & Environment* 27 (4): 381-391. https://doi.org/10.1111/j.1365-3040.2003.01151.x

Rasulov B, Hüve K, Välbe M, Laisk A, Niinemets U (2009) Evidence that light, carbon dioxide, and oxygen dependencies of leaf isoprene emission are driven by energy status in hybrid aspen. *Plant Physiology* 151 (1):448-60. https://doi.org/10.1104/pp.109.141978

Rasulov B, Talts E, Bichele I, Niinemets Ü (2018) Evidence That Isoprene Emission Is Not Limited by Cytosolic Metabolites. Exogenous Malate Does Not Invert the Reverse Sensitivity of Isoprene Emission to High [CO_2]. *Plant Physiology* 176 (2):1573-1586. https://doi.org/10.1104/pp.17.01463

Rodrigues TB, Baker CR, Walker AP, McDowell N, Rogers A, Higuchi N, Chambers JQ, Jardine KJ (2020) Stimulation of isoprene emissions and electron transport rates as key mechanisms of thermal tolerance in the tropical species *Vismia guianensis*. *Global Change Biology* 26 (10):5928-5941. https://doi.org/10.1111/gcb.15213

Rohmer M (1999) The discovery of a mevalonate-independent pathway for isoprenoid biosynthesis in bacteria, algae and higher plants. *Natural Product Reports* 16 (5):565-574. http://dx.doi.org/10.1039/A709175C

Rosenstiel TN, Fisher AJ, Fall R, Monson RK (2002) Differential accumulation of dimethylallyl diphosphate in leaves and needles of isoprene- and methylbutenol-emitting and nonemitting species. *Plant Physiology* 129 (3):1276-84. https://doi.org/10.1104/pp.002717

Sasaki K, Ohara K, Yazaki K (2005) Gene expression and characterization of isoprene synthase from *Populus alba*. *FEBS Letters* 579 (11):2514-2518. https://doi.org/10.1016/j.febslet.2005.03.066.

Schwender J, Zeidler J, Gröner R, Müller C, Focke M, Braun S, Lichtenthaler FW, Lichtenthaler HK (1997) Incorporation of 1-deoxy-D-xylulose into isoprene and phytol by higher plants and algae. *FEBS Letters* 414:129-134. https://doi.org/10.1016/S0014-5793(97)01002-8

Sharkey TD, Loreto F, Delwiche CF (1991) High carbon dioxide and sun/shade effects on isoprene emission from oak and aspen tree leaves. *Plant, Cell & Environment* 14 (3):333-338. https://doi.org/10.1111/j.1365-3040.1991.tb01509.x

Sharkey T, Singsaas E (1995) Why plants emit isoprene. *Nature* 374(6525). https://doi.org/10.1038/374769a0

Silver GM, Fall R (1991) Enzymatic synthesis of isoprene from dimethylallyl diphosphate in aspen leaf extracts. *Plant Physiology* 97 (4):1588-91. https://doi.org/10.1104/pp.97.4.1588

Siwko ME, Marrink SJ, Vries AH, Kozubek A, Uiterkamp AJ, Mark AE (2007) Does isoprene protect plant membranes from thermal shock? A molecular dynamics study. *Biochimica Et Biophysica Acta (BBA) - Biomembranes* 1768 (2):198-206. https://doi.org/10.1016/j.bbamem.2006.09.023

Suzuki S (1996) Illustrations of Japanese *Bambusaceae* (Revised Edition). *Self-published*.

Tani A, Kawawata Y (2008) Isoprene emission from the major native *Quercus* spp. in Japan. *Atmospheric Environment* 42 (19):4540-4550. https://doi.org/10.1016/j.atmosenv.2008.01.059

Tingey DT, Manning M, Grothaus LC, Burns WF (1979) The influence of light and temperature on isoprene emission rates from live oak. *Physiologia Plantarum* 47 (2):112-118. https://doi.org/10.1111/j.1399-3054.1979.tb03200.x

Vickers CE, Possell M, Laothawornkitul J, Ryan AC, Hewitt CN, Mullineaux PM (2011) Isoprene synthesis in plants: lessons from a transgenic tobacco model. *Plant, Cell & Environment* 34 (6): 1043-1053. https://doi.org/10.1111/j.1365-3040.2011.02303.x

Way DA, Schnitzler JP, Monson RK, Jackson RB (2011) Enhanced isoprene-related tolerance of heat- and light-stressed photosynthesis at low, but not high, CO_2 concentrations. *Oecologia* 166 (1):273-282. https://doi.org/10.1007/s00442-011-1947-7

Wiberley AE, Donohue AR, Westphal MM, Sharkey TD (2009) Regulation of isoprene emission from poplar leaves throughout a day. *Plant, Cell & Environment* 32 (7):939-947. https://doi.org/10.1111/j.1365-3040.2009.01980.x

Wildermuth MC, Fall R (1996) Light-Dependent Isoprene Emission (Characterization of a Thylakoid-Bound Isoprene Synthase in *Salix* discolor Chloroplasts). *Plant Physiology* 112 (1):171-182. https://doi.org/10.1104/pp.112.1.171

Wildermuth MC, Fall R. (1998) Biochemical characterization of stromal and thylakoid-bound isoforms of isoprene synthase in willow leaves. *Plant Physiology* 116 (3):1111-23. https://doi.org/10.1104/pp.116.3.11

Chapter 5

Conclusions

This study measured leaf-scale isoprene emission fluxes for multiple bamboo species. For this, the responses of leaf isoprene emission flux to potential meteorological, morphological, and physiological controllers such as leaf temperature, light intensity, LMA, leaf nitrogen concentration, photosynthetic rate, and ETR were examined. This study verifies the relationships of isoprene emission flux from bamboo leaves with several factors that control representative isoprene emission flux, and aids in a better estimation of bamboo isoprene emissions using the current model.

In Chapter 2, the isoprene emission flux of the leaves of *P. pubescens*, a woody bamboo, in response to varied leaf temperature and light intensity was examined. The results of here confirm that *P. pubescens* is a major isoprene emitter, equivalent to or even stronger than previously reported emitters. When validating the reproducibility of the G93 model, the isoprene emission flux in response to light was well reproduced. However, the model did not reproduce the response to leaf temperature owing to overestimation of isoprene emission fluxes under low temperatures. Although the issue was substantially corrected by applying an optimization on certain parameters in the model, the large variation among leaves led to difficulties in reproducing isoprene emission flux from *P. pubescens* with a constant basal isoprene emission rate. Further investigation of the controlling factors by considering the seasonal and inter-leaf variation in isoprene emission is suggested.

In Chapter 3, the results of Chapter 2, and knowledge of the process-based sense, were used to determine the morphologic and physiologic factors that could alter the isoprene emission capacity of bamboo leaves. After examining the dependence of isoprene emission on LMA, photosynthetic rate, and leaf nitrogen concentration, I found a strong correlation between LMA and area-based isoprene emission flux. However, mass-based photosynthetic rate and leaf nitrogen concentration did not exhibit any correlation with the mass-based isoprene emission flux. By combining data from *P.*

pubescens LMA from other sites, under constant light (1000 μmol m^{-2} s^{-1}) and leaf temperature (~30 °C), a constant correlation was demonstrated across these sites. This dependency on LMA could be attributed to the thicker mesophylls and consequently higher quantity of chloroplasts per unit leaf area for leaves with higher LMA, when assuming consistent leaf density. This result partly explains the inter-leaf variation in isoprene emission flux, and suggests that detection of LMA can effectively determine the representative isoprene emission flux of bamboo leaves.

In Chapter 4, isoprene flux, LMA, photosynthetic rate, and ETR were recorded for 18 bamboo species within 5 genera, incorporating different growth types (woody and dwarf) and climates of the region of origin (temperate, warm-temperate, and subtropical). Dwarf bamboos showed negligible to no emissions; in contrast, woody bamboos demonstrated considerable isoprene emission fluxes, mainly in August and September, at temperatures >30 °C. For woody bamboos, isoprene emission fluxes, photosynthetic rate, and ETR in area-based units were correlated with LMA. To exclude the systematic correlation among these parameters, correlations among the values of mass-based units were also tested, and the results demonstrated significant positive correlations. The different isoprene emission traits between woody and dwarf bamboos were independent of LMA, photosynthetic rate, and ETR. This implies that differences in isoprene emissions were caused by genetic dissimilarities. Low isoprene emission from dwarf bamboos is expected because they usually grow in areas with relatively low heat stress and light, where the production of isoprene could be futile due to carbon loss. This study suggests separating the two bamboo types on the basis of isoprene emissions.

This study shows that some bamboo species emit a considerable amount of isoprene. Previous studies have revealed that species-average basal isoprene emission flux from plant leaves ranged from 0 to 100 nmol m^{-2} s^{-1} in area-based units and 0 to 173 μg g^{-1} h^{-1} in mass-based units (Table 1-1). Some of the highest isoprene emissions have been recorded in *Elaeis* sp. (172.9 μg g^{-1} h^{-1}), *Populus* sp. (165 μg g^{-1} h^{-1}), *Quercus* sp. (157 μg g^{-1} h^{-1}), and *Salix* sp. (133 μg g^{-1} h^{-1}) in mass-based units; the area-based values of *Populus* sp., *Quercus* sp., and *Salix* sp. were 74, 93, and 37 nmol m^{-2} s^{-1}, respectively. In Chapter 2, an isoprene emission flux of 30.6 nmol m^{-2} s^{-1} from *P. pubescens* was recorded under light intensity of 1000 μmol m^{-2} s^{-1} and leaf temperature of around 25.9 °C in September, which were normalized as a basal flux of 54.4 nmol m^{-2} s^{-1} with the G93 model. Chapter 3 documents a series of varied isoprene emission rates among leaves (1.4–32.2 nmol m^{-2} s^{-1}) under light intensity of 1000 µmol m^{-2} s^{-1} and leaf temperature of around 30 °C in August, depending on the LMA of each leaf, by direct measurement from overtopped plant culms. Chapter 4 discusses differences in isoprene emissions between woody and dwarf bamboos, where the isoprene emission flux of woody bamboos ranged from 4.9 to 43.0 nmol m^{-2} s^{-1} ('basal' flux normalized with G93 parameter sets : 5.0 to 37.1 nmol m^{-2} s^{-1}) in area-based unit and 24.6 to 157.8 µg g^{-1} h^{-1} (normalized: 25.1 to 135.0 µg g^{-1} h^{-1}) in mass-based unit, while that of dwarf bamboos ranged from 0.2 to 7.0 (0.2 to 5.6 nmol m^{-2} s^{-1}) nmol m^{-2} s^{-1} and 0.7 to 22.3 µg g^{-1} h^{-1} (0.7 to 18.0 µg g^{-1} h^{-1}), respectively, in August. In winter, both plant types exhibited little to no emission. The isoprene emissions of certain bamboo species were found equivalent to those of known high-emitter species. This observation increases the necessity of mitigating the impact on regional BVOC emissions from expanding bamboo habitats.

The data from multiple sites and bamboo species aid in expanding the database of BVOC emissions from bamboo leaves. In addition, by quantifying the variability of isoprene emission rates, in response to factors such as leaf temperature, light intensity, LMA, and ETR, from bamboo leaves of different species, this study allows us to better understand isoprene emission characteristics of bamboo species. With this knowledge we can effectively determine isoprene emissions from bamboos and make efforts to better estimate global BVOC emissions.

ACKNOWLEDGEMENTS

I would like to express the sincerest gratitude to Prof. Yoshiko Kosugi. She is a great researcher, scientist, advisor, and mentor. I cannot complete this thesis without her kindly guidance and support. I would like to thank Prof. Kanehiro Kitayama (Laboratory of Forest Ecology), Prof. Shouzo Shibata (Laboratory of Landscape Architecture) and Prof. Masahiro Sakamoto (Laboratory of Forest Biochemistry) in Kyoto University for reviewing this thesis and giving insightful comments. I also want to give thanks to Dr. Okumura. He teaches me all my techiques to complete the experiment. I also want to give a special acknowledgement to Prof. Kume. He is a kind teacher and I learn almost every knowledge about forest climate from him.

I would like to express appreciation to Mrs. Yi-Jen Pan for the support of the laboratory works. Also, thanks to Prof. Liang for providing great advises and equipments.

The field works were conduct smoothly because of the support from all the people that manage the sites. I need to thank National Taiwan University Experimental Forest, Kasuya Research Forest of Kyushu University and Kamigamo Experimental Station of Kyoto University for the great management and welcome.

I am very grateful to all the members and former members in Laboratory of Forest Hydrology. They are good teachers, learners and great friends.

Finally, I want to thank my family. They give all the guiding and supporting to let me have a chance to become a researcher.